

NASA TECHNICAL NOTE



NASA TN D-5617

c. 1

NASA TN D-5617



LOAN COPY: RETURN TO
AFWL (WL0L)
KIRTLAND AFB, N MEX

REVIEW OF PROPULSION-INDUCED EFFECTS ON AERODYNAMICS OF JET/STOL AIRCRAFT

by Richard J. Margason
Langley Research Center
Langley Station, Hampton, Va.



0132417

1. Report No. NASA TN D-5617	2. Government Accession No.	3. Recipient's Catalog No.		
4. Title and Subtitle REVIEW OF PROPULSION-INDUCED EFFECTS ON AERODYNAMICS OF JET V/STOL AIRCRAFT		5. Report Date February 1970		
7. Author(s) Richard J. Margason		6. Performing Organization Code		
9. Performing Organization Name and Address NASA Langley Research Center Hampton, Va. 23365		8. Performing Organization Report No. L-6565		
12. Sponsoring Agency Name and Address National Aeronautics and Space Administration Washington, D.C. 20546		10. Work Unit No. 721-01-11-05-23		
15. Supplementary Notes This material was originally presented as a lecture at the University of Tennessee Space Institute Short Course on V/STOL, November 1968.		11. Contract or Grant No.		
16. Abstract This paper reviews several aspects of the effects induced on the aerodynamics of V/STOL aircraft in hover and transition flight by the interference of wakes from relatively high disk-loading propulsion devices. Four problem areas are treated: (1) the performance losses sustained when hovering out of ground effect, (2) induced aerodynamic effects in transition flight out of ground effect, (3) the problems caused by hot-gas ingestion, and (4) the effects induced on performance during hover in ground effect. Some of the conflicts among the design requirements imposed by these different modes of flight are discussed, along with the present state of the art of solutions to some of the problems.		13. Type of Report and Period Covered Technical Note		
17. Key Words Suggested by Author(s) Jet V/STOL transition V/STOL Hovering aircraft Ground effects Hot-gas ingestion		14. Sponsoring Agency Code		
	18. Distribution Statement Unclassified - Unlimited			
19. Security Classif. (of this report) Unclassified	20. Security Classif. (of this page) Unclassified	21. No. of Pages 67	22. Price* \$3.00	

REVIEW OF PROPULSION-INDUCED EFFECTS ON
AERODYNAMICS OF JET V/STOL AIRCRAFT*

By Richard J. Margason
Langley Research Center

SUMMARY

This paper reviews several aspects of the effects induced on the aerodynamics of V/STOL aircraft in hover and transition flight by the interference of wakes from relatively high disk-loading propulsion devices. Four problem areas are treated: (1) the performance losses sustained when hovering out of ground effect, (2) induced aerodynamic effects in transition flight out of ground effect, (3) the problems caused by hot-gas ingestion, and (4) the effects induced on performance during hover in ground effect. Some of the conflicts among the design requirements imposed by these different modes of flight are discussed, along with the present state of the art of solutions to some of the problems.

INTRODUCTION

This paper summarizes some of the propulsion-induced effects on the aerodynamics of V/STOL aircraft when in and out of ground effect, both in hover and in transition flight. Descriptions of the fluid-flow phenomena are presented, along with an indication of the trends obtained from experimental investigations. In several cases, empirical or analytic approaches are discussed. The specific examples relate directly to effects caused by turbojet, turbofan, or high-disk-loading lift-fan propulsion devices.

In particular, four problem areas are reviewed: (1) the performance losses sustained by a VTOL aircraft hovering out of ground effect, (2) the induced aerodynamic effects as a V/STOL aircraft flies on a combination of powered and aerodynamic lift between hover and cruise out of ground effect, (3) some results of investigations of hot-gas ingestion by the inlets of the propulsion devices when a jet V/STOL airplane is on or near the ground, and (4) propulsion-induced effects on the performance of a VTOL aircraft hovering near the ground. Additional descriptions of some of these problem areas can be found in references 1 to 9.

*This material was originally presented as a lecture at the University of Tennessee Space Institute Short Course on V/STOL, November 1968.

SYMBOLS

A_j	total area of nozzle exit or exits, ft ² (m ²)
b	wing span, ft (m)
C_m	pitching-moment coefficient, $\frac{\text{Pitching moment}}{q_\infty S c}$
C_p	pressure coefficient, $\frac{p_l - p_\infty}{q_\infty}$ (in fig. 3 only, $\frac{p_l - p}{q_j}$)
C_T	thrust coefficient, $\frac{T}{q_\infty S}$
c	wing chord, ft (m)
D	diameter of a single jet, ft (m)
D_e	equivalent diameter; the diameter of a circle whose area equals the sum of the areas of all the nozzles of a multiple configuration, ft (m)
d	fuselage diameter, ft (m)
h	height of jet exit above ground, ft (m)
I_X	moment of inertia about the X body axis, slug-ft ² (kg-m ²)
k	constant of proportionality
ΔL	propulsion-induced increment of lift, lb (N)
ΔL_b	propulsion-induced increment of lift out of ground effect, lb (N)
ΔL_g	change in propulsion-induced increment of lift caused by ground effect, lb (N)
l	distance between the center lines of two nozzles, ft (m)
M	Mach number
M_X	rolling moment about the X body axis, ft-lb (m-N)

ΔM_y	propulsion-induced increment of pitching moment, ft-lb (m-N)
p	atmospheric pressure, psi (N/m ²)
p_l	local pressure, psi (N/m ²)
p_t	total pressure, psi (N/m ²)
p_∞	free-stream static pressure
q	dynamic pressure, psi (N/m ²)
q_x	maximum dynamic pressure in jet wake a distance x downstream of the jet exit plane, psi (N/m ²)
R	radius of the nozzle, ft (m)
r	local radius measured from the center line of the jet nozzle, ft (m)
S	area, ft ² (m ²)
T	thrust, lb (N)
t	time, sec
V	velocity, fps (m/s)
W	weight, lb (N)
x,y,z	Cartesian coordinates, ft (m)
$(x/D_e)_i$	location of maximum slope on dynamic-pressure decay curve
α	angle of attack, deg
β	sideslip angle, deg
δ_f	flap deflection angle, deg

δ_j jet nozzle deflection angle, deg
 ρ density, slugs/ft³ (kg-m³)

Subscripts:

j jet exit
max maximum
 ∞ free stream

PERFORMANCE LOSSES OF VTOL AIRCRAFT
HOVERING OUT OF GROUND EFFECT

The rated thrust of a jet engine, whether for conventional aircraft or for VTOL aircraft, is based on its performance with a bell-mouth inlet on a test stand, using the nozzle designed for the engine. The actual performance of the engine when installed in the airplane is degraded from the test-stand rating by various installation losses. Even though each of these losses may be only a few percent of rated thrust, an accurate knowledge of each is required for a realistic estimate of the aircraft performance. An error of as little as 3 percent in the total lifting capability in hover would mean a reduction of 3 percent in gross weight, which would cause a like reduction in fuel capacity. This would result in a reduction in design range of about 10 percent. There are several sources of thrust loss in hover when an engine is installed in an airplane which might be considered. These losses include inlet flow distortion, hot-gas ingestion, hot day conditions, control bleed, internal nozzle flow, thrust vectoring, static ground effect, and base loss. The present paper is concerned primarily with the aerodynamic lift loss in hover resulting from suction forces on the undersurface of the airplane; this is commonly referred to as base loss. This paper also includes a summary of some hot-gas ingestion investigations. Finally, the aerodynamic ground effect on the base loss is discussed.

The flow phenomena that cause base loss in hover are illustrated in figure 1. This photograph and several other photographs in later figures were taken from a motion-picture film entitled "Flows With Large Velocity Fluctuations" obtained from the Office National d'Etudes et de Recherches Aérospatiale (O.N.E.R.A.). The film is based on work done by Henri Werlé in an O.N.E.R.A. water tunnel. This photograph shows a jet ejecting into still water. The air bubbles being entrained into the jet show that flow is induced from the quiescent surroundings into the jet. This has been called the douche (shower) effect.

A nozzle is shown in figure 2 with the jet exhausting normal to a flat plate. The jet is entraining fluid, some of which is coming from behind the plate. The swirling air bubbles near the edge of the plate indicate that this fluid separates as it flows from behind the plate around to the jet. The pressure distribution induced radially on the plate is presented in figure 3. Near the edge of the plate, the separation region is indicated by an increased pressure coefficient. As the separation is relieved inboard of the edge of the plate, the pressure coefficient is reduced. The pressure coefficient increases again as the induced flow approaches and is entrained into the exhaust jet.

Propulsion-Induced Lift Loss for a Single Jet

In a program aimed at understanding these base losses and perhaps estimating their magnitude, a plenum chamber was constructed which would fit inside a long rectangular fuselage (ref. 10). In checking out this rectangular plenum chamber, the induced losses were compared with those obtained with a round plenum chamber. The round plenum chamber had a large contraction ratio between the plenum and the nozzle exit. Some results of this investigation are presented in figure 4. The round plenum chamber with a simple convergent nozzle gave a lift loss on the plate of a little less than 1 percent. The rectangular plenum chamber initially gave quite a large lift loss. This difference in results between the two plenum chambers (both with simple convergent nozzles) caused considerable concern. It was noted that the round plenum chamber had a flat distribution of dynamic pressure at the exit of the nozzle, while the dynamic pressure from the rectangular plenum chamber was depressed near the center line of the nozzle. The rectangular plenum chamber also had rather poor internal flow and a great deal of separation, so that the flow from the nozzle was quite turbulent. A change in the internal lines of the plenum chamber improved the flow, as indicated by the flatter pressure profiles and the reduction in thrust loss from more than 3 percent to approximately $1\frac{1}{2}$ percent. To determine whether it was the character of the flow coming out the nozzle that determined this thrust-loss level, the round plenum chamber had a restriction placed in its nozzle which almost completely eliminated the pressure at the center line of the nozzle. The base loss for the nozzle with the restriction increased from slightly under 1 percent to nearly the level obtained with the improved rectangular plenum chamber. This result indicated that the type of flow coming out the nozzle has an important influence on the induced interference in hover. The exit pressure profiles at the bottom of figure 4 do not explain the variations in lift loss.

A picture of a nozzle in a water tunnel with some colored milk introduced just upstream of the nozzle is presented in figure 5. The milk is entrained into the jet and mixes in a turbulent mixing region. This is a different look at the same flow illustrated in figure 1, concentrating on the flow inside the jet wake. It is illustrated schematically in figure 6 to show the decay and spread of the jet efflux from the nozzle. Starting at the

nozzle exit plane, there is a rectangular dynamic pressure distribution; 2 diameters downstream, this pressure profile is spread. At a distance downstream between 4 and 6 diameters, the peak dynamic pressure in the pressure profile has dropped below that at the exit. The conically shaped region where the peak pressure exists is the core of the jet. Outside the core region are the bounding surfaces of the turbulent mixing. In this region, air is entrained and slows the efflux as indicated by the further reductions in the height of the dynamic-pressure profiles.

In an effort to relate the lift loss to the characteristics of the jet core, the jet decay, and the turbulent mixing of the jet wake, an attempt was made to find a correlating parameter. The parameter finally chosen was the maximum dynamic pressure in the jet at different stations downstream of the exit of the jet, nondimensionalized by the dynamic pressure at the jet exit. Data for the same four plenum conditions shown in figure 4 are presented in figure 7. These data show the dynamic-pressure decay and the lift loss for surfaces of several sizes. At the top of the figure, the lift loss divided by thrust is plotted as a function of the square root of the ratio of surface area to jet area. With these parameters, there is a linear variation in the data. The round plenum chamber with no restriction in the nozzle had the smallest lift loss and the slowest decay of jet dynamic pressure. The round plenum chamber with the restriction in the nozzle gave an increased lift loss and a more rapid decay of jet dynamic pressure. The rectangular plenum chamber with the poor internal flow gave the largest lift loss and the most rapid decay of dynamic pressure. The rectangular plenum chamber with the improved internal flow gave about the same results as the round plenum chamber with the restriction. These data indicate that a relation exists between the lift loss and the rate of decay of nozzle dynamic pressure. However, more work was required to identify the exact relation.

Propulsion-Induced Lift Losses for Multiple Jets

In order to compare the induced lift loss of a single jet with the induced lift loss of multiple-jet arrangements, additional jet-exit configurations were investigated. Results for a single jet on the improved rectangular plenum chamber with the fuselage mounted around it, for a pattern of four jets, and for a pattern of four slot jets are presented in figure 8. The three configurations have different slopes of the lift-loss curve. These results show that there is a correspondence between increasing slopes of the lift-loss curve and increasing dynamic-pressure decay rates.

A comparison was also made between the small-scale cold jets and large-scale hot jets (ref. 11). Data are presented in figure 9 for a single jet and for a pattern of four jets exiting through a plate. The small-scale and large-scale lift-loss results are similar. The dynamic decay characteristics are also similar.

Correlation of Propulsion-Induced Lift Losses

The experimental results just presented were used to develop a correlation between the lift-loss curve and another parameter indicative of the dynamic-pressure decay. The parameter selected is the maximum slope of dynamic-pressure decay $\left[\frac{\partial(q_x/q_j)}{\partial(x/D_e)} \right]_{\max}$ divided by the distance downstream $(x/D_e)_i$ where that slope occurs. By using figure 8 for the jet dynamic-pressure decay characteristics and for the geometry of the configuration, the lift loss can be estimated from the equation given in the legend of figure 10. The correlation obtained is shown in figure 10.

It should be pointed out, however, that the dynamic-pressure decay parameter is quite sensitive to the fairing of the data. Unless the dynamic-pressure decay is well defined with an adequate number of data points, there may be some error in application of this procedure. It should also be noted that since the levels of lift loss tend to be small for most of the data presented, this potential error is not very serious. Subsequent investigations have shown that this type of correlation can be suitable for additional configurations (ref. 12). For these data, the effect of jet pressure ratio is included in the constant of proportionality between the two parameters.

Some information on the effect of nozzle shape on the rate of decay of dynamic pressure can be obtained from references 13 and 14, which present the results of investigations of the effect of nozzle shape on ground erosion. In general, an increase in the rate of decay of dynamic pressure reduces the potential for ground erosion. Results of these investigations relating nozzle shape and dynamic-pressure decay, presented in figure 11, indicate in general an increasing rate of dynamic-pressure decay with increasing nozzle perimeter per unit of exit area. This same trend is obtained with sound-suppressor nozzles (ref. 15) and nozzles designed to promote mixing of secondary and primary efflux from a turbofan engine (ref. 16). The purpose of presenting these data in figure 11 is to illustrate the conflicting requirements and conflicting solutions to problems that confront the designer of V/STOL aircraft. This example shows that a nozzle with a rapid rate of decay of dynamic pressure tends to reduce ground erosion and noise by promoting rapid entrainment of ambient air, but it has the undesirable feature of increased lift loss.

PROPULSION-INDUCED AERODYNAMIC EFFECTS ON V/STOL AIRCRAFT IN TRANSITION FLIGHT

The second part of this paper presents the jet-induced effects on the airplane in a cross wind out of ground effect. The aerodynamic interference effects experienced in the transition speed range between hovering and conventional flight have been the subject

of a large number of experimental investigations (refs. 17 to 21). Most of this research effort has been the investigation of the forces and moments induced on the aircraft by the interaction of the vertical jets with the free-stream air during transition flight.

During transition flight, the jets issuing from the aircraft are swept rearward by the free-stream flow and are rapidly rolled up in a pair of vortices (fig. 12). These rolled-up vortices induce suction pressures on the fuselage and a distribution of downwash over the aircraft. This downwash is in effect an induced twist on the wing and tail and an induced camber over the length of the airplane.

The general trend of these jet-induced effects is illustrated in figure 13. There is usually a loss in lift which tends to increase with increasing forward velocity. The loss in lift is about the same with the tail off the vehicle and with the tail on. There is an increment of nose-up pitching moment in transition flight which tends to increase with increasing velocity. Because of the change in downwash in the vicinity of the tail, an additional increment of pitching moment is induced when the tail is on.

Visualization of Transition Flow Phenomena

In this section, the flow phenomena involved in the transition problem are described. The shape of the jet wake when influenced by the free stream is presented in figure 14 from an experimental investigation (ref. 22) where the wake exits from the nozzle at a deflection angle (δ_j) to the free stream. As the wake exits from the jet nozzle, the free stream deflects the wake back until it tends to become parallel with the free-stream flow. As a result of this investigation, the empirical equation given in the legend of figure 14 was obtained. It describes the path of the jet as a function of the ratio of the free-stream dynamic pressure to jet dynamic pressure and as a function of the deflection of the jets.

By means of water-tunnel flow visualization, a more detailed look at the jet in the cross flow is presented in figure 15, which shows the flows induced in and around the jet. A flat plate is shown with the free stream from the left and a jet exhausting through the plate, perpendicular to the free stream. Near the leading edge of the plate are orifices through which colored milk is emitted. When the colored milk filament on the center line of the jet exit gets to the vicinity of the jet exit, it has a stagnation point near the front of the jet and then it is swept around the jet exit. The visible portion of the jet wake indicates that some of the milk flow from the free stream is sucked into the jet. The milk flow filament adjacent to the jet passes beside the jet and is then induced upward into the turbulent wake region behind the jet. Even the colored milk filaments farthest from the center line of the exit are sucked toward the jet and into the wake region. In the wake region, a considerable amount of entrainment into the jet can be seen.

Two photographs of oil flow on the surface of the plate are presented in figure 16. The lower one is a closeup view near the jet exit. There is a line trailing diagonally

back from the jet which bounds the wake region. Careful inspection of the streamlines on the surface reveals that the free-stream flow is deflected around the surface of the jet and into the bounding flow. In the wake region, the flow near the jet is entrained forward into the jet. Farther downstream of the jet exit, the wake flow is deflected away and carried off with the boundary of the wake on the surface of the plate.

The pressure distribution which is induced on the surface of the plate is illustrated in figure 17 (ref. 23). These particular data were obtained with the square root of the ratio of the free-stream dynamic pressure to jet dynamic pressure equal to 0.25. This parameter, called the effective velocity ratio, is 0.25 with a cold jet. Ahead of the jet, there is a region of positive pressure indicating a force augmenting the jet thrust. Adjacent to and aft of the jet, there is a negative pressure region which indicates a force opposing the jet thrust behind the jet. This is why a nose-up moment is induced by the jet wake interference. The area covered by negative pressure is noticeably larger than the area covered by positive pressure. This difference causes the lift loss. In the region aft of the jet near the center line, it is difficult to define the pressure contours. This is the wake region where there is the very turbulent, disturbed flow seen in figure 16.

Examples of Experimental Data Showing Induced Interference in Transition Flight

The data in figures 15 to 17 illustrate the pressures induced on the airplane in transition flight. In addition to this effect, there is a distribution of downwash on the aircraft. Results showing both effects on one experimental model are illustrated in figure 18 (ref. 24). The increment of interference lift divided by thrust is plotted as a function of the effective velocity ratio. Also presented is the increment of interference pitching moment divided by the product of thrust and effective nozzle diameter. Data for the airplane with all five jets operating show the expected increments of lift loss and nose-up pitching moment. With the front three lift jets operating alone, there is an increased lift loss and reduced pitching-moment increment. A similar test with the two lift-cruise jets operating alone shows contrasting results – an increase in both lift and pitching moment. The two lift-cruise jets in effect induce an increased angle of attack on the wing in addition to the pressures on the fuselage.

These results indicate that the induced interference effects could be reduced with proper location of the engines. A generalized investigation was undertaken to explore this possibility more systematically (ref. 25). This investigation used a wing-fuselage model that had an unswept, untapered wing with an aspect ratio of 6 and a 30-percent-chord slotted Fowler-type flap. The model was mounted on a sting with a strain-gage balance. Two jets, one on either side of the fuselage, were positioned spanwise at about

the 25-percent wing station and at various longitudinal and vertical positions shown by the plus marks in figure 19. The jets were mounted independently of the wing so that only the aerodynamic forces and interference effects were measured on the wing. These results show that with the exits on the wing-chord plane, considerable jet interference was experienced even with the jet as far as 4 chords ahead of the wing. Favorable interference effects, however, were encountered with the jets beneath and behind the 50-percent-chord point of the wing, and the interference effects were most favorable for positions closest to the flap. These data show general agreement with the results for the five-jet model in figure 18, with results reported in reference 26, with data obtained on a fan-in-wing configuration in reference 27, and with data reported in reference 28. These favorable interference increments indicate that the jet was probably helping the wing and flap achieve its full lift potential.

Examples of analytic approaches.- Efforts have been made to represent the jet wake analytically and then compute the interference effects. Figure 20 shows the wake portion of one representation used to describe a fan-in-wing configuration (refs. 29 and 30). The jet wake is deflected along a path given by the equation which was presented in figure 14 (from ref. 22). The wake itself is represented by a cylinder around this path. The cylinder has a constant cross section which is essentially circular. On this cross section there are eight dots that represent filaments of vorticity which run parallel to the jet path. Laterally across the path there are additional filaments of vorticity. All these filaments combine to form quadrilateral panels of vorticity on the surface of the jet. The boundary condition of flow tangent to these panels is maintained for the solution of the vorticity strength of the vortex filaments which describe the jet wake. Once the strengths of the vorticity have been established, the flow induced in the vicinity of the jet can be computed. In particular, the pressure coefficients on the surface of a vehicle from which the jet is exiting can be computed, and the pressure distributions on the surface can be estimated. One deficiency in this representation of a jet wake is the constant cross section.

Figure 21 is a photograph of the cross section of a real jet wake in a water tunnel. The white region at the top is the jet itself, and the white dots are air bubbles around the jet. The primary features are the swirl of the two elements of vorticity in this jet cross section and the fact that the cross section is kidney shaped. At the present time, work is being undertaken at the Langley Research Center to develop a more accurate representation of the wake cross section. Equations from reference 31 are being used to describe the cross-sectional shape of the jet. The results of this work are indicated by the cross sections presented in figure 22. The wake has a circular cross section at the jet exit, and the cross section deforms as the jet progresses downstream. Eventually it develops into the kidney shape shown in section C-C; farther downstream the kidney shape

becomes even more distorted. It is hoped that this presentation will provide a better estimate of the interference effects induced on a vehicle.

Induced transition effects on stability and control.- The jet-induced suction pressures described earlier act on the fuselage and wing undersurfaces. The moment induced by these pressures is essentially independent of angle of attack. Another aspect of this jet-induced interference is the downwash induced at the horizontal tail and over the wing. Figure 23 schematically illustrates the path of the vortex developed along the leading edge of the inboard portion of a highly swept wing. The vortex trails aft above the wing and the tail in cruise. In figure 24 the leading-edge vortex flow is seen clearly to go aft above the trailing edge of the wing. Transition is shown in figure 25 where the lift jets are operating, as indicated by the wakes. The effect of these lift jets is to pull the vortices above the wings down so that they sometimes interfere with the horizontal tail and cause trim changes and possibly some stability problems. The lift jets also reduce the lift of the airplane as described earlier. These effects can be seen in figure 26, a photograph taken in the water tunnel with the lift jet operating, where the flow of vorticity over the upper surface of the wing is now deflected down and actually goes aft below the trailing edge of the delta wing.

These photographs show that the downwash field induced by the lifting jets behind the wing depends to a large degree on the flow field generated by the parts of the aircraft ahead of the wing itself. Furthermore, unlike the moment on the wing-body from jet-induced suction pressures, the downwash behind the wing is a function of angle of attack and can, therefore, change both the trim and the stability of the tail-on configuration. As a result, the severity of the problem depends on many configuration variables, not all of which have been determined. A particularly severe example is presented in figure 27 for a four-jet configuration with a fixed forewing and large inlets placed well forward (ref. 32). With the power off, there is a linear and stable variation of pitching moment with angle of attack and a stable break at the stall. With the power on, there is a nose-up increment, but it is not invariant with angle of attack. It increases very rapidly as the angle of attack is increased and results in an extremely unstable configuration.

Data for two other configurations are shown in figure 28 (refs. 2 and 24). For the configuration with short inlets and no variable-sweep wing glove, the power effect on stability is essentially zero, as indicated by the fact that the two curves are nearly parallel. For the other configuration, which has long inlets and a fixed forewing, a reduction in stability due to power is encountered. However, it is not as severe as that shown for the configuration in figure 27. The most significant difference between the configurations appears to be the size and length of the lifting elements forward of the wing. The differences in tail length and tail configuration may also contribute to the differences in stability. The destabilizing influence of elements that carry lift and are located ahead

of the main wing has been described in reference 33. This effect can be seen by comparing the two power-off curves in figure 28. The primary point here is that the effects of power on longitudinal stability can be kept small.

Another aspect of the interference effects is the jet-induced effects on the lateral control characteristics. The jet-induced suction pressures which cause a nose-up pitching moment can also cause a rolling moment in a sideslipping condition. In figure 29, the effect of sideslip on rolling moment is presented. The sideslip angle resulting from an assumed 30-knot cross wind increases as the velocity decreases and would reach 90° at zero velocity. In the plot at the bottom of the figure, the rolling-moment parameter is plotted as a function of the velocity for a 30 000-pound airplane. The curve with the circles indicates the rolling moment that would be encountered. This rolling moment must be canceled by the control available, shown by the long-dash—short-dash curve. The control available at forward speeds is that due to the roll from the tip jets plus the rolling moment obtained from the aerodynamic control surfaces on the airplane. The lower speed range, where the induced moments are quite large, is most critical, as can be seen by comparing the control-required curve with the hover control that would be provided for an airplane of this size. This available hover control, shown by the diamond, corresponds to a rolling acceleration of $1.2 \text{ radians/second}^2$ and is supplied by roll jets near the wing tips. Unfortunately, the amount of roll control available from the tip jets decreases with increasing speed because of the interference effects between the jets and the wing area surrounding them (ref. 34). For the configuration shown, the total control available is slightly greater than that required, but there is little margin for complacency. Obviously, operation in cross winds is undesirable, but not always avoidable. When an airplane is close to the ground, a pilot tends to sense velocity and direction with respect to the ground and can thus lose track of the direction of the approaching wind. The point is that these rolling moments can be quite large and must be accounted for in the design of the airplane.

HOT-GAS INGESTION

Hot-gas ingestion is a serious problem for jet V/STOL aircraft when operating near the ground. Hot-gas ingestion is the taking into the engine inlet of the hot exhaust gases or air heated by the exhaust. It should be emphasized that the problem is not the ingestion of contaminated air, but the elevated temperature of the inlet air.

The general flow patterns that cause hot-gas ingestion are shown in figure 30. In still air, the exhaust gases that strike the ground and spread outward to the far field present very little problem since the gases will be cooled before they are recirculated back to the inlets. The multiple-jet configuration in figure 30, however, can have a serious problem with the fountain of hot gases that occurs beneath the aircraft when the exhausts

of widely spaced engines collide after striking the ground. These rapidly flow upward around the fuselage and reach the vicinity of the inlets while the gases are still hot. The other configuration in figure 30 has a single engine or closely grouped cluster of engines which would be expected in still air to result in low inlet temperatures, since the exhaust would be blown far away. With wind, however, the exhaust gases are blown back toward the inlet and ingested. This effect can result in very high inlet air temperatures.

Hot-gas ingestion is a serious problem for jet V/STOL aircraft. Hot-gas ingestion causes a thrust loss; for example, an inlet temperature rise of about 40° F (22° C) would result in a 15-percent thrust loss. However, it should be noted that much higher temperature rises and, as a result, greater thrust losses occur in some of the subsequent figures. Another reason for concern is that the engine compressor may stall as a result of rapid increase in inlet air temperature or as a result of uneven distribution of temperature across the engine face. In summary, some of the factors that cause hot-gas ingestion are the fountain effect, surface winds, and configuration effects, in particular, the location of the inlets and exhausts.

Hot-Gas Ingestion Investigations

Although hot-gas ingestion has long been recognized as a serious problem, until recently very little systematic research of a generalized nature had been done. In 1965, the National Aeronautics and Space Administration initiated some projects to study the problem in detail. Illustrated in figure 31 are two large-scale models. One model was tested at the Ames Research Center in cooperation with the Northrop Corporation (ref. 35) and the other model was tested at the Langley Research Center (ref. 36). In addition to these projects, several models were tested by Bell Aerosystems Company, including a small-scale version of the Langley model (refs. 37 and 38). In other Ames investigations, described in references 39 and 40, a half-scale model representing a high-performance V/STOL lift-engine fighter airplane was used. A German facility for small-scale model tests is described in reference 41.

To illustrate the problem of hot-gas ingestion, results from the large-scale tests at Langley are presented here. Most of the material is taken from references 3 and 4. Sketches of the hot-gas ingestion model in figure 32 show the exit arrangements for the nozzles as well as the inlet arrangement. One pattern has four exits in a rectangular arrangement at the base of the fuselage, the in-line pattern has four exits along the center line of the fuselage, the third configuration has a single exit located at the center of gravity, and finally, there is a side-exit configuration similar to the P. 1127 airplane nozzle arrangement. It should be noted that this last configuration has hot exhaust from all four nozzles, in contrast to the P. 1127, which has only two rear nozzles with hot gases. These arrangements were tested with scoop inlets in front (as in fig. 32) and also

with inlets at the top of the fuselage. In addition to these configuration variables, the models were tested for a range of nozzle heights above the ground and for several velocities of head winds and side winds. Because it was realized that the problem of hot-gas ingestion would be highly time dependent, the data acquisition system used 36 high-response thermocouples in the inlets to record temperatures. The data were in the form of time histories on oscillograph records.

Some method was needed to duct the hot gases away from the model during the starting cycle to prevent ingestion from occurring before the test was started. This problem would also exist for an actual airplane. After discussions with several researchers, including NASA VTOL pilots, the investigator decided to conduct the tests in the following manner:

The engines would be started and brought to about 80 percent rpm with the exhaust nozzles deflected 25° rearward. This prevented early ingestion and provided a time zero for the test. At this point, the nozzles were deflected straight down, followed by a 3- to 4-second pause to simulate time for the final pilot checkout. Then the throttle was quickly advanced to full rpm. The tests continued for 5 to 10 seconds following full rpm and then shut down.

A typical time history is presented in figure 33. For clarity, only two temperature traces and one nozzle-pressure trace are shown. The temperature data are for the left-hand side inlet with a rectangular exit-nozzle configuration. There are three points that should be emphasized. First, the inlet temperatures are very high. It is not known exactly how much thrust loss is caused by these high temperatures, but the pressure trace indicates that after the 3- or 4-second pause for pilot checkout the engine is operating at only about half of normal thrust. The second thing to note is that the temperatures increase very quickly and are very unsteady. These rapid changes in temperature can cause compressor stall. The final thing to note is the large temperature variation across the face of the engine, as indicated by the difference in the two temperature traces. This temperature distortion can cause compressor stall.

Hot-Gas Ingestion Due to the Fountain Effect

The fountain effect illustrated in figure 34 exists with multiple-nozzle configurations. The fountain of high-temperature air between the nozzles flows upward rapidly and is ingested by the inlets.

Some data illustrating this problem are shown in figure 35, where inlet temperature rise is plotted as a function of nozzle height above the ground. The first plot shows the data for the model with inlets on top; the second plot shows the data for the side

inlets. For the single-nozzle arrangement in both cases, there are relatively low levels of temperature rise. In other words, with the single nozzle there is no fountain. With in-line nozzles, the jets are very close together. As a result, the upflow is not significant, and the inlet temperature rises are small. However, with the rectangular nozzle arrangement and with four nozzles on the sides of the fuselage, there are fairly large temperature rises in the inlets.

In addition to the obvious configuration variables of inlet and nozzle arrangement, the placement of the wing on the fuselage was found to be an important parameter. The effect of wing height on the temperature rise of the top inlets for the rectangular and the in-line nozzle arrangements with a zero wind condition is shown in figure 36. Inlet temperature rise is shown as a function of model height above the ground in equivalent nozzle diameters. The wing in a low position is seen to greatly reduce the inlet air temperatures at all test heights of the rectangular nozzle configuration, but has little effect on the in-line nozzle configuration, which has very low inlet air temperatures with both wing positions. Observations of smoke from the exhaust nozzles indicated that the low wing caused the upward-flowing hot gases to be deflected outward and away from the inlets. These effects are discussed in more detail later in a section entitled "Characteristics of the Upflow from a Square Pattern of Nozzles."

Hot-Gas Ingestion Due to a Cross Wind

Hot-gas ingestion caused by the cross wind is considered next. In figure 37, there is an illustration of a jet engine operating, the hot gases flowing outward, and then at some distance away from the engine, the wind deflecting these hot gases back into the inlet. The rapidity with which this occurs is shown in figure 38 by a sequence of photographs of the hot-gas cloud from an engine operating at full power. The aircraft has a single nozzle exit and a single inlet in the top and is operating in a 5- to 8-knot cross wind. At time zero, the nozzle is deflected straight down from an initial rearward deflection of 25° and oil is injected into the hot exhaust jet to produce smoke. At a time 0.2 of a second later, the smoke is progressing outward. At 0.4 of a second later it starts to rise, and at 0.6 of a second later the cross winds are starting to blow it back to the vehicle. By the time 1 second has elapsed, the vehicle is practically immersed in the exhaust gas. This rapid temperature rise tends to cause compressor stall, which may be a more serious problem than the maximum level of temperature.

A summary plot of the data obtained with a range of head winds is presented in figure 39. The inlet temperature-rise data are plotted as a function of wind speed; in the first plot, the data are for the model with the top inlets, and in the second plot, for the model with the side inlets. The single-jet arrangement, which before showed very little temperature effect, now causes a noticeable temperature rise in the top inlet and quite a disastrous temperature rise in the side inlets. The in-line nozzle arrangement still

causes fairly low temperature rises in the top inlets. However, at a speed of 20 knots with the side inlets, the in-line arrangement causes significant rises. The rectangular nozzle arrangement with either the top inlets or the side inlets causes high inlet temperature rises for speeds up to 30 knots. For the side exits, which were tested only with the side inlets, the inlet temperature rise is high with no head wind (a rise of about 60° F or 33° C). It then drops off rapidly and reaches 0° at a wind speed of 15 knots.

These and other data are summarized in figure 40. Results are presented for the basic configurations of the Langley model with side inlets – the single exit, the in-line nozzles, the pattern of rectangular nozzles, and the side nozzles. The first two arrangements show very little temperature rise with no wind, but the second two arrangements show significant temperature rises with no wind. For comparison, results from the Ames-Northrop model are indicated at the bottom of the figure for the no-wind case. On this configuration, both the lift engine inlets in the front and the lift-cruise engine inlets at the rear experienced noticeable temperature rises. With either a head wind or a side wind, all four of the Langley configurations have a significant problem with inlet temperature rise.

The Impact of Hot-Gas Ingestion

It can readily be seen that some arrangements are more ingestion-prone than others, but when one considers all possibilities of wind and configuration, hot-gas ingestion problems seem to be unavoidable. The inlet temperature rise as a function of forward speed, presented in figure 39, showed that the ingestion rapidly decreased toward no ingestion with speeds of 30 knots or greater. This fact suggests a take-off technique that has been proposed many times and has come to be called rolling vertical take-off. This is illustrated in figure 41. It is assumed that the aircraft can be turned into the wind with the nozzles deflected rearward to prevent ingestion during start and check-out. The power is increased until the brakes can no longer hold, and as the brakes are released, full throttle is applied. When the speed required to prevent ingestion is reached, the nozzles are rotated downward, and the aircraft takes off. In order to illustrate this rolling vertical take-off and to see how vertical this procedure really is, calculations were made of take-off profiles of two configurations.

The calculations were made for side and rectangular nozzle configurations for thrust-weight ratios of 1.05 and 1.10. An important difference between these configurations is that the nozzles of the side arrangement could be deflected directly rearward for maximum acceleration, while the nozzles of the rectangular configuration could be rotated rearward only about 25°. The lift-off speeds were determined from the minimum speed required to avoid any hot-gas ingestion from any wind direction. In reality, these estimates may be too conservative. However, there is a fundamental problem involved which

has not been worked on. We do not know what levels of hot-gas ingestion can be tolerated by the engine. The take-off distances are quite long, from 300 to 500 feet to clear a 50-foot obstacle. It is certainly questionable whether these should be classed as vertical take-offs.

Of course, all of this does not mean that jet aircraft cannot land and take off vertically. This type of operation can be performed. What it does mean is that there are some operating conditions of each configuration that result in low to no ingestion, but if all the possible operating conditions that have to be contended with are considered, then all configurations at some time will experience the problem of hot-gas ingestion. Several European investigators have been using raised porous gratings to operate with some degree of success, but this solution has the serious drawback of limiting operation to places that have these platforms.

In summary, it should be stated that hot-gas ingestion is a very serious problem for jet VTOL aircraft. A great deal is known about the flow fields and causes of ingestion, and results of current investigations using small-scale models will add further to this knowledge. It is believed, however, that more work will be required before the ingestion characteristics of a particular configuration can be predicted accurately. Even then, the ingestion problem will not be solved.

PROPULSION-INDUCED EFFECTS DURING HOVER IN GROUND EFFECT

There are propulsion-induced effects when a jet-lift aircraft is hovering in ground effect. Figure 42 shows schematically how the ambient air is entrained around the lower surface of the vehicle into the jet; it then strikes the ground and flows outward as a wall jet. The entrainment induces a download on the vehicle. These phenomena are well understood for the case of a single jet. Downloads can be calculated by using the empirical methods of L. A. Wyatt (ref. 42). The data shown in figure 43 are for the X-14A airplane, which has two jets placed close together under the center of gravity. They are close enough together to be considered a single jet. The full-scale and model data are in good agreement with the calculation.

Unfortunately, the phenomena for the multiple-jet case are not so well understood. In figure 42 the flow characteristics of the single jet are contrasted with the flow of the multiple jet. The primary difference is the fountain of hot gas between the two jets. This upflow between the jets causes large positive pressures on the lower surface of the fuselage. There is also a circulatory flow between the jets and the fountain. To get a better understanding of this fountain effect, the results of some investigations of the upflow are presented in the following sections.

Characteristics of the Upflow From a Pair of Nozzles

The results of some work done in Germany by Hertel (ref. 43) are presented in figure 44. The sketch shows the two nozzles exhausting near the ground with an upflow. Starting at the center line between the two jets, the velocity of the upflow was measured with both jets operating; these results are indicated by the circles. There is a gradual dropoff in the upflow velocity from the line of symmetry. Then a reflection plane was placed at the plane of symmetry. The velocities were measured and plotted as the triangles. There is a large upflow velocity at the line of symmetry which drops off sharply. This shows that the use of a vertical reflection plane is not appropriate for measuring data with jets in ground effect. Further, the results show that there is not a true line of symmetry; instead, there is quite a bit of mixing and interaction between the upflows from the two jets.

The reflection plane also has an effect on the inlet temperature rise. Data obtained by Bell Aerosystems Company (ref. 38) with their small-scale hot-gas ingestion model are presented in figure 45 to show this effect. The two jets, impinging on the ground with a fountain between them, are moved from a height of 2 diameters from the ground to a height of 10 diameters above the ground. When no reflection plane is located between the two jets, the inlet temperature rise is large at a height-diameter ratio of 2. It drops off sharply and approaches zero at a height-diameter ratio above 10. In contrast, with the reflection plane, there is a temperature rise of about 30° F (17° C) close to the ground, which increases steadily as the inlets move away from the ground. When the nozzles are close to the ground, high velocities on the reflection plane carry the gases up above the inlet and disperse them away from the inlet. Consequently, inlets near the ground are not influenced by the hot gases when the reflection plane is in place. As the exits of the jets are moved away from the ground, the inlets gradually move into the region where these hot gases are carried up, furnishing results in sharp contrast to the data without the reflection plane. Figures 44 and 45 indicate the importance of the modeling techniques used in investigating these problems.

The flow pattern from a pair of vertical jets above a horizontal ground plane with equal nozzle pressure ratios (ref. 44) is presented in figure 46. The flow on the ground plane, the bottom half of the photograph, is away from the jet pair in the form of a wall jet reinforced to form a large roach in the plane of symmetry between the pair of jets. In the vertical plane, the flow may be divided into two zones. The zone outboard of the nozzles is very similar to the wall jet arising from the interaction of a single jet with a normal plane. The second zone is the flow between the jets. Its major features are the large upflow of the fountain and the two rather large counter-rotating vortices. The impinging flow from the two jets is forced upward into the fountain, but a strong entrainment from the jet wakes causes much of this flow to double back and form the vortices.

Some of the flow, however, carries on upward, where it eventually meets a downflow moving toward the inlets and is bent back downward. The stagnation region formed in the plane of symmetry is very unstable, as illustrated previously in figures 44 and 45.

A dramatic change takes place in this flow pattern with the introduction of asymmetry in the configuration. The nozzles have been canted about 6° from the vertical in figure 47. The flow on the ground plane is largely unchanged except for the curved path of the roach from the plane of symmetry. In the vertical plane, the left vortex has opened out, and the flow comprising it is now partially drawn into the right jet wake. The right vortex has become tightly wound very near the right jet wake. Of major significance in this asymmetric configuration is the direction of the flow between the jets, which is now downward because of the viscous entrainment of the free air by the flow between the jets. A similar asymmetric flow structure occurs with vertical jets if there are small differences in the two nozzle pressure ratios. The inlet temperature rise experienced with these asymmetric flows is considerably reduced from the levels experienced with the symmetric flow situation in figure 46.

Characteristics of the Upflow From a Square Pattern of Nozzles

The upflow characteristics from a square pattern of jets hovering in ground effect was examined by Hertel (ref. 43). The velocity contours obtained in the exit plane are shown in figure 48. The contours in the center of the jet pattern represent the highest velocities; successive planes of lower constant velocity are indicated at increasing distances from the center of the jet pattern. To compare the results for different model configurations, Hertel integrated the mass flow and velocities in these contours to get an upflow impulse – essentially, a thrust type of expression to represent the energy contained in this upflow. The upflow velocity contours were investigated for square jet arrangements located various distances apart as illustrated in figure 49. A cylindrical body between the jets was included to represent a fuselage. In addition to varying the jet spacing by changing the distance l between the jets, the relation of the fuselage diameter to the jet exit diameter was varied. The key gives the values of these two variables: the spread of the jet exits l/D and the size of the fuselage between the jets d/D . The upflow impulse is nondimensionalized by the combined thrust of the four jets and plotted as a function of the height above the ground divided by the spread of the jets in the pattern. The shaded area represents the band of results. With these parameters, the upflow energy contained in the fountain is indicated.

Several regions of ground effect can be inferred from these data. One region exists when the ratio of height to spread h/l is greater than 3. This might exist for two different conditions: (1) near the ground when the spread is small, as with a single jet or a tight cluster of jets; (2) when the height is large with any pattern of jets. In this first

region a downward flow exists in the vicinity of the airplane, and causes a lift loss. A second region exists for a ratio of height to spread between 1 and 3. Here the upflow velocity increases with decreasing values of the ratio of height to spread. A third region exists for configurations which experience the entire range of h/l between 0 and 3. This might apply over a wide range of ground heights for configurations with a large spread of the jet exits or for most multiple-jet configurations over a limited range of heights near the ground. This range of conditions causes the airplane to experience large fluctuations in the patterns of upflow velocity. Results of investigations in references 36 and 38 on the effect of aircraft configuration changes on hot-gas ingestion with a given nozzle arrangement show that the results are sensitive to height above the ground. In general, if the wing, strake, or other surface on the airplane deflects the upflow outward or downward with sufficient velocity to direct the flow away from the airplane, beneficial effects may occur which can influence the aerodynamic lift or perhaps reduce hot-gas ingestion. If, however, the upflow is redirected with a low velocity, it tends to flow around the deflecting surface and continues to drift upward with little or no beneficial effect.

Some of the effects of the fuselage on the upflow impulse have been examined in reference 43 and are presented in figure 50. Four jets are arranged in a square pattern measuring 12 nozzle diameters on a side. Results showing the effect of a cylindrical fuselage located between the jets are presented, along with results showing the effect of adding strakes to the fuselage. When the four jets are operating without the fuselage, a very large upflow impulse exists in the exit plane of the jets at all heights up to $h/D = 20$. With the fuselage in place, the upflow impulse has been reduced noticeably in the vicinity of $h/D = 5$. However, at higher values of h/D the upflow impulse rapidly goes back to the level it had without the fuselage. These results indicate that the flow is not stopped by the fuselage, but is diverted around it and upward. Then data are presented for the fuselage fitted with strakes which are rather long and have a width of about 10 percent of the diameter of the fuselage. The data show that at heights above 4 diameters these large strakes are effective in reducing the upflow from the fountain. As described earlier, this has important implications for hot-gas problems in hover near the ground. The results also indicate that the fuselage might be feeling a lift force because the strakes are redirecting the upflow.

Aerodynamic Lift Loss for Multiple-Jet Configurations

The aerodynamic lift loss for many multijet configurations in ground effect has been investigated experimentally (refs. 1, 2, 5 to 11, and 45 to 48). While the story is not as clear for the multiple jets as for the single jet at this time, an interesting trend can be seen in figure 51. These data are based on a systematic investigation of a delta wing and body combination (wing in a middle position) with several different arrangements

of multiple jets, reported in reference 48, and are consistent with results in figures 49 and 50. The ratio of interference lift to thrust is plotted as a function of height of the fuselage lower surface above the ground, expressed in equivalent nozzle diameters. The basic configuration consisted of four engines arranged in a cluster near the center of the wing-body. The single-jet configuration was obtained by ejecting air from the right rear nozzle only, and the results are indicative of the general trends previously shown for single jets. The two rear jets were also tested together. These jets were spaced farther apart than those of the X-14A airplane which was shown in figure 43. As a result, these data show a reversal of the lift loss due to ground at very low heights. When the number of jets is increased to four, the lift losses become smaller. When the spacing between the jet exits is increased, as shown by the other two four-jet configurations, the jets have a favorable effect on lift at heights above approximately 2 effective diameters. The trend of these results is consistent. For a given range of heights, there is a reduction of lift loss with a multiple-jet engine as the exits are spaced farther apart and thus enlarge the model area that experiences favorable pressures from the fountain of jet gases reflected up from the ground. However, this increase in spacing would be expected to aggravate the hot-gas ingestion problem because of a reduction in shielding of the inlets and the higher sensitivity to cross winds.

Another factor influencing the lift loss of multiple-jet configurations near the ground is the lateral deflection angle or cant of the nozzles. The ground effect on a model having either a single row of jets in the fuselage or a rectangular array of jets with and without outboard cant is presented in figure 52 (from ref. 4). The model had a low wing with an aspect ratio of 5.8, a taper ratio of 0.32, and a quarter-chord sweep of 28.2° . The lift loss due to ground effect is divided by the thrust and plotted as a function of ground height divided by equivalent nozzle diameter. The loss is less with the rectangular array than with the single row of jets, and an additional benefit can be realized by canting the nozzles outboard 10° from the vertical. This effect is similar to an increase in jet spacing as shown in figure 51, since canting the engines increases the spacing of the jet impingement on the ground. The effect of canting the engines on the hot-gas reingestion is unknown at this time, but indications are that engine canting will have some unfavorable effects.

Only the general trends of lift interference by multiple jets near the ground have been illustrated in figures 51 and 52. The results for many different multiple-jet configurations have been documented (refs. 45 to 48). They indicate that the magnitude of lift interference due to ground effect in hovering flight is dependent on the model configuration as well as the nozzle arrangement. Therefore, in spite of the fact that these two sets of data seem to show consistent trends, attempts to correlate the effect of ground on the interference lift for multiple-jet configurations has not as yet produced acceptable results.

CONCLUDING REMARKS

The material presented in this review paper has concentrated on several aspects of the induced effects on aircraft aerodynamics in hover and transition flight which are caused by the interference of wakes from relatively high-disk-loading V/STOL propulsion devices. Only a few of the major factors discussed are emphasized below to illustrate the conflicts among the spectrum of design requirements facing the airplane designer or to illustrate the state of the art of the solutions to some of the problems.

The first part of this paper described in detail the lift losses sustained by a VTOL hovering out of ground effect. It was shown that minimum losses in lift are obtained from lifting propulsion devices which maintain their maximum jet dynamic pressure for large distances (4 to 6 nozzle diameters) away from the nozzle exit. However, a rapid reduction in jet dynamic pressure with distance from the nozzle exit is desired to reduce the adverse effects caused by hot-gas ingestion and ground erosion and to promote sound suppression and mixing of primary and bypass air in a turbofan engine.

The problem of V/STOL transition out of ground effect to wingborne forward flight has been examined in many experimental investigations. Although the general trends are understood, the problem of estimating the propulsion-induced interference effects on a specific configuration is not well understood. Some efforts are being made to represent analytically the jet wake in a cross wind and to derive a procedure for estimating the jet-induced forces and moments. Further work in this area is required to develop the required generalized design methods.

Next, the hot-gas ingestion problem was presented. This is a very serious one for jet VTOL aircraft. A great deal is known about the flow fields from the engine nozzles and about the causes of ingestion. Experiments are being made with small-scale models to further this knowledge. It is believed, however, that more work will be required before the ingestion characteristics of a particular configuration can be accurately predicted. Even then, the ingestion problem will not be solved. It appears, for the present time at least, that the only sure cure for this hot-gas ingestion problem, for all operating conditions, is to make rolling vertical take-offs.

In the final section of the paper, some of the aerodynamic characteristics of jet VTOL hovering near the ground were discussed. The fountain effect which is obtained with multiple-jet configurations was emphasized in the discussion. Some detailed studies

of these flows were presented along with their effects on lift. It was emphasized that there is a strong connection between the fountain effect and hot-gas ingestion by multiple-jet configurations.

Langley Research Center,
National Aeronautics and Space Administration,
Langley Station, Hampton, Va., October 27, 1969.

REFERENCES

1. Hammond, Alexander D.: Thrust Losses in Hovering for Jet VTOL Aircraft. Conference on V/STOL and STOL Aircraft, NASA SP-116, 1966, pp. 163-176.
2. Margason, Richard J.: Jet-Induced Effects in Transition Flight. Conference on V/STOL and STOL Aircraft, NASA SP-116, 1966, pp. 177-189.
3. McLemore, H. Clyde: Considerations of Hot-Gas Ingestion for Jet V/STOL Aircraft. Conference on V/STOL and STOL Aircraft, NASA SP-116, 1966, pp. 191-204.
4. Hammond, Alexander D.; and McLemore, H. Clyde: Hot-Gas Ingestion and Jet Interference Effects for Jet V/STOL Aircraft. Integration of Propulsion Systems in Airframes, AGARD Conf. Proc. No. 27, Sept. 1967, pp. 8-1 - 8-27.
5. Kuhn, Richard E.: Technological Gaps in V/STOL Development. Paper presented at the University of Tennessee Space Institute Short Course "Modern Developments in Low Speed Aerodynamics With Application to VTOL," Tullahoma, Tenn., Sept.-Oct. 1967.
6. Schwantes, E.: Survey of the Ground Effect of V/STOL Aircrafts With Jet Propulsion - Report of Literature. NASA TT F-12,573, 1969.
7. Seidel, M.: Der Einfluss eines geneigten Strahles auf das Strömungsfeld in der Umgebung eines Leitwerks sowie auf dessen Luftkraftbeiwerte - Teil II: Literaturübersicht. DFL-Ber. Nr. 0532, 1969.
8. Skifstad, J. G.: Aerodynamics of Jets Pertinent to VTOL Aircraft. AFAPL-TR-69-28, U.S. Air Force, Mar. 1969.
9. Carrière, Pierre: Effets de l'Écoulement Interne sur le Comportement Aérodynamique d'un Avion a Réaction. (Effects of Internal Flow on the Aerodynamic Behavior of a Jet Aircraft.) ICAS Paper No. 68-03, Sept. 1968. (Also available in English translation as publication B-798, The Boeing Co.)
10. Gentry, Garl L.; and Margason, Richard J.: Jet-Induced Lift Losses on VTOL Configurations Hovering In and Out of Ground Effect. NASA TN D-3166, 1966.
11. McLemore, H. Clyde: Jet-Induced Lift Loss of Jet VTOL Configurations in Hovering Condition. NASA TN D-3435, 1966.
12. Shumpert, P. K.; and Tibbetts, J. G.: Model Tests of Jet-Induced Lift Effects on a VTOL Aircraft in Hover. NASA CR-1297, 1969.
13. Higgins, C. C.; and Wainwright, T. W.: Dynamic Pressure and Thrust Characteristics of Cold Jets Discharging From Several Exhaust Nozzles Designed For VTOL Downwash Suppression. NASA TN D-2263, 1964.

14. Higgins, C. C.; Kelly, D. P.; and Wainwright, T. W.: Exhaust Jet Wake and Thrust Characteristics of Several Nozzles Designed for VTOL Downwash Suppression – Tests In and Out of Ground Effect With 70° F and 1200° F Nozzle Discharge Temperatures. NASA CR-373, 1966.
15. Kuhn, Richard E.: An Investigation to Determine Conditions Under Which Downwash From VTOL Aircraft Will Start Surface Erosion From Various Types of Terrain. NASA TN D-56, 1959.
16. Hartmann, A.: Theoretical and Experimental Investigation on Fanengines With Mixing; Optimal Layout of Fanengines With and Without Mixing. AIAA Paper No. 67-416, July 1967.
17. Spreemann, Kenneth P.: Investigation of Interference of a Deflected Jet With Free Stream and Ground on Aerodynamic Characteristics of a Semispan Delta-Wing VTOL Model. NASA TN D-915, 1961.
18. Otis, James H., Jr.: Induced Interference Effects on a Four-Jet VTOL Configuration With Various Wing Planforms in the Transition Speed Range. NASA TN D-1400, 1962.
19. Vogler, Raymond D.: Surface Pressure Distributions Induced on a Flat Plate by a Cold Air Jet Issuing Perpendicularly From the Plate and Normal to a Low-Speed Free-Stream Flow. NASA TN D-1629, 1963.
20. Vogler, Raymond D.: Interference Effects of Single and Multiple Round or Slotted Jets on a VTOL Model in Transition. NASA TN D-2380, 1964.
21. Davenport, Edwin E.; and Kuhn, Richard E.: Wind-Tunnel-Wall Effects and Scale Effects on a VTOL Configuration With a Fan Mounted in the Fuselage. NASA TN D-2560, 1965.
22. Margason, Richard J.: The Path of a Jet Directed at Large Angles to a Subsonic Free Stream. NASA TN D-4919, 1968.
23. Bradbury, L. J. S.; and Wood, M. N.: The Static Pressure Distribution Around a Circular Jet Exhausting Normally From a Plane Wall Into an Airstream. C.P. No. 822, Brit. A.R.C., 1965.
24. Margason, Richard J.; and Gentry, Garl L., Jr.: Aerodynamic Characteristics of a Five-Jet VTOL Configuration in the Transition Speed Range. NASA TN D-4812, 1968.
25. Carter, Arthur W.: Effects of Jet-Exhaust Location on the Longitudinal Aerodynamic Characteristics of a Jet V/STOL Model. NASA TN D-5333, 1969.

26. Williams, John; and Wood, Maurice N.: Aerodynamic Interference Effects With Jet-Lift V/STOL Aircraft Under Static and Forward-Speed Conditions. Tech. Rep. No. 66403, Brit. R.A.E., Dec. 1966.
27. Hickey, David H.; Kirk, Jerry V.; and Hall, Leo P.: Aerodynamic Characteristics of a V/STOL Transport Model With Lift and Lift-Cruise Fan Power Plants. Conference on V/STOL and STOL Aircraft, NASA SP-116, 1966, pp. 81-96.
28. Seidel, M.: Der Einfluss eines geneigten Strahles auf das Strömungsfeld in der Umgebung eines Leitwerks sowie auf dessen Luftkraftbeiwerte – Teil I: Versuchseinrichtung, Vorversuche und Kraftmessungen mit horizontalem und vertikalem Strahl. DFL-Ber. Nr. 0487, 1968.
29. Rubbert, P. E.; and Saaris, G. R.: A General Three-Dimensional Potential-Flow Method Applied to V/STOL Aerodynamics. [Preprint] 680304, Soc. Automot. Eng., Apr.-May 1968.
30. Rubbert, P. E.; Saaris, G. R.; Scholey, M. B.; Standen, N. M.; and Wallace, R. E.: A General Method for Determining Aerodynamic Characteristics of Fan-In-Wing Configurations. Vol. 1 – Theory and Application. USAAVLABS Tech. Rep. 67-61A, U.S. Army, Dec. 1967.
31. Chang-Lu, Hsiu-Chen: Aufrollung eines zylindrischen Strahles durch Querwind (Rollup of a Cylindrical Jet in a Crosswind). Doctorial Dissertation, Univ. of Göttingen, 1942.
32. Vogler, Raymond D.; and Kuhn, Richard E.: Longitudinal and Lateral Stability Characteristics of Two Four-Jet VTOL Models in the Transition Speed Range. NASA TM X-1092, 1965.
33. Alford, William J., Jr.; and Harris, Roy V., Jr.: Cruise Performance and Stability Considerations for Jet V/STOL Aircraft. Conference on V/STOL and STOL Aircraft, NASA SP-116, 1966, pp. 139-161.
34. Spreemann, Kenneth P.: Free-Stream Interference Effects on Effectiveness of Control Jets Near the Wing Tip of a VTOL Aircraft Model. NASA TN D-4084, 1967.
35. Lavi, Rahim; Hall, Gordon R.; and Stark, Wilbur W.: Full-Scale Ground Proximity Investigation of a VTOL Fighter Model Aircraft. NASA CR-1098, 1968.
36. McLemore, H. Clyde; and Smith, Charles C., Jr.: Hot-Gas Ingestion Investigation of Large-Scale Jet VTOL Fighter-Type Models. NASA TN D-4609, 1968.

37. Speth, Robert F.; and Ryan, P. E.: A Generalized Experimental Study of Inlet Temperature Rise of Jet V/STOL Aircraft in Ground Effect. Rep. No. 2099-928003 (Contract No. N600(19)63320), Bell Aerosyst. Co., Apr. 5, 1966. (Available from DDC as AD 641 610.)
38. Ryan, Patrick E.; Heim, Richard J.; and Cosgrove, Wayne J.: A Generalized Experimental Investigation of Hot Gas Recirculation and Ingestion for Jet VTOL Aircraft. NASA CR-1147, 1968.
39. Kirk, Jerry V.; and Barrack, Jerry P.: Reingestion Characteristics and Inlet Flow Distortion of V/STOL Lift Engine Fighter Configurations. AIAA Paper No. 68-78, Jan. 1968.
40. Barrack, Jerry, P.; and Kirk, Jerry V.: Low-Speed Characteristics of High-Performance Lift-Engine V/STOL Aircraft. [Preprint] 680644, Soc. Automot. Eng., Oct. 1968.
41. Dissen, H.; and Schwantes, E.: Versuchsanlage für Bodeneffekt-Untersuchungen bei Kurz- und Senkrechtstartern. (Experimental Plant for Investigations of Ground Effects on V/STOL Aircraft.) DLR-Mitteilung 68-29, 1968.
42. Wyatt, L. A.: Static Tests of Ground Effect on Planforms Fitted With a Centrally-Located Round Lifting Jet. C.P. No. 749, Brit. A.R.C., 1964.
43. Hertel, Heinrich: Wandströmungen und Aufströme aus der Umlenkung von Freistrahlguppen (Wall Flows and Up-Streams Due to the Diversion of Free Jet Groups). Fortschritt Berichte VDI Zeitschrift Fortschr., vol. 12, no. 11, pp. 1-72, July 1966.
44. Hall, Gordon R.; and Rogers, Kenneth H.: Recirculation Effects Produced by a Pair of Heated Jets Impinging on a Ground Plane. NASA CR-1307, 1969.
45. Spreemann, Kenneth P.; and Sherman, Irving R.: Effects of Ground Proximity on the Thrust of a Simple Downward-Directed Jet Beneath a Flat Surface. NASA TN D-4407, 1958.
46. Davenport, Edwin E.; and Spreemann, Kenneth P.: Thrust Characteristics of Multiple Lifting Jets in Ground Proximity. NASA TN D-513, 1960.
47. Vogler, Raymond D.: Ground Effects on Single- and Multiple-Jet VTOL Models at Transition Speeds Over Stationary and Moving Ground Planes. NASA TN D-3213, 1966.
48. Seibold, Wilhelm: Untersuchungen über die von Hubstrahlen an Senkrechtstartern Erzeugten Sekundärkräfte. Jahrb. 1962 WGLR.

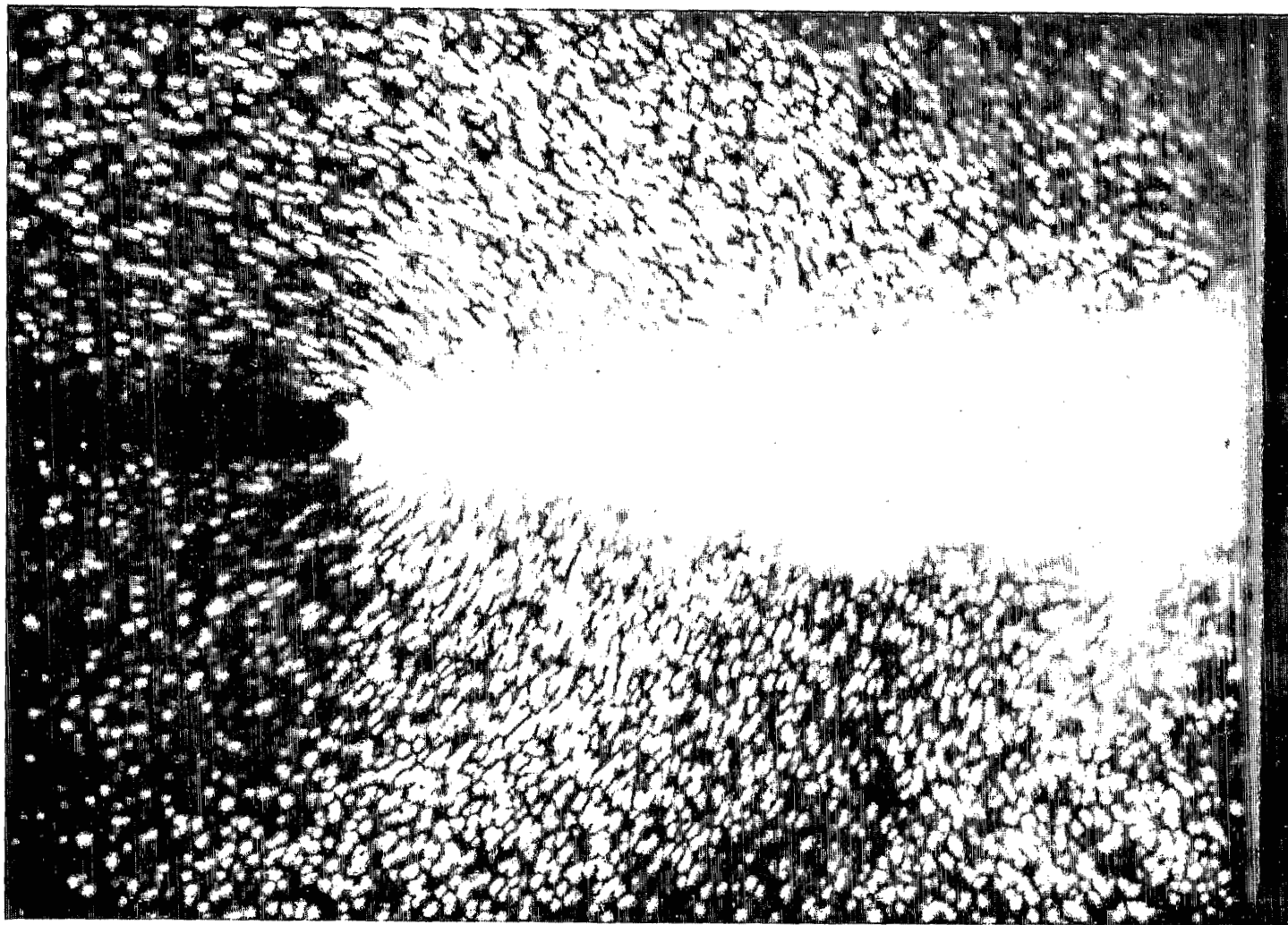


Figure 1.- Photograph of a jet in a water tunnel illustrating with air bubbles the "douche" effect -- entrainment of air from quiescent surroundings. (Photograph from O.N.E.R.A. Film No. 575, "Flows With Large Velocity Fluctuations.")

L-69-5103

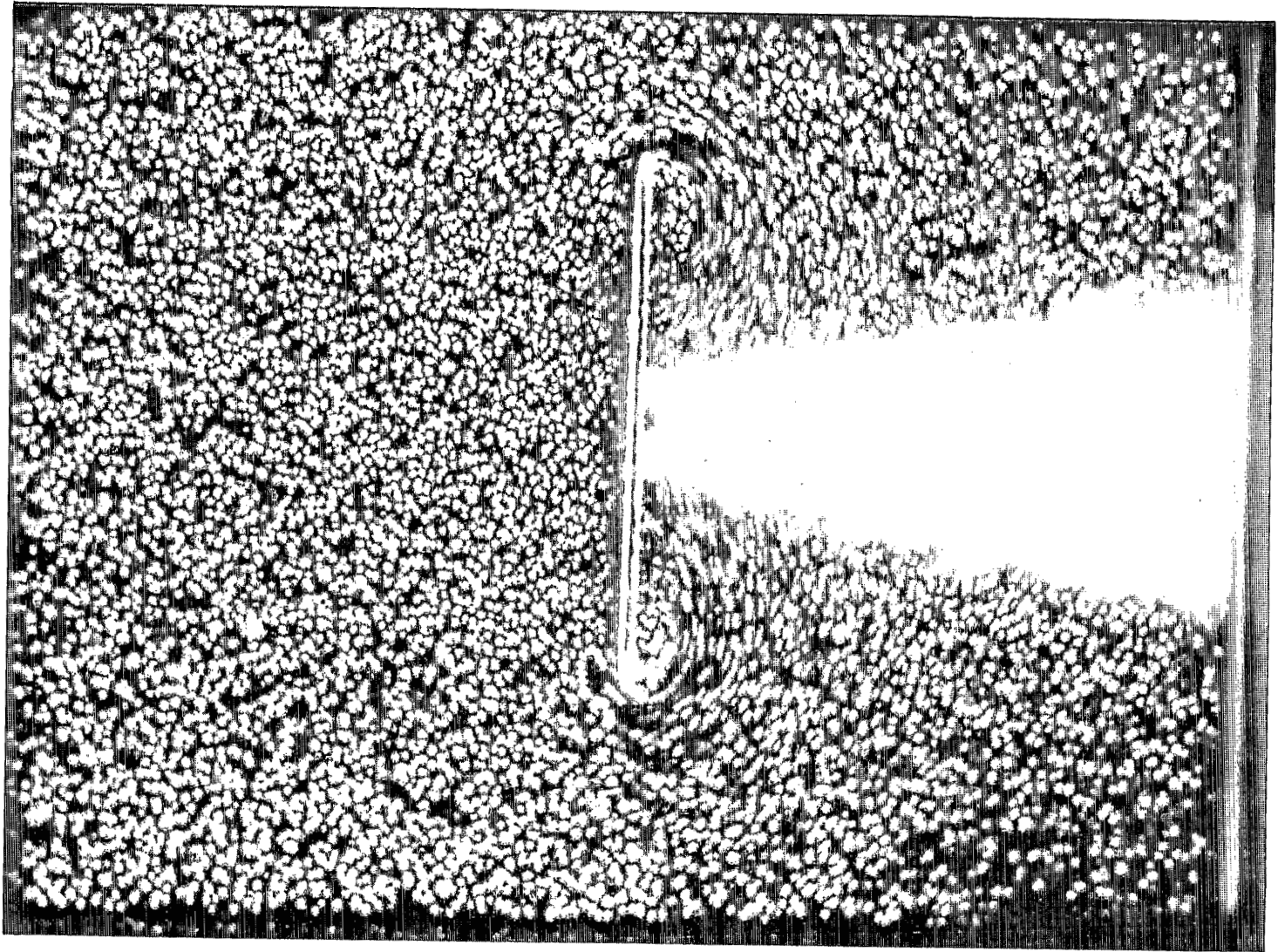


Figure 2.- Photograph of a jet in water tunnel exiting through a circular flat plate to illustrate the entrainment of air from quiescent surroundings around the edge of the plate. (Photograph from O.N.E.R.A. Film No. 575, "Flows With Large Velocity Fluctuations.")

L-69-5104

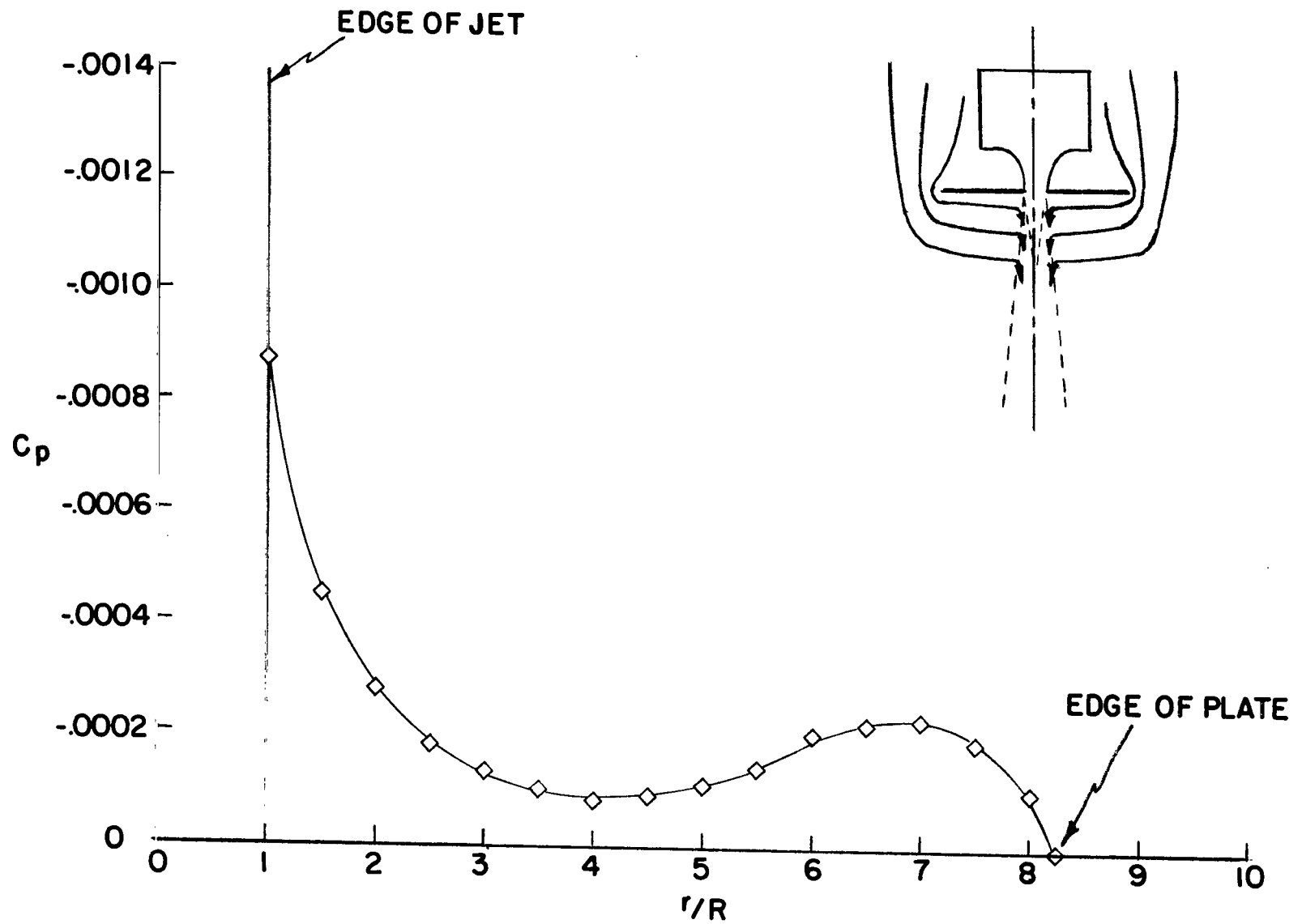


Figure 3.- Radial pressure distribution induced on a circular flat plate by a jet exiting through the plate. (From ref. 10.)

- ROUND PLENUM - CLEAR NOZZLE
- ROUND PLENUM - RESTRICTED NOZZLE
- ◇ RECTANGULAR PLENUM - POOR INTERNAL FLOW
- △ RECTANGULAR PLENUM - IMPROVED INTERNAL FLOW

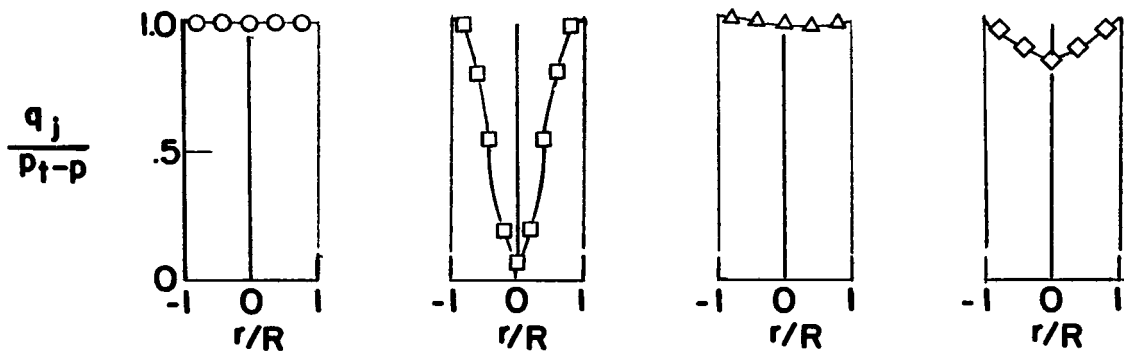
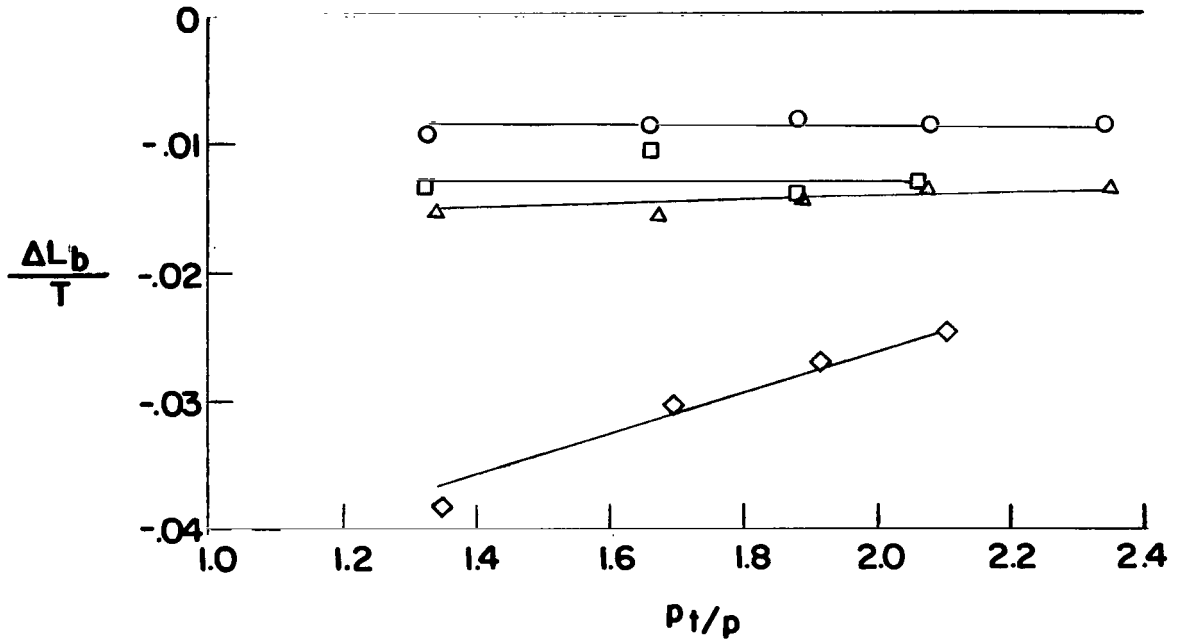


Figure 4.- Induced loads on a circular flat plate ($S/A_j = 69.5$) and exit dynamic-pressure distributions for several single-jet configurations. (From ref. 10.)

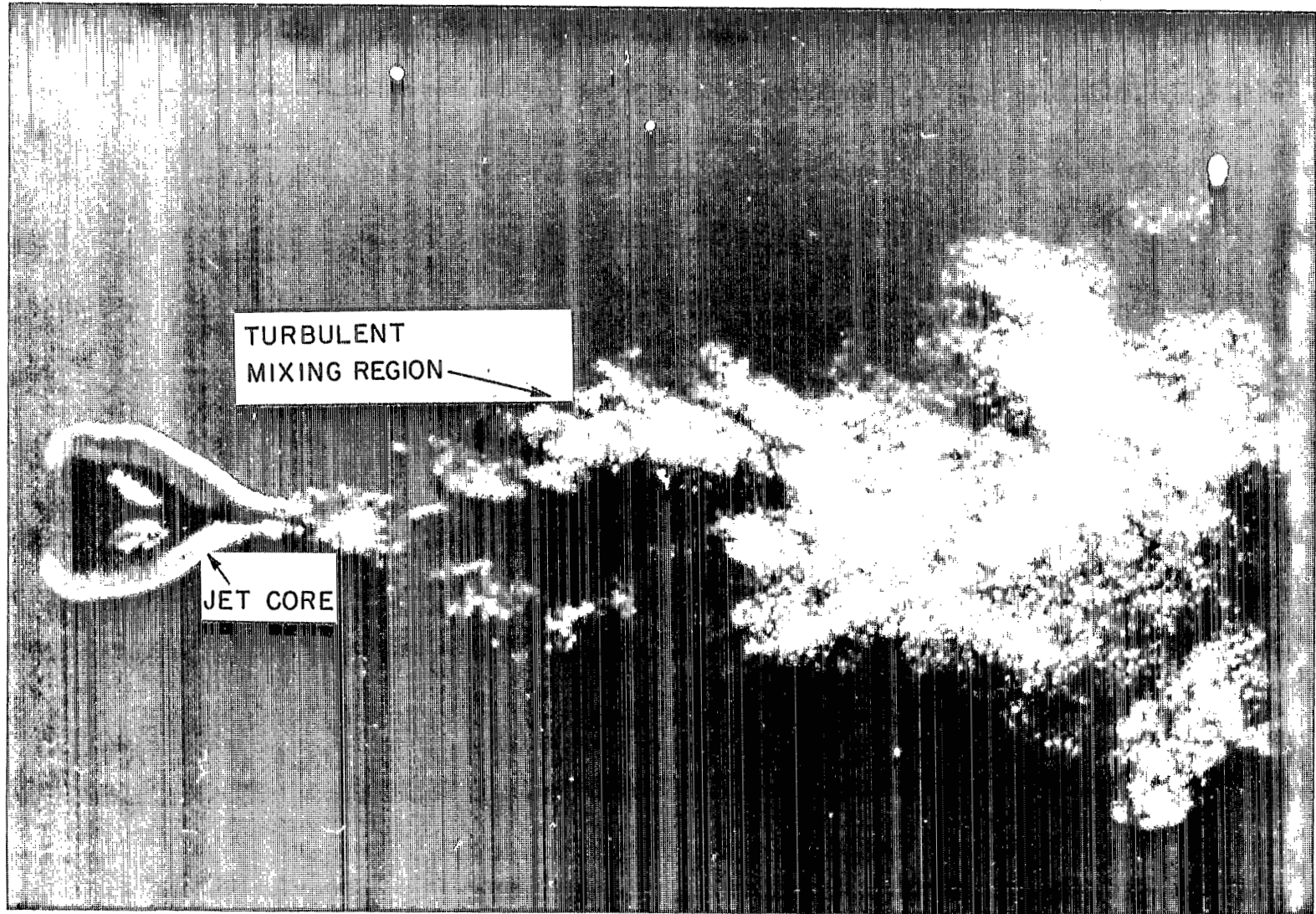


Figure 5.- Photograph of a jet exiting into quiescent surroundings, showing the undisturbed jet core and entrainment into the turbulent mixing region. (Photograph from O.N.E.R.A. Film No. 575, "Flows With Large Velocity Fluctuations.")

L-69-5105

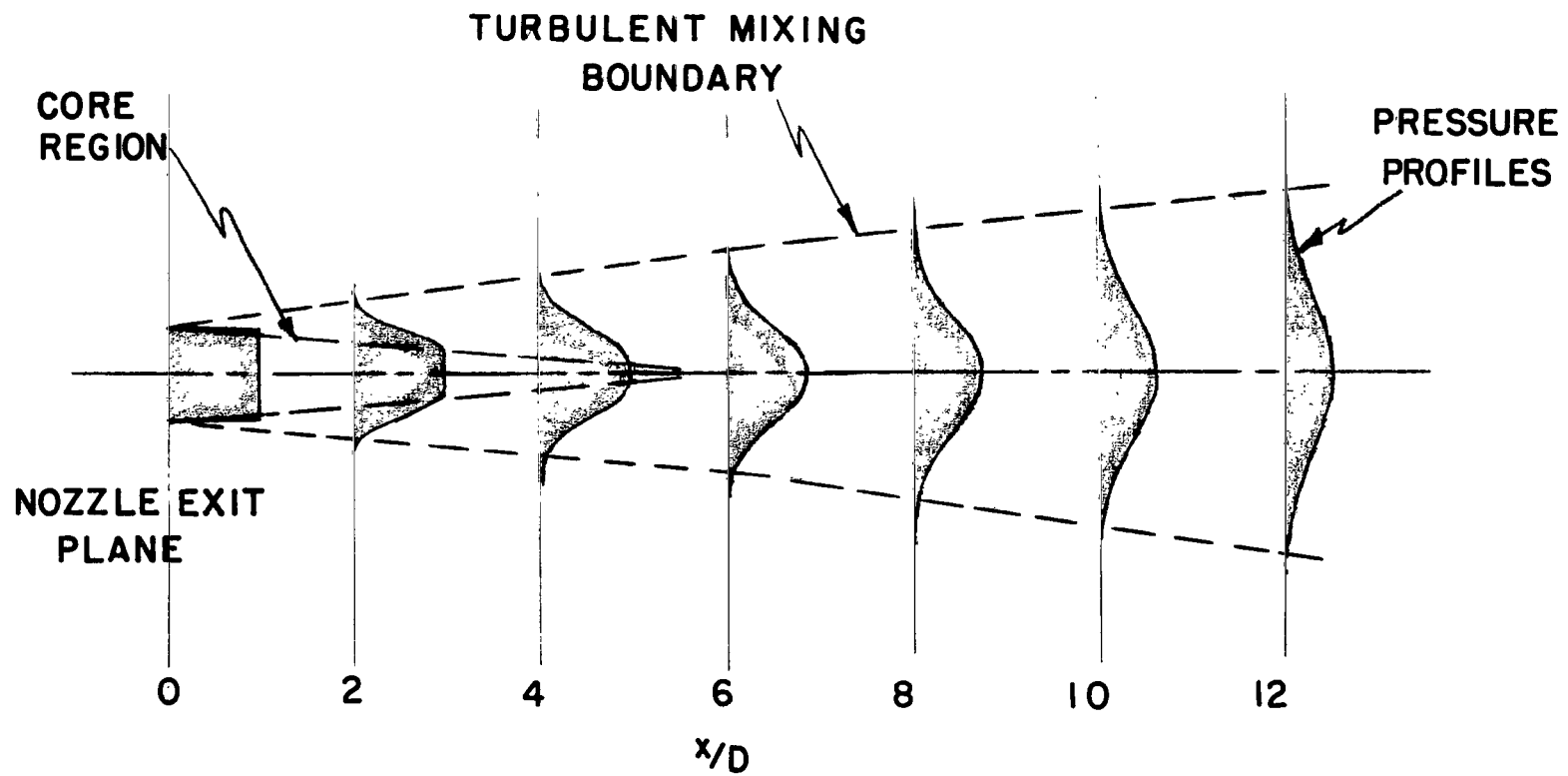


Figure 6.- Schematic sketch of the decay and spread of the jet efflux with distance downstream of the nozzle exit.

- ROUND PLENUM - CLEAR NOZZLE
- ROUND PLENUM - RESTRICTED NOZZLE
- ◇ RECTANGULAR PLENUM - POOR INTERNAL FLOW
- △ RECTANGULAR PLENUM - IMPROVED INTERNAL FLOW

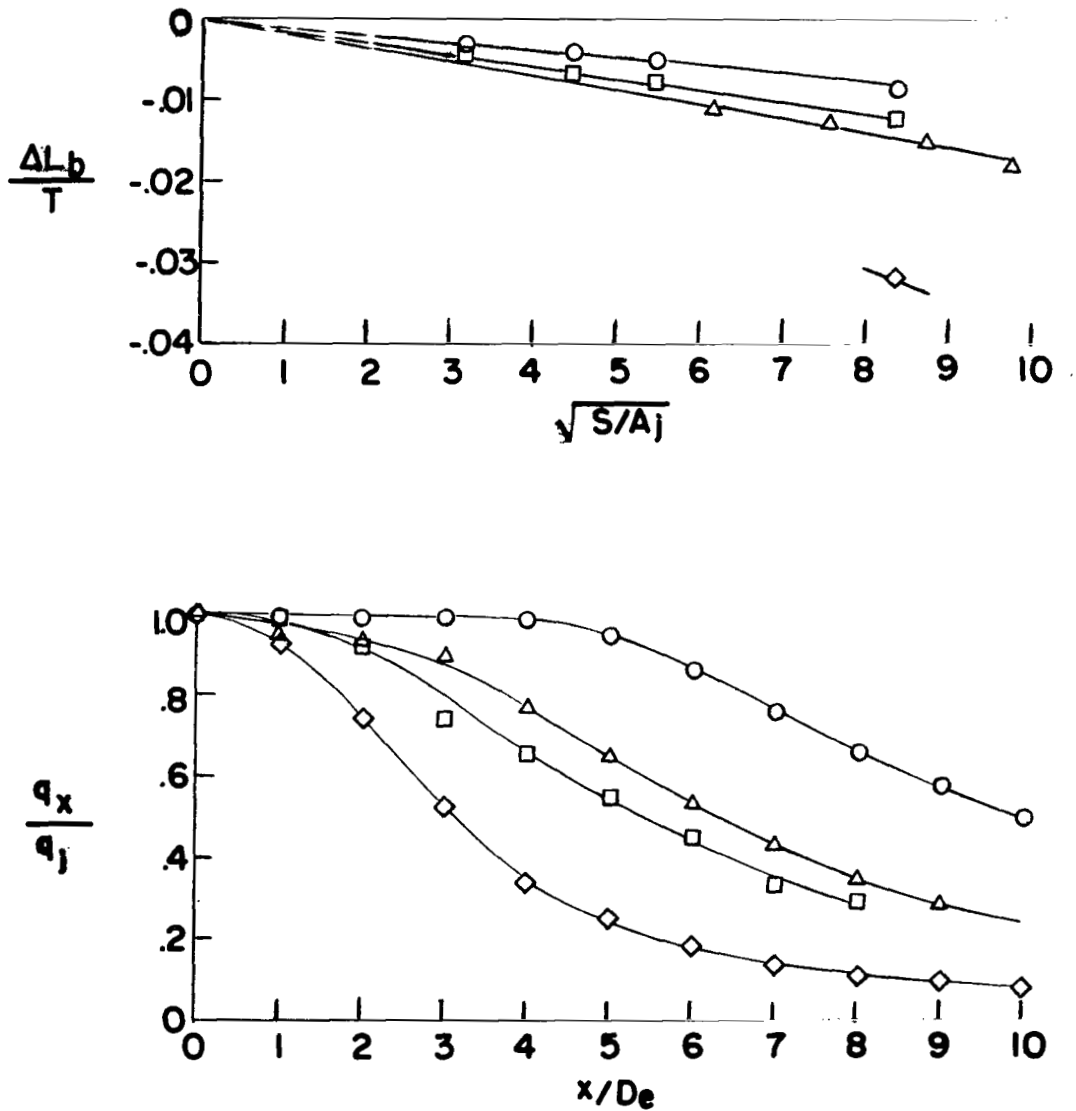


Figure 7.- Induced loads on a series of circular flat plates with several different jets exiting through their centers and the dynamic-pressure decay of the efflux from these jets. (From ref. 10.)

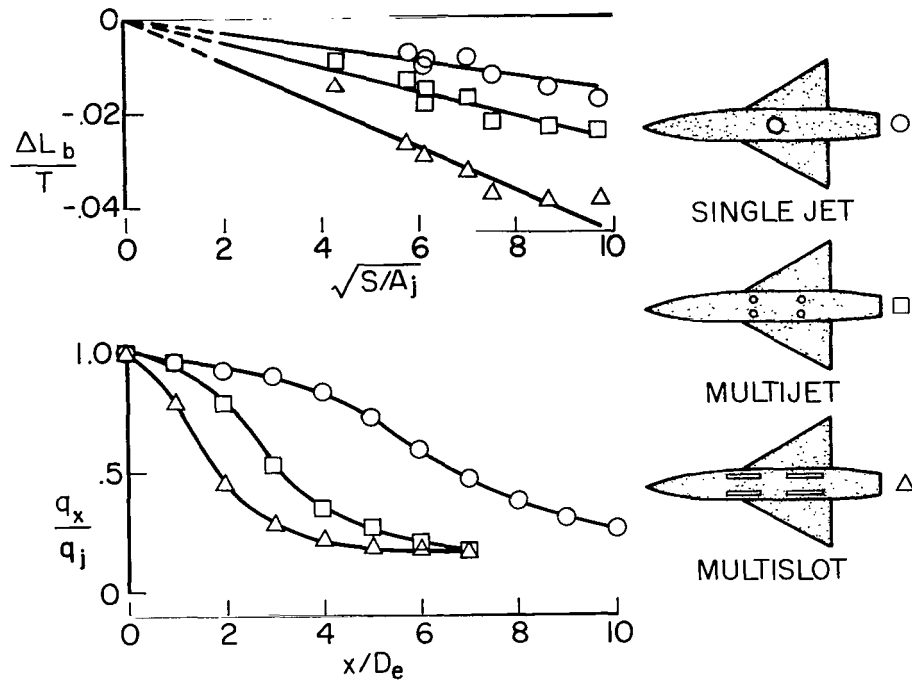


Figure 8.- Effect of jet arrangement on the lift loss and dynamic-pressure decay. (From ref. 10.)

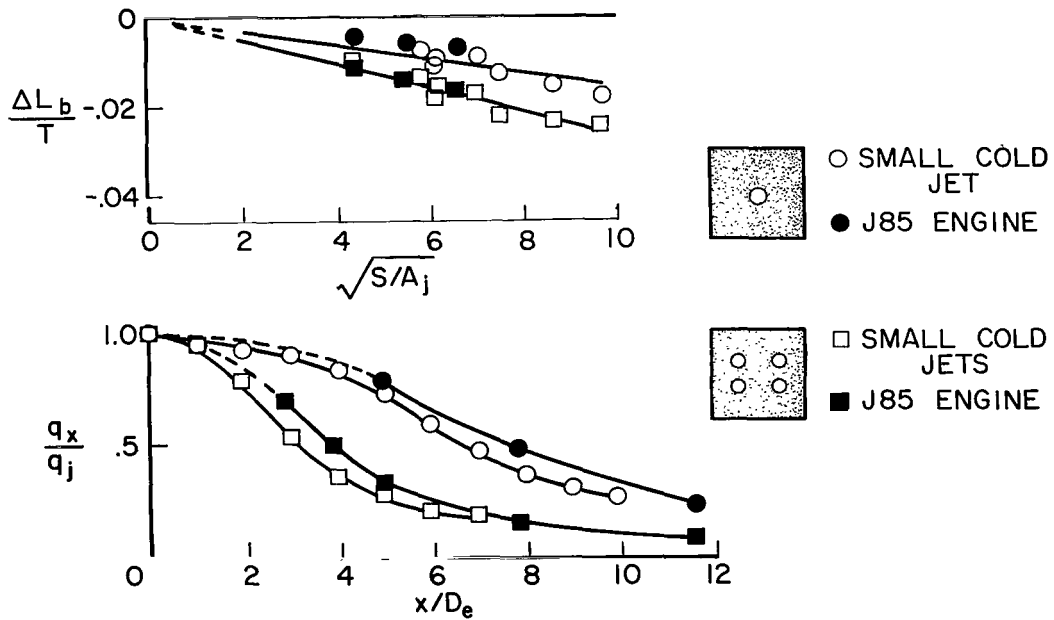


Figure 9.- Comparison of small-scale cold jet with large-scale hot jet, showing the effect on lift loss and the dynamic-pressure decay. (From ref. 11.)

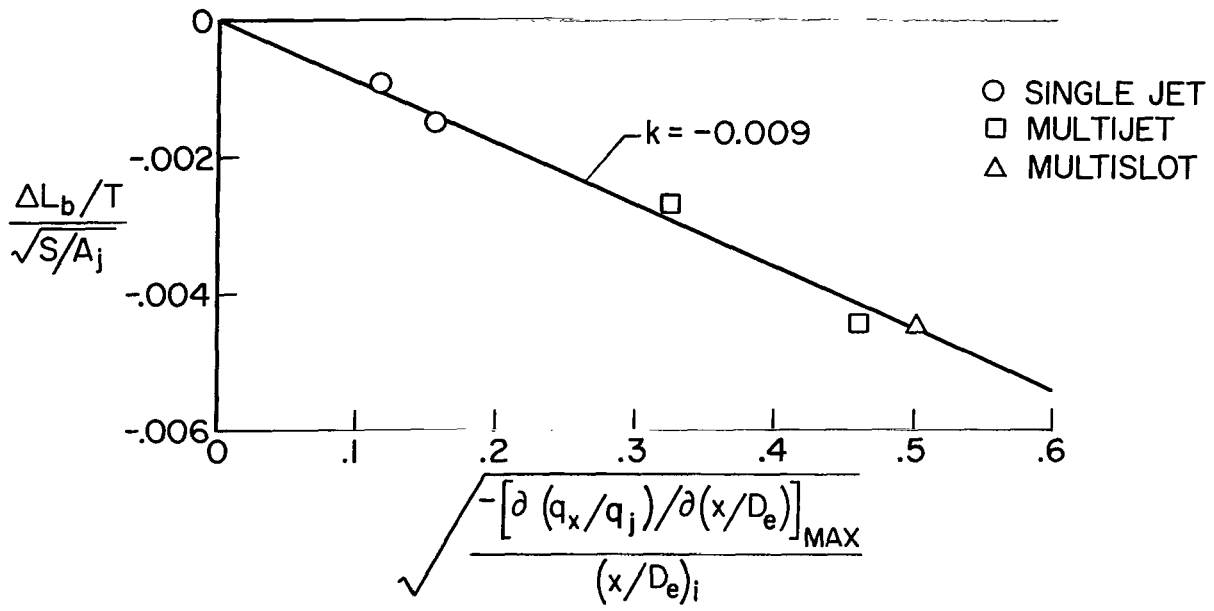


Figure 10.- Correlation of induced loads with the jet dynamic-pressure decay parameter. $\frac{\Delta L_b}{T} = k\sqrt{S/A_j} \sqrt{\frac{-[\partial(q_x/q_j)/\partial(x/D_e)]_{MAX}}{(x/D_e)_i}}$. (From ref. 10.)

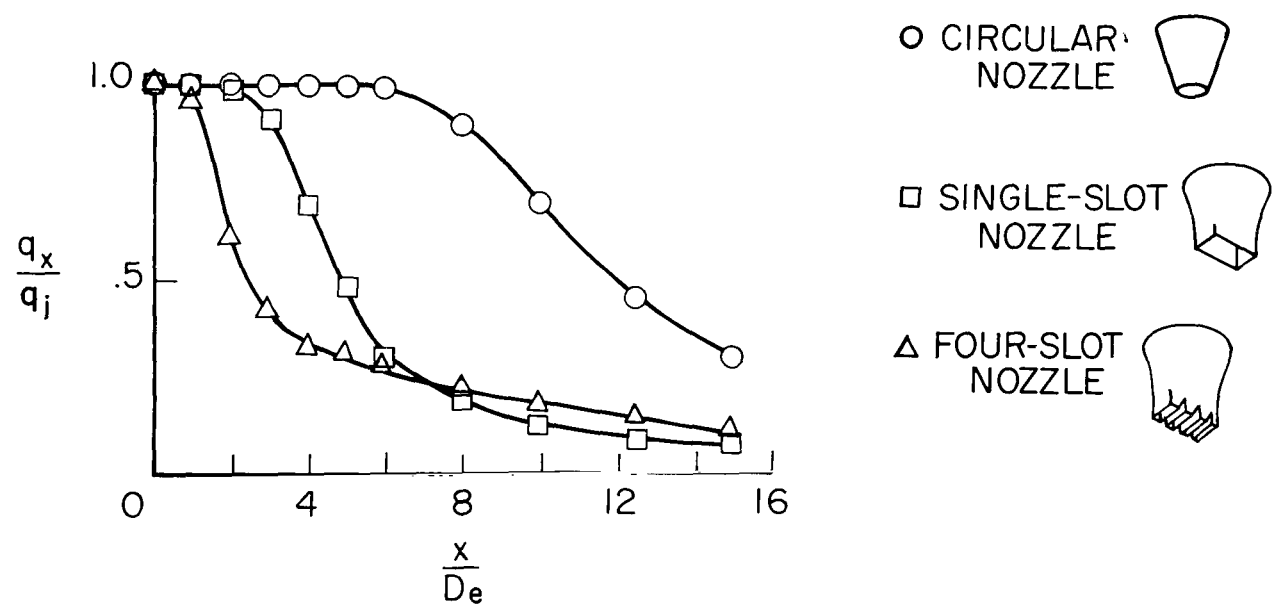


Figure 11.- Effect of nozzle configuration on jet dynamic-pressure decay. (From ref. 13.)

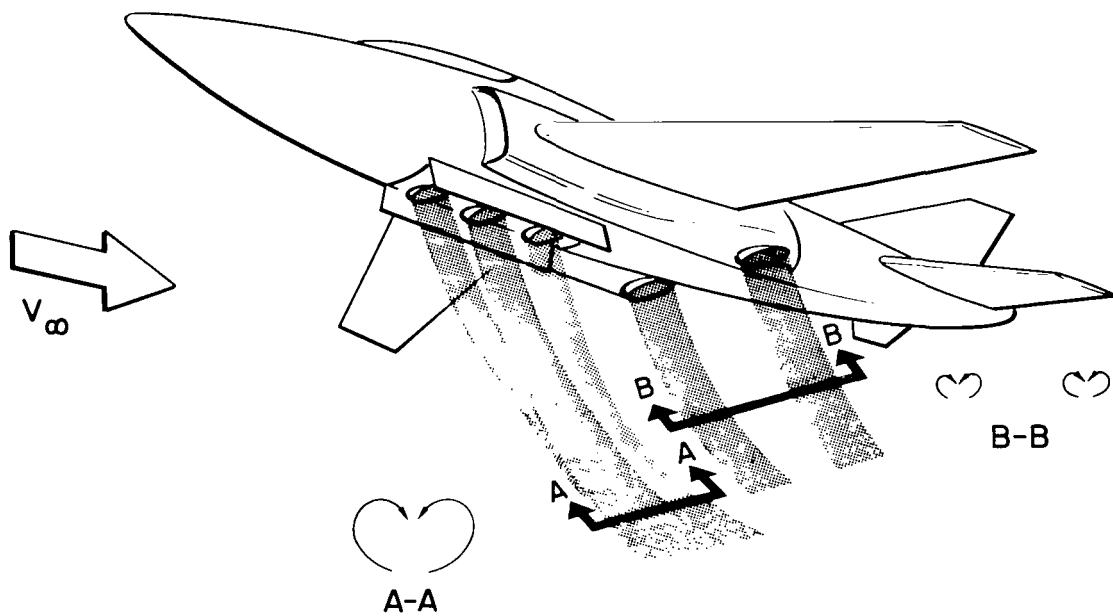


Figure 12.- Jet wakes from an aircraft in transition flight roll up into vortex pairs.

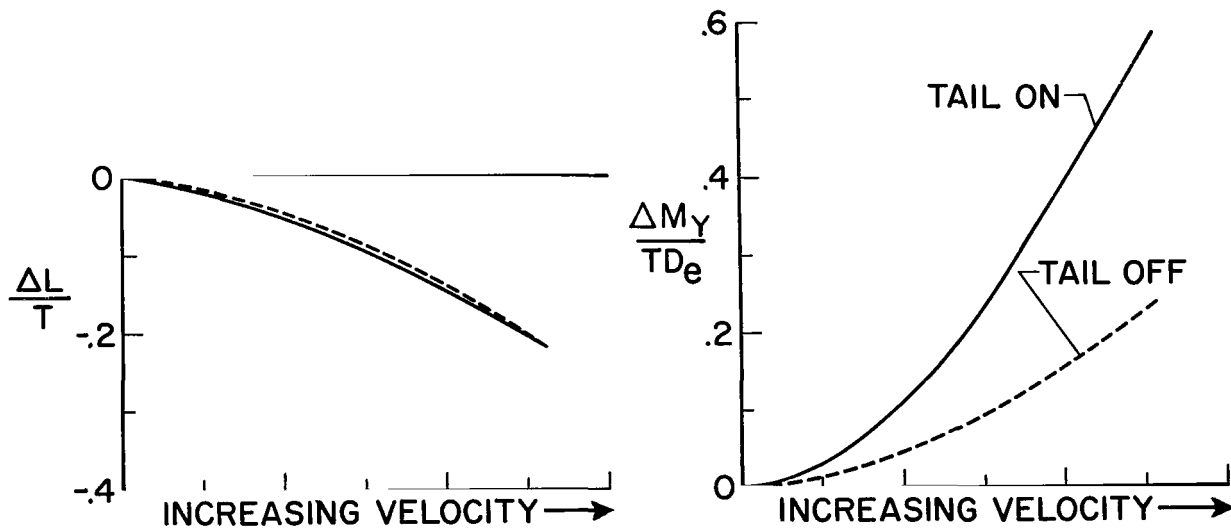


Figure 13.- The general trend of jet-induced lift loss and pitching moment in transition flight.

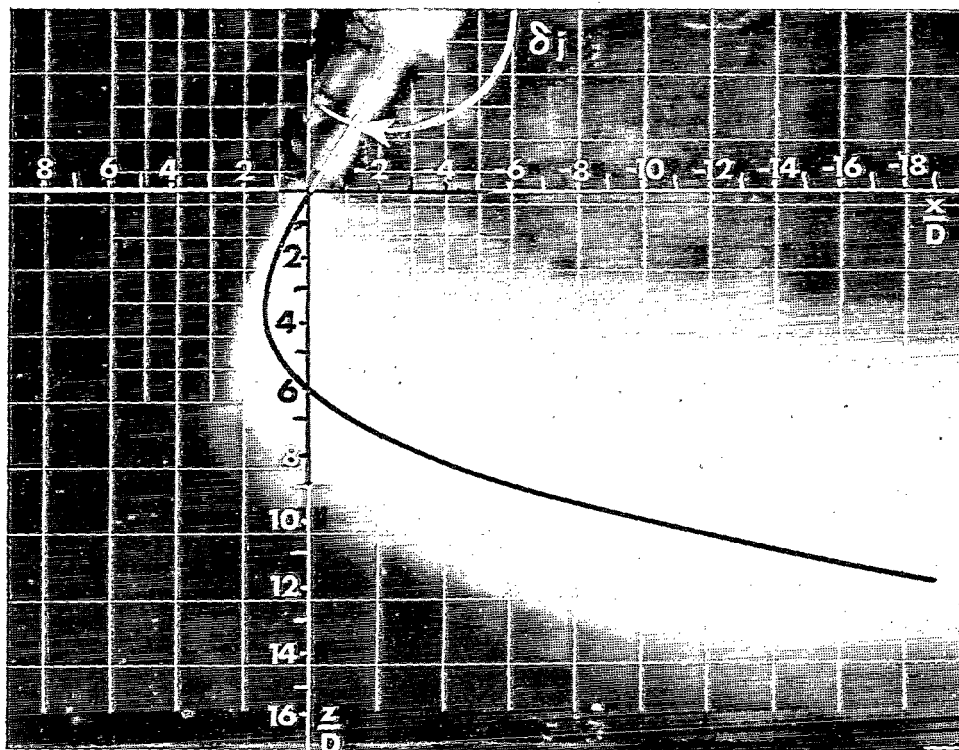
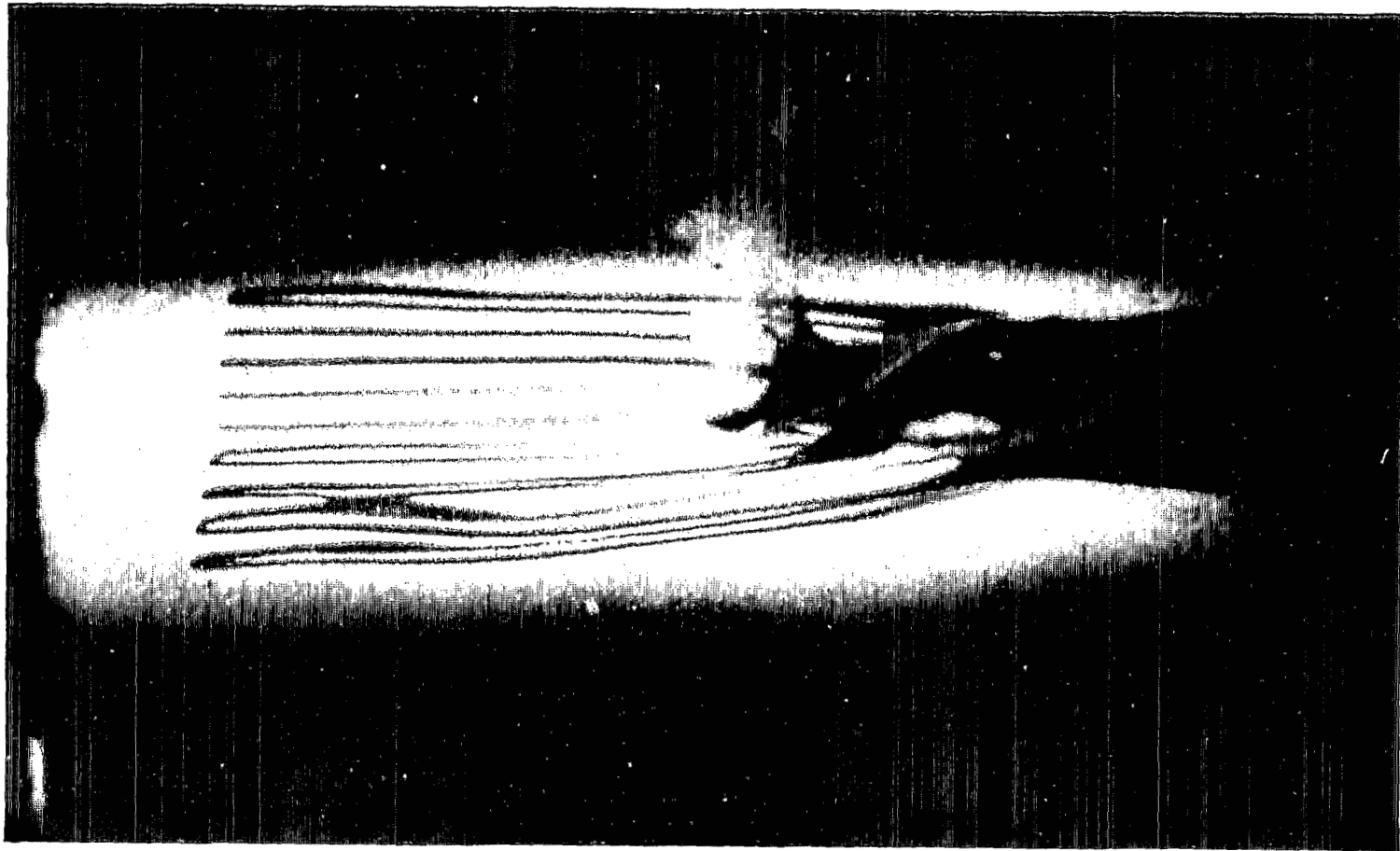


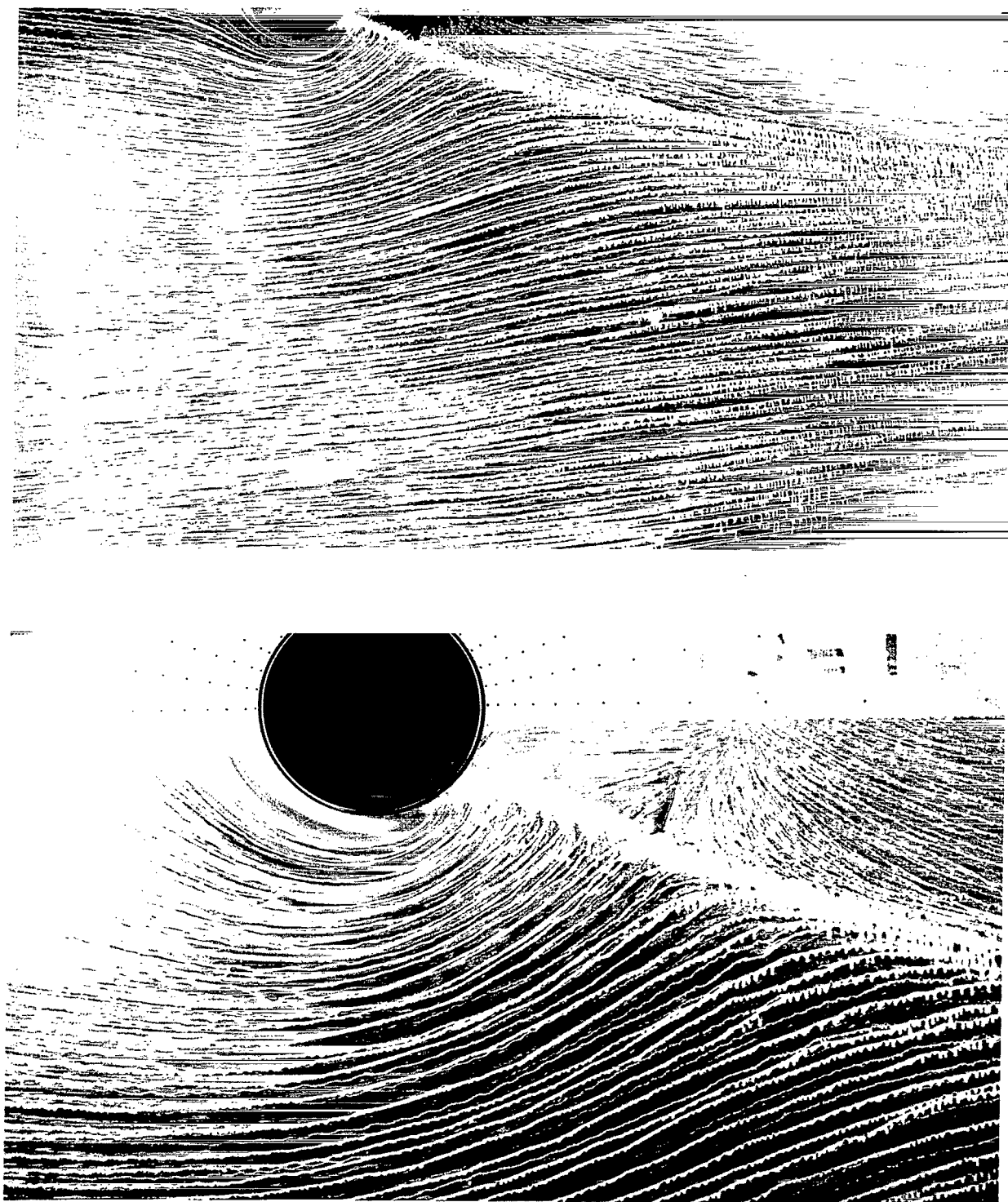
Figure 14.- The center-line path of jet wakes obtained from flow visualization studies. The jet wake path is given empirically by

$$\frac{x}{D} = -\frac{q_{\infty}/q_j}{4 \sin^2 \delta_j} \left(\frac{z}{D}\right)^3 - \frac{z}{D} \cos \delta_j. \quad (\text{From ref. 22.})$$



L-69-5106

Figure 15.- Photograph of the flow induced around and into a jet exhausting normal to the free stream. (Photograph from O.N.E.R.A. Film No. 575, "Flows With Large Velocity Fluctuations.")



L-69-5107

Figure 16.- Photographs of oil flow on the surface of a plate through which a jet is exhausting normal to the plate and to a free stream. $M_\infty = 0.18$; $\frac{M_j}{M_\infty} = 5.5$. (O.N.E.R.A. photograph.)

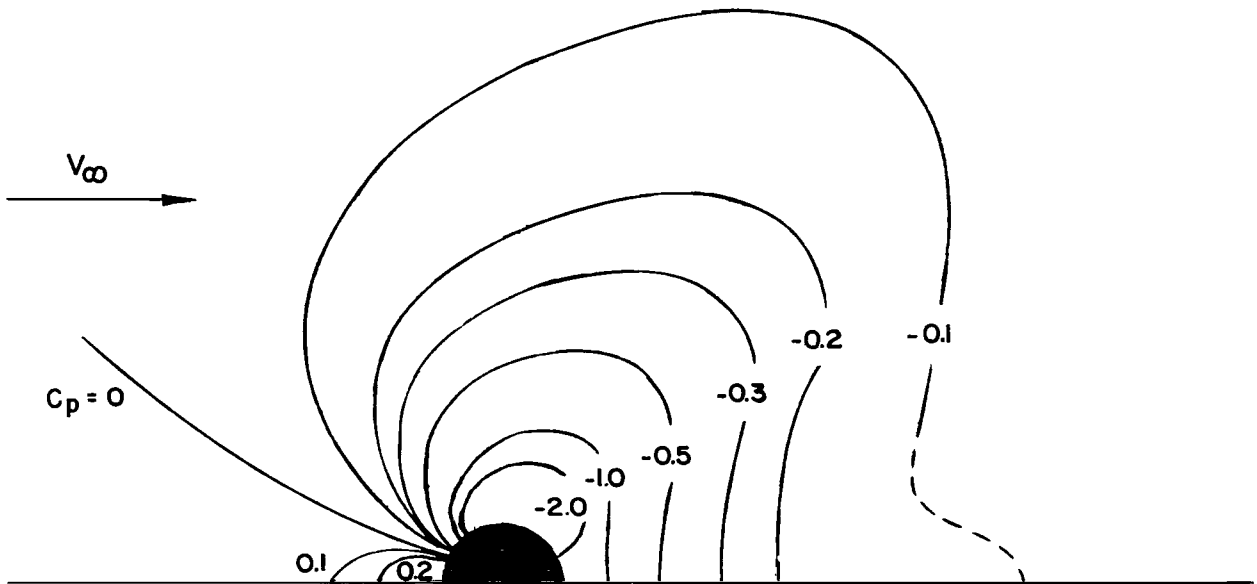


Figure 17.- Pressure distribution on the surface of a plate through which a jet is exhausting normal to the plate and to a free stream. $\sqrt{\frac{\rho_{\infty} V_{\infty}^2}{\rho_j V_j^2}} = 0.25$. (From ref. 23.)

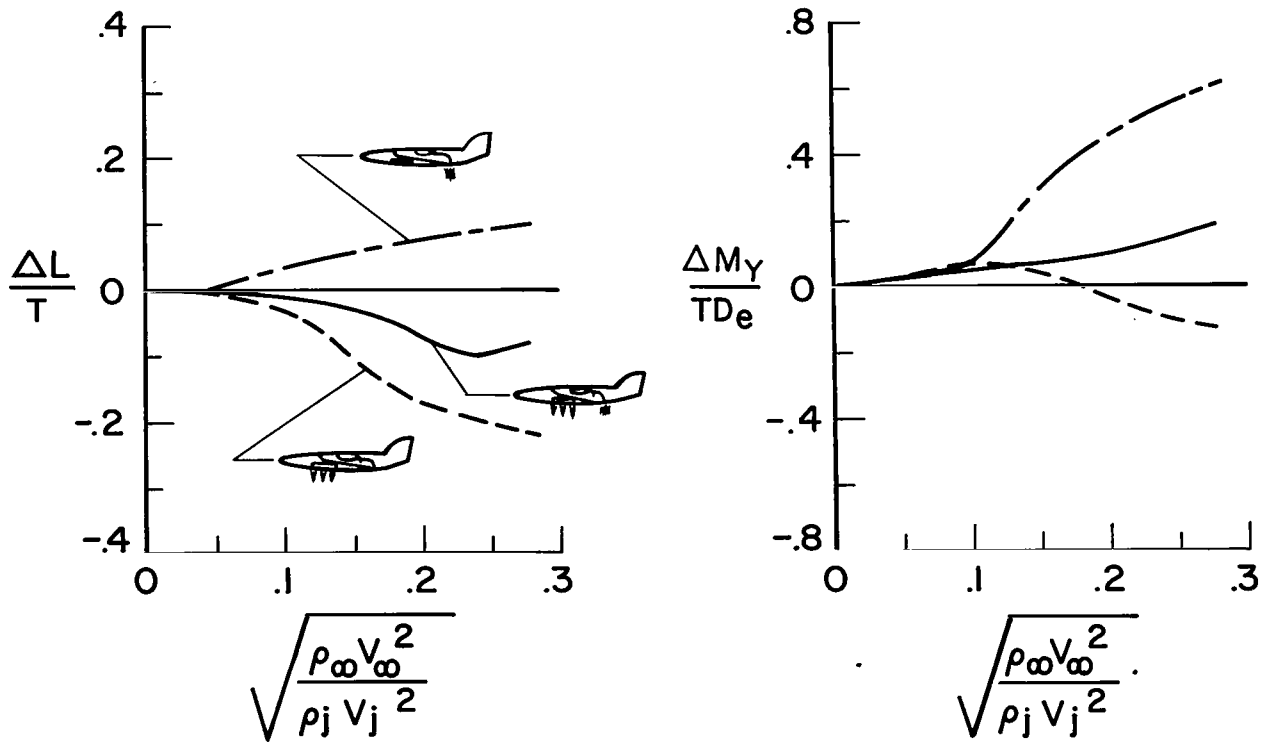


Figure 18.- Increments of interference lift and pitching moment during transition flight, showing the effect of the location of the lift-jet exits on a fighter-type configuration. (From ref. 24.)

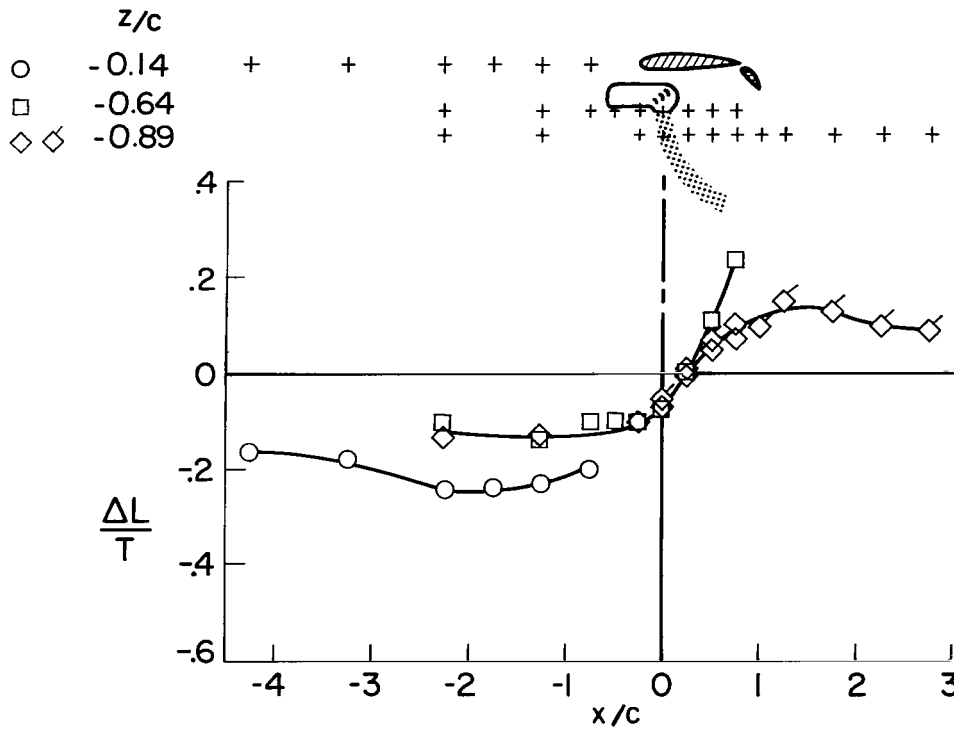


Figure 19.- Increments of interference lift during transition flight, showing the effect of varying the chordwise location of the jet.

$$\delta_f = 40^\circ; \delta_j = 90^\circ; C_T = 1.0; \sqrt{\frac{\rho_\infty V_\infty^2}{\rho_j V_j^2}} = 0.18. \text{ (From ref. 25.)}$$

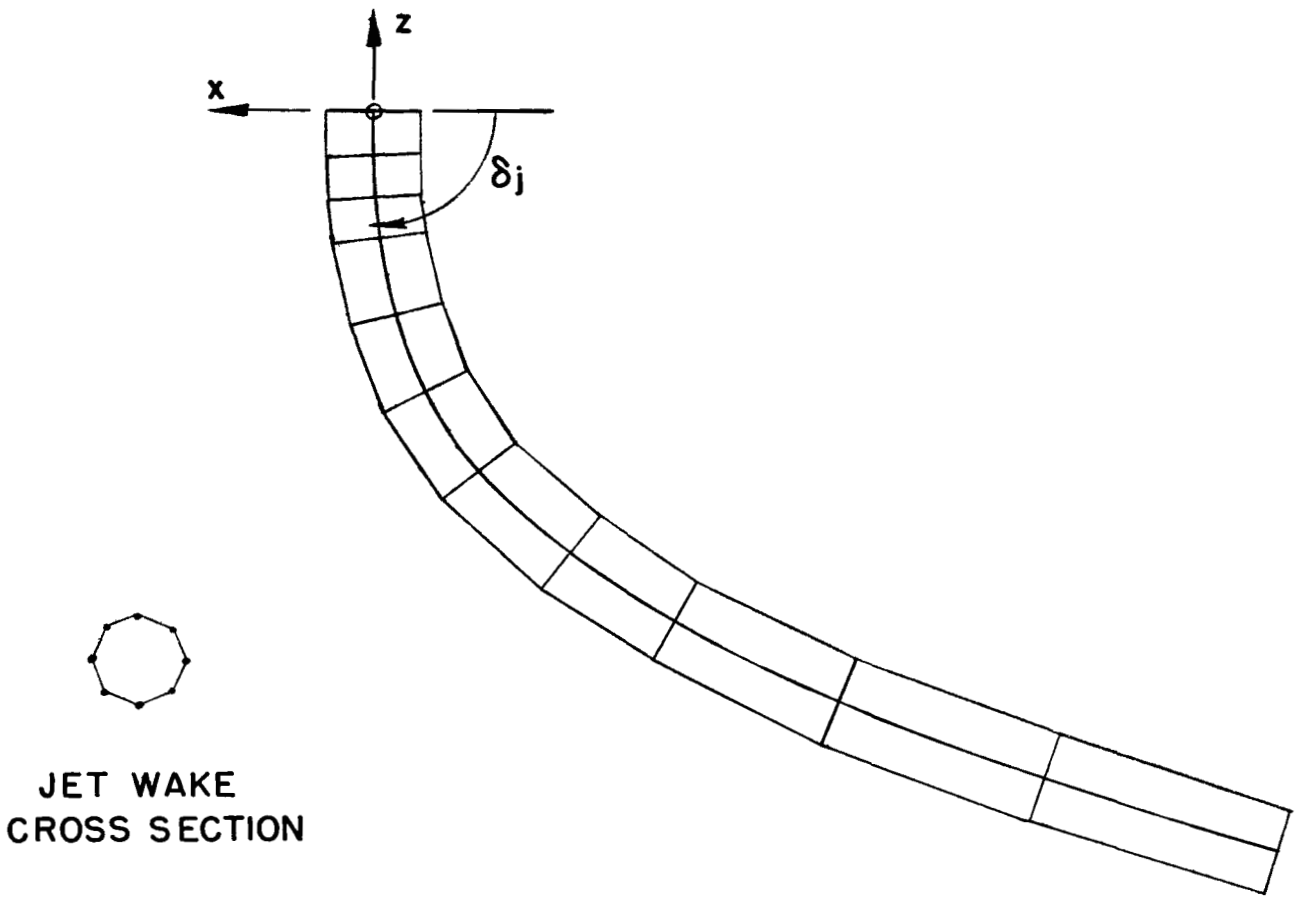


Figure 20.- Sketch of an analytic representation of a jet wake with an unchanging circular cross section, consisting of a quadrilateral vortex system superimposed on an empirically determined jet wake path $\frac{x}{D} = -\frac{q_{\infty}/q_j}{4 \sin^2 \delta_j} \left(\frac{z}{D}\right)^3 - \frac{z}{D} \cos \delta_j$. (From refs. 29 and 30.)

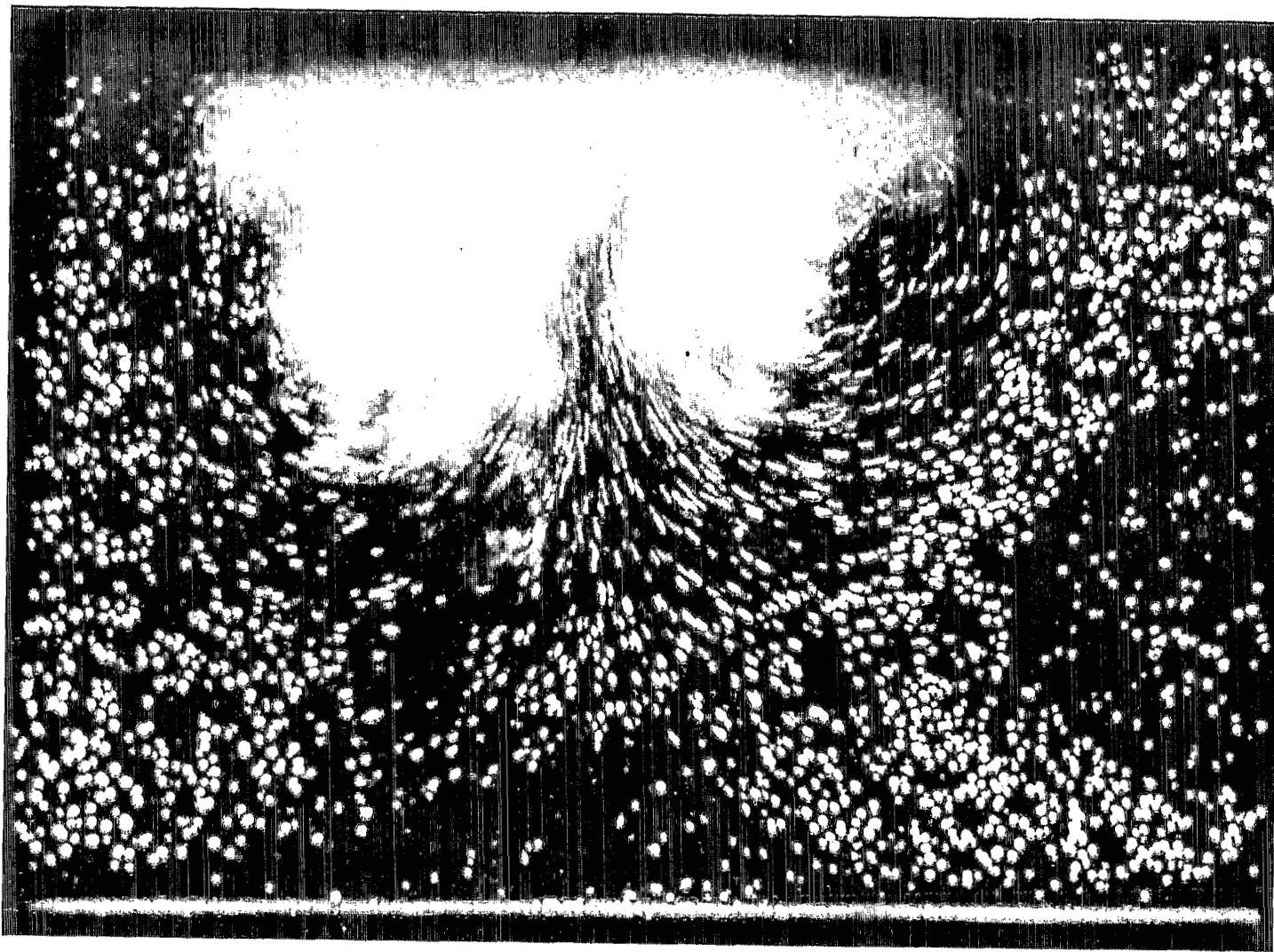


Figure 21.- Photograph of the cross section of the wake of a jet exiting perpendicular to the free stream in a water tunnel. This cross section is approximately 6 nozzle diameters downstream of the nozzle exit. (Photograph from O.N.E.R.A. Film No. 575, "Flows With Large Velocity Fluctuations.")

L-69-5108

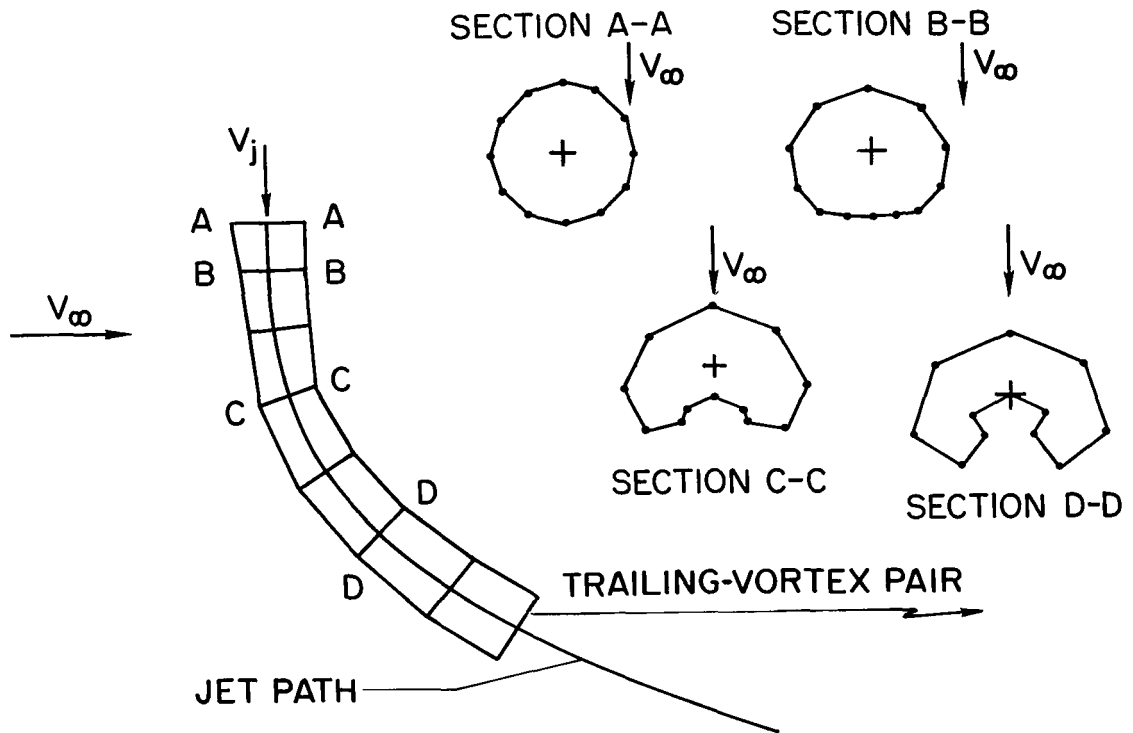


Figure 22.- Sketch of an analytic representation of a jet wake with a changing cross section, consisting of a quadrilateral vortex system superimposed on an empirically determined jet wake path.

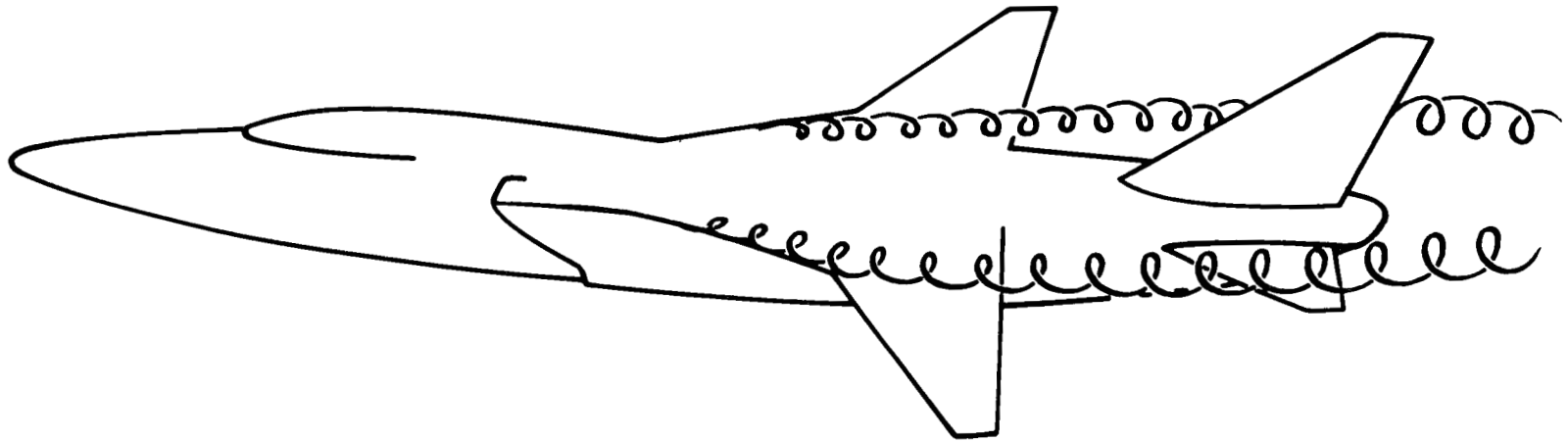
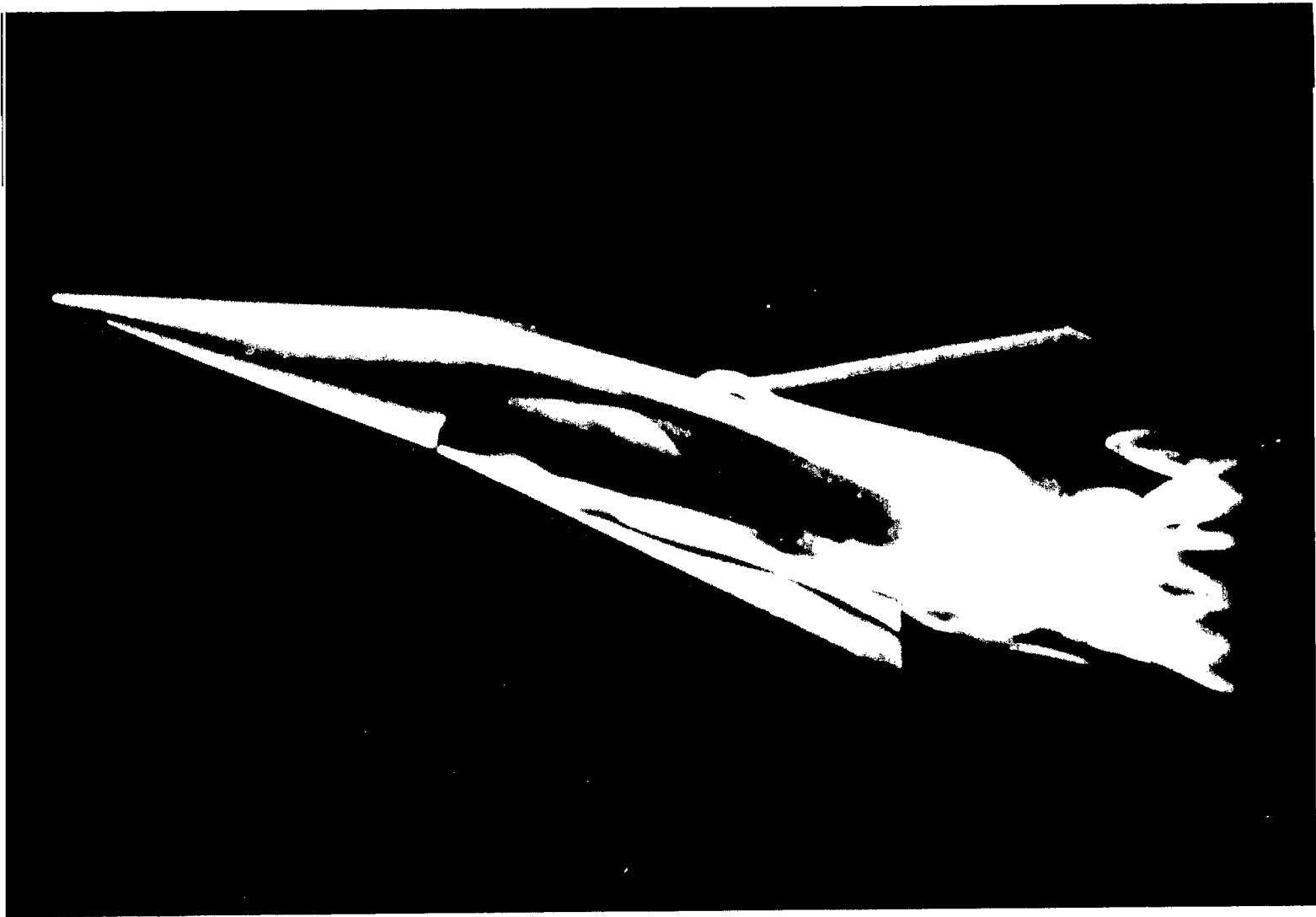


Figure 23.- Sketch of vortex paths developed along the leading edge of a highly swept inboard portion of a wing in cruise flight.



L-69-5109

Figure 24.- Photograph of vortex paths developed along the leading edge of a delta wing in cruise flight. (Photograph from O.N.E.R.A. Film No. 575, "Flows With Large Velocity Fluctuations.")

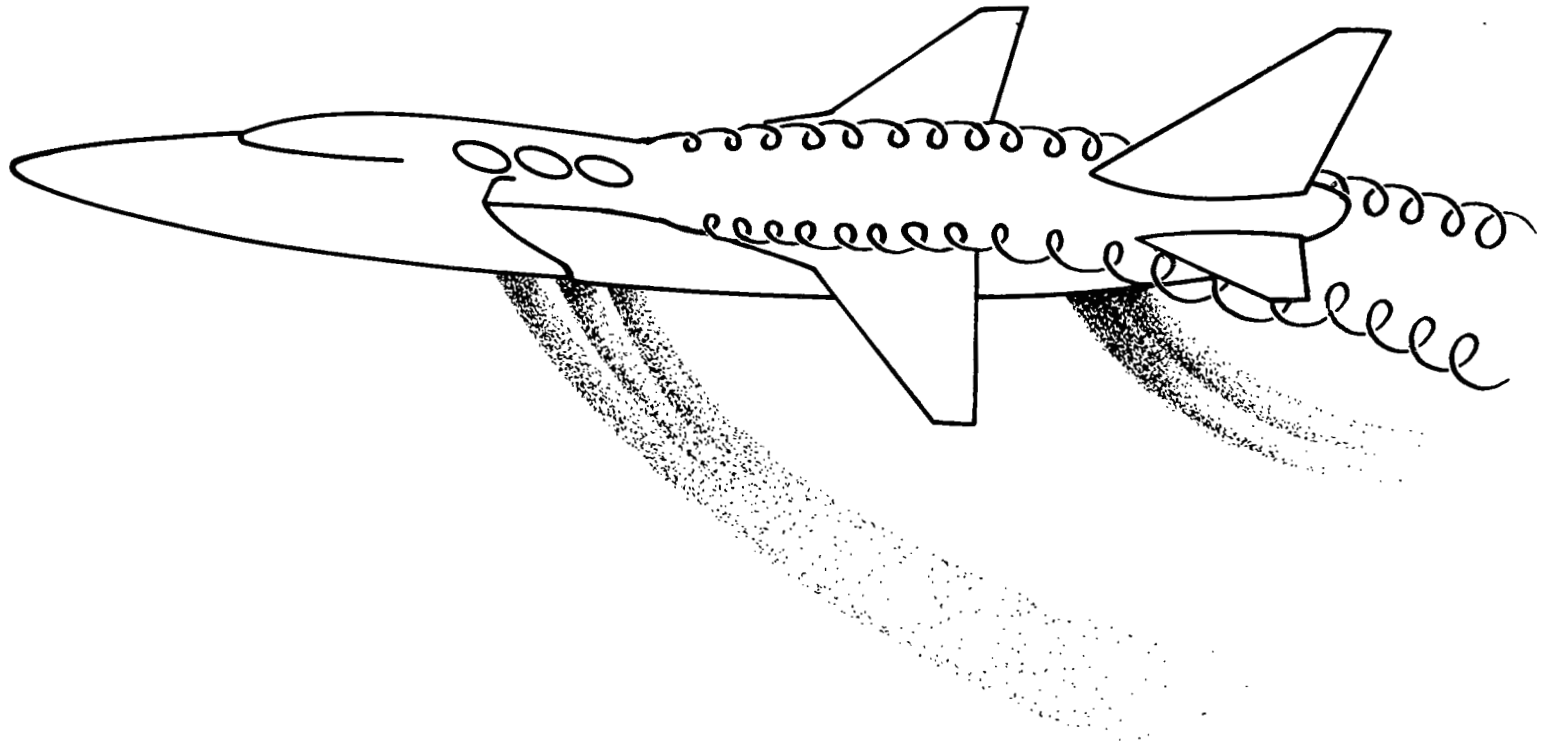
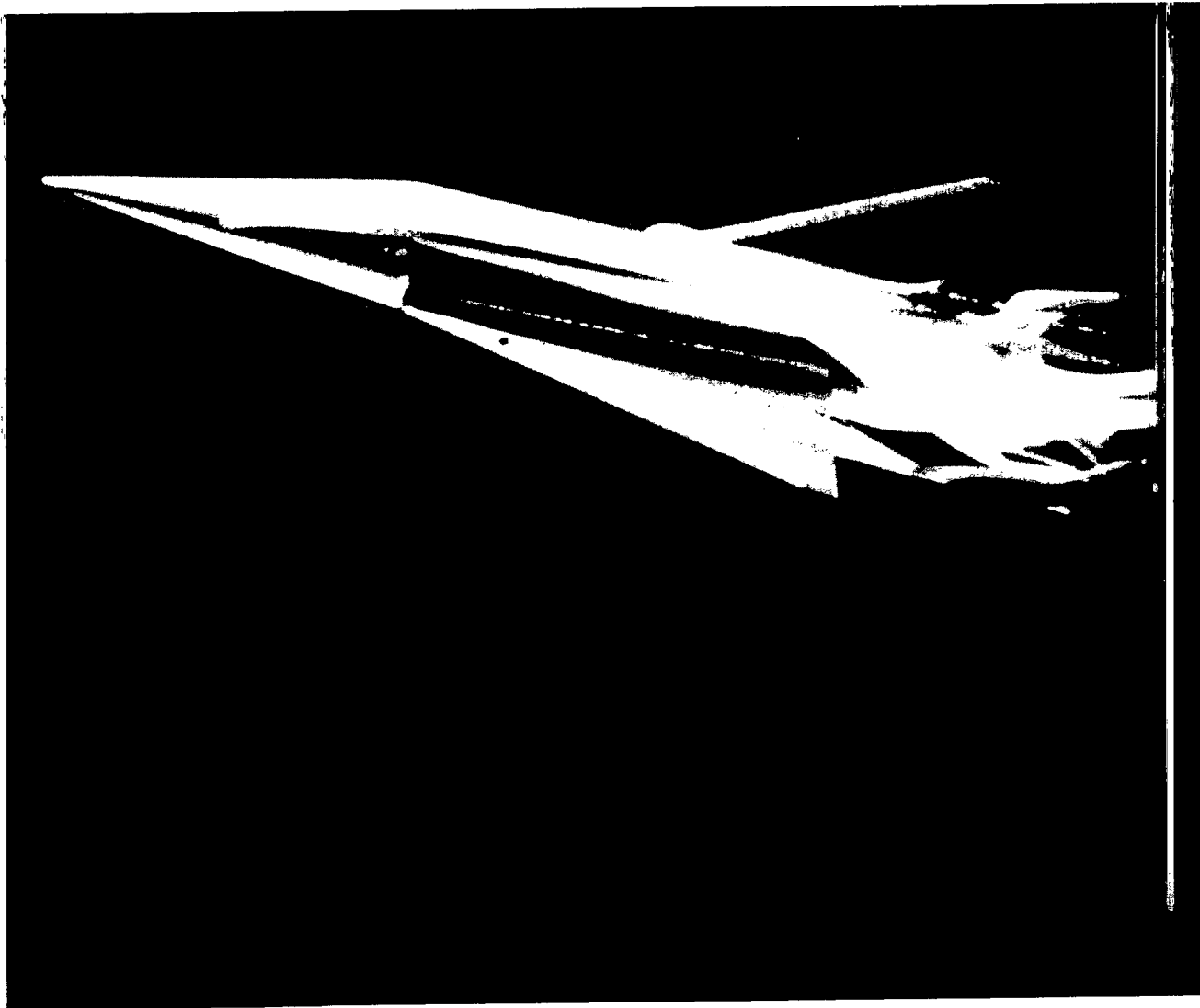


Figure 25.- Sketch of vortex paths developed along the leading edge of a highly swept inboard portion of a wing in transition flight.



L-69-5110

Figure 26.- Photograph of vortex paths developed along the leading edge of a delta wing in transition flight. (Photograph from O.N.E.R.A. Film No. 575, "Flows With Large Velocity Fluctuations.")

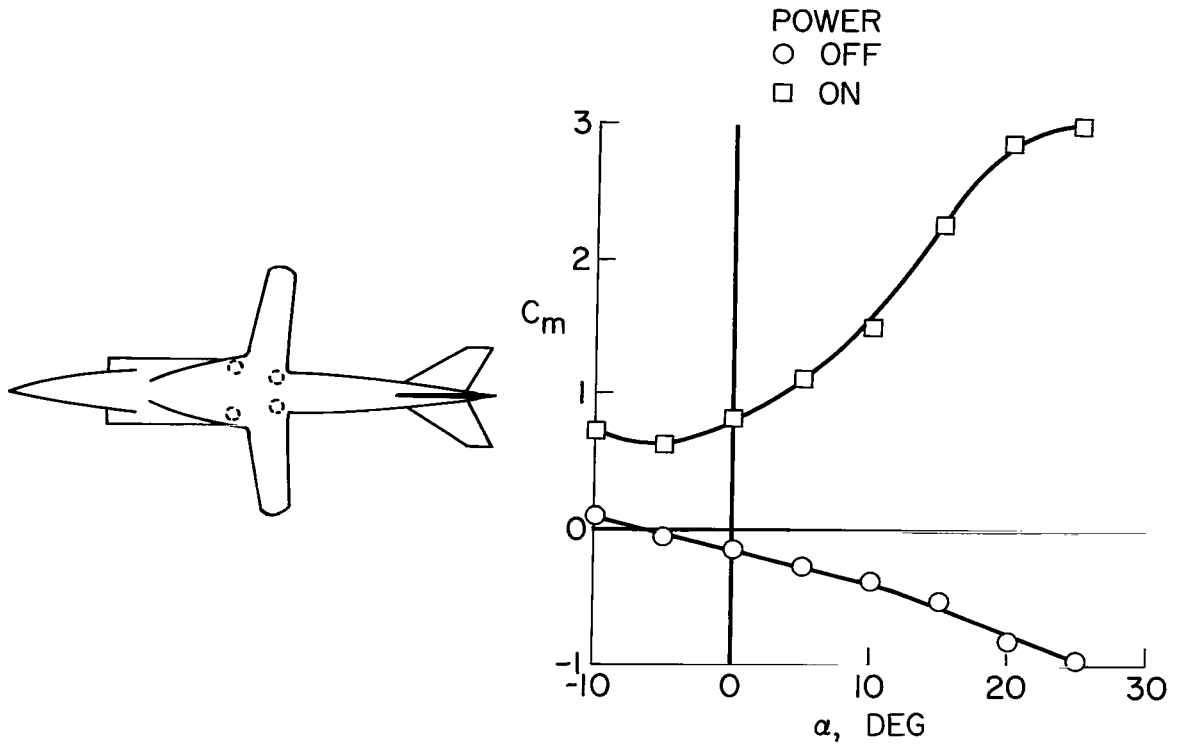


Figure 27.- Effect of power from vectored lift nozzles on the longitudinal stability of a four-jet fighter configuration with a large forebody and a small wing. (From ref. 32.)

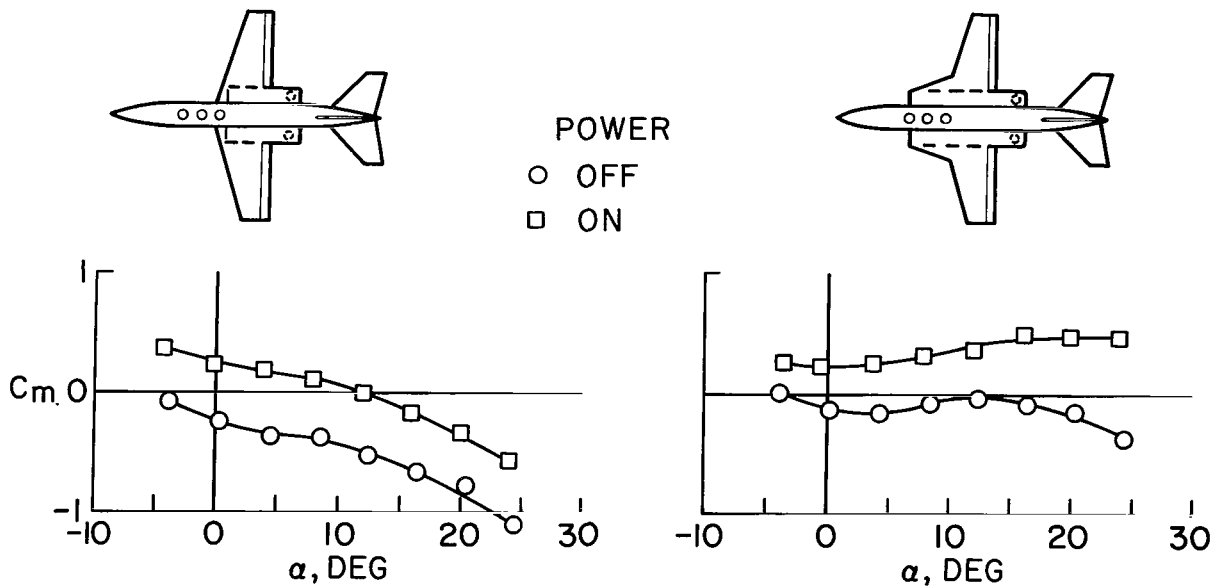


Figure 28.- Effect of power from lift-jet engines on the longitudinal stability of a five-jet fighter configuration with a varying forebody shape and varying wing planform. (From ref. 2.)

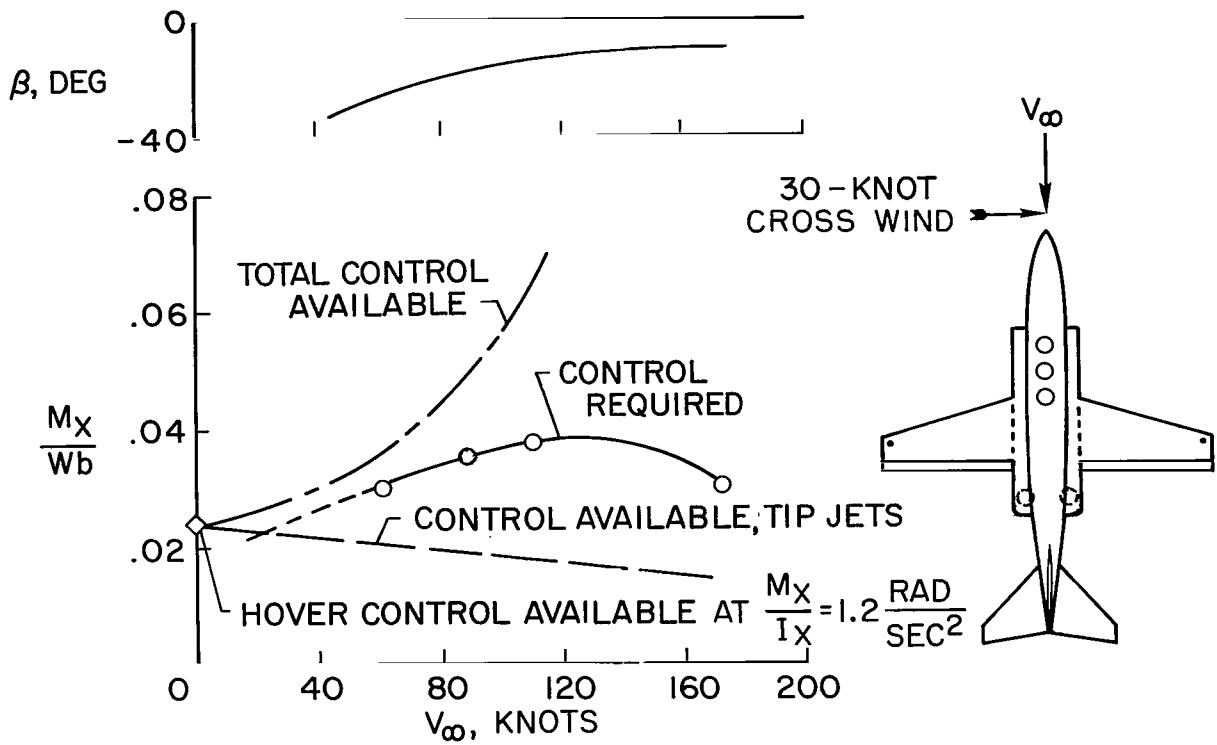
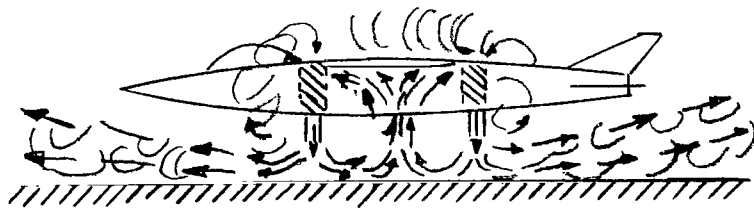
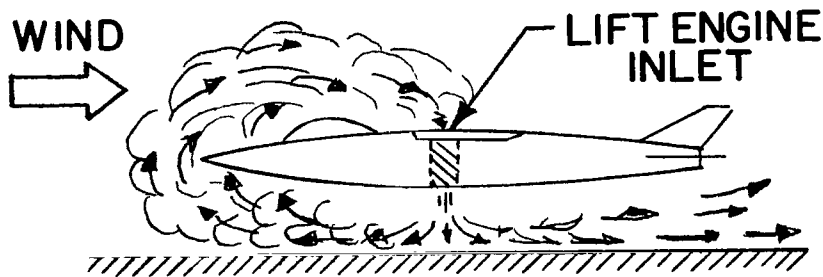


Figure 29.- Effect of power from lift-jet engines on the lateral control requirements of an airplane in transition from cruise flight to hover in a 30-knot cross wind. (From ref. 2.)



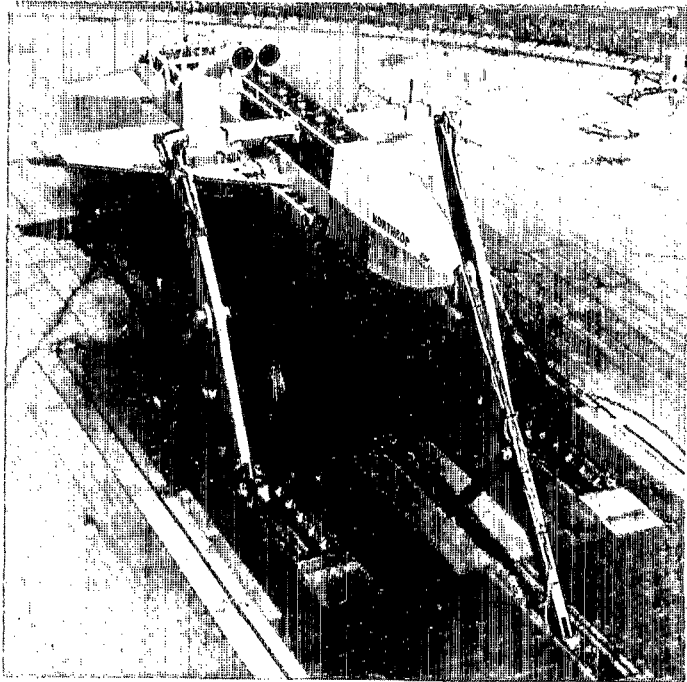
(a) Still air.



(b) Surface winds.

Figure 30.- The general flow patterns which cause hot-gas ingestion.

AMES-NORTHROP
FULL-SCALE MODEL



LANGLEY
1/3-SCALE MODEL

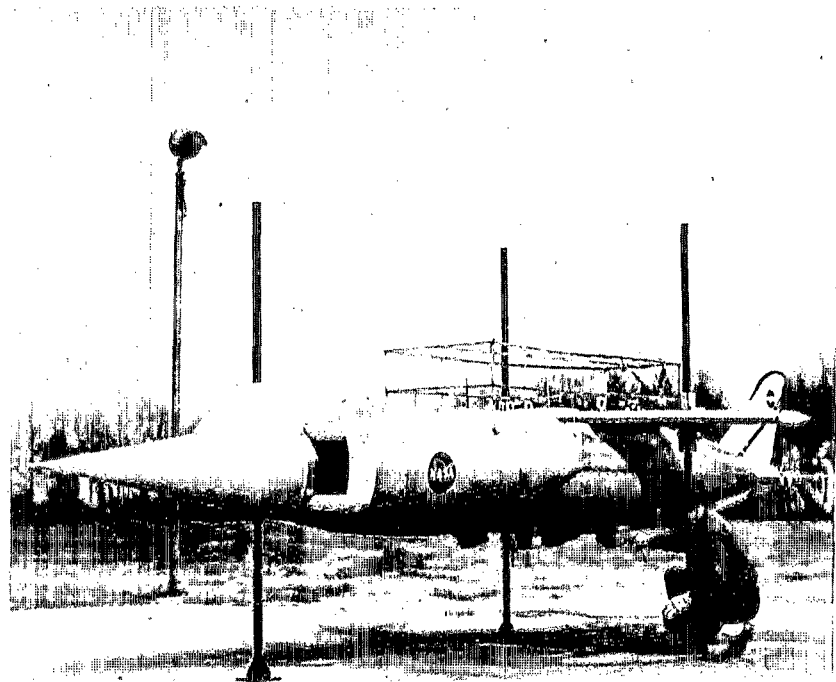


Figure 31.- Large-scale models used by NASA for investigation of hot-gas ingestion.

L-69-5111

+ UPPER-SURFACE INLETS
 ○ EXITS

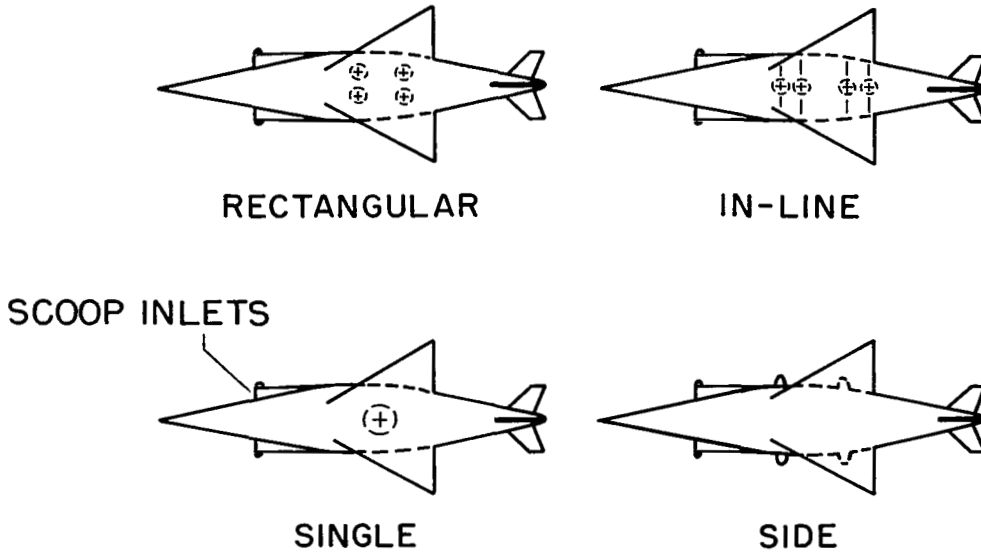


Figure 32.- Sketches of the exit-nozzle arrangements represented by the hot-gas ingestion model at NASA Langley Research Center. All configurations had the scoop inlets and all except the side-nozzle configuration had alternate inlets on the fuselage upper surface.

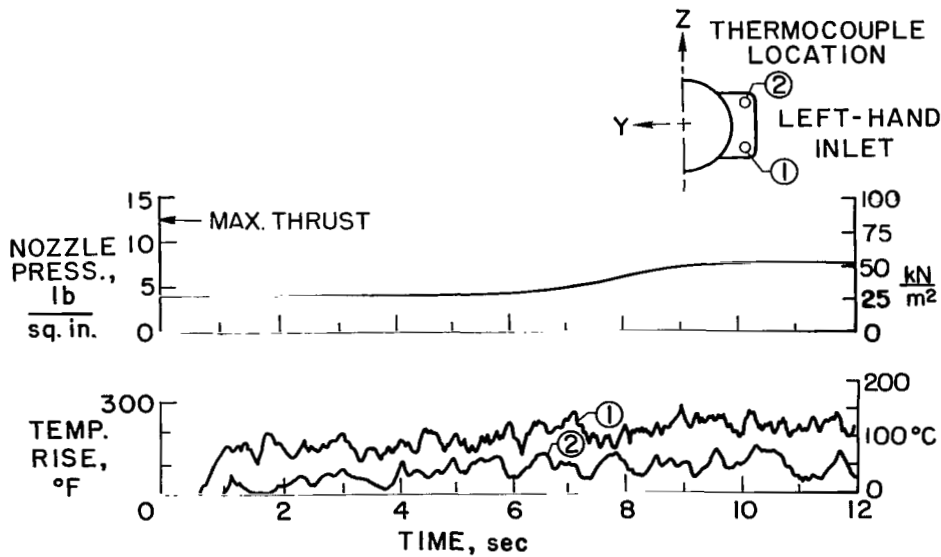


Figure 33.- Typical time history of inlet temperature rise and nozzle pressure obtained on the NASA Langley hot-gas ingestion model with the rectangular exit-nozzle arrangement and side inlets. $H/D_e = 1.17$.

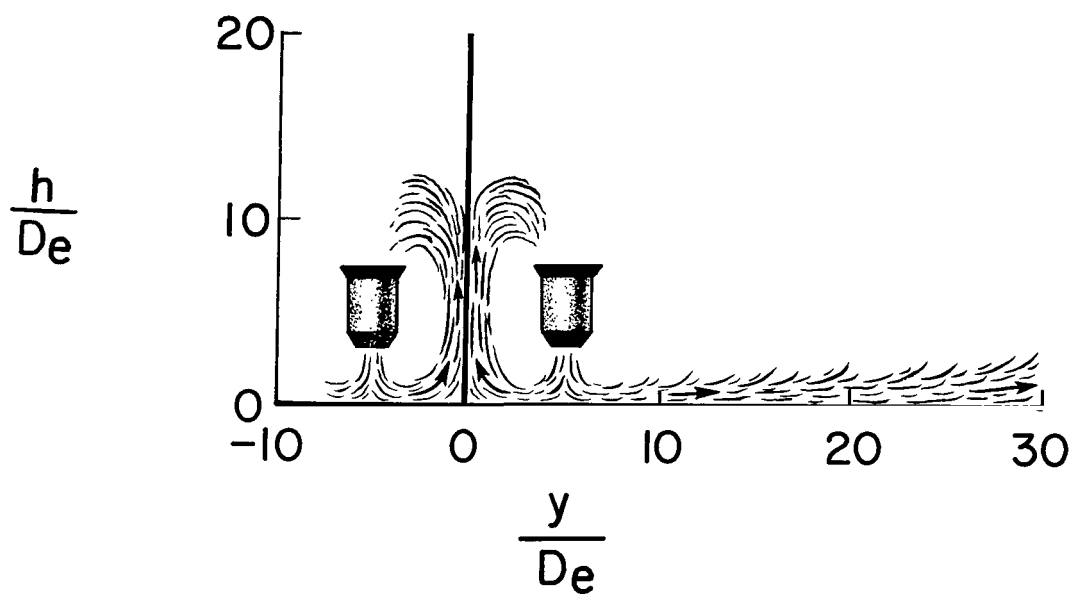


Figure 34.- Sketch showing the extent of the hot-gas cloud in still air (fountain effect) obtained when multiple nozzles exit vertically near the ground.

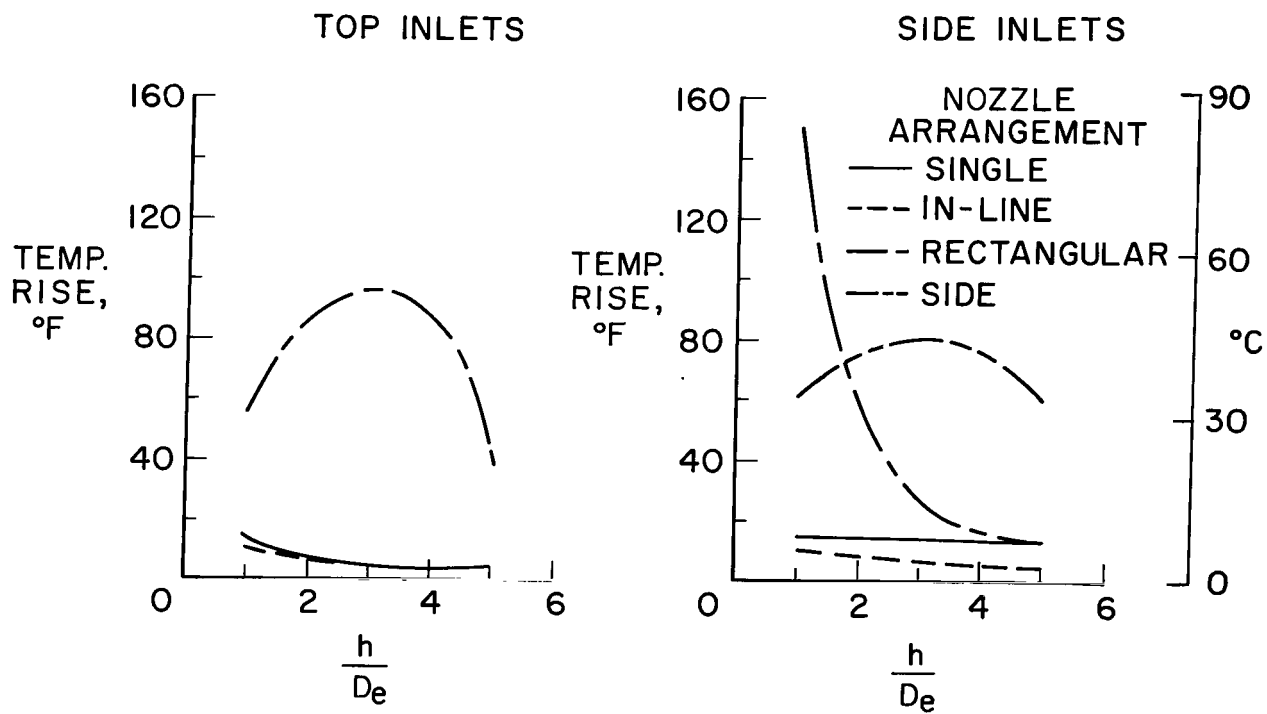


Figure 35.- Inlet air temperature rise in still air caused by the fountain effect on several configurations.

— HIGH DELTA WING
 --- LOW DELTA WING

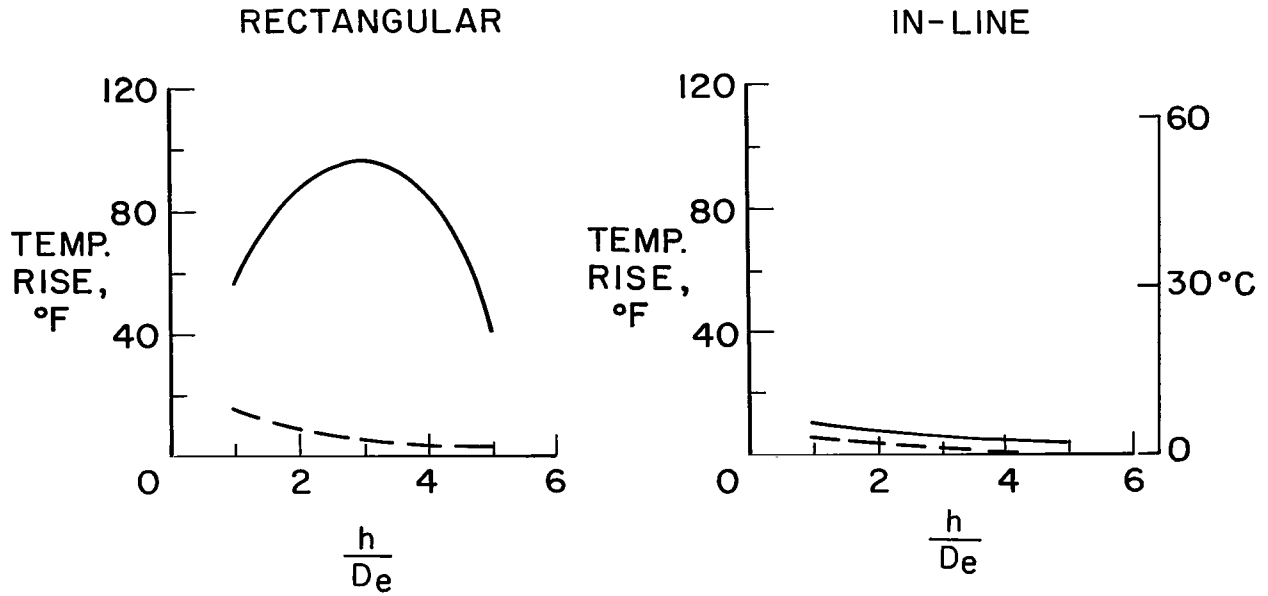


Figure 36.- Effect of wing height on air temperature rise in top inlets caused by the fountain effect on two nozzle configurations in still air.

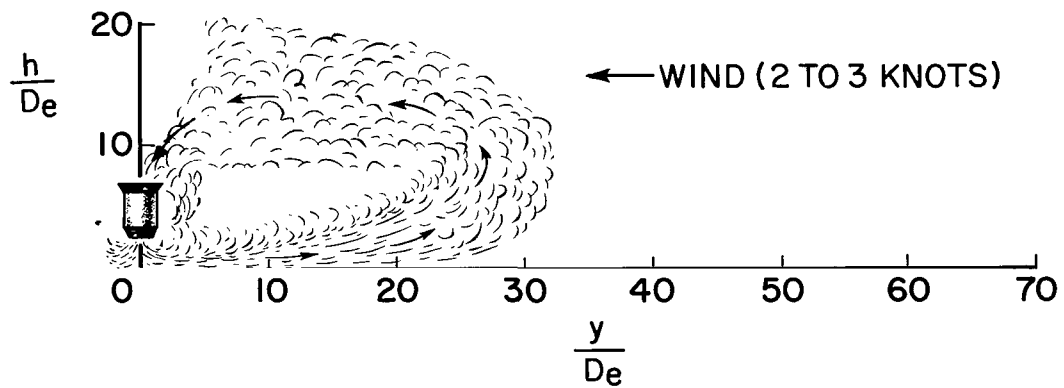


Figure 37.- Sketch showing extent of hot-gas cloud caused by the wind blowing the exhaust of a single nozzle exiting vertically near the ground.

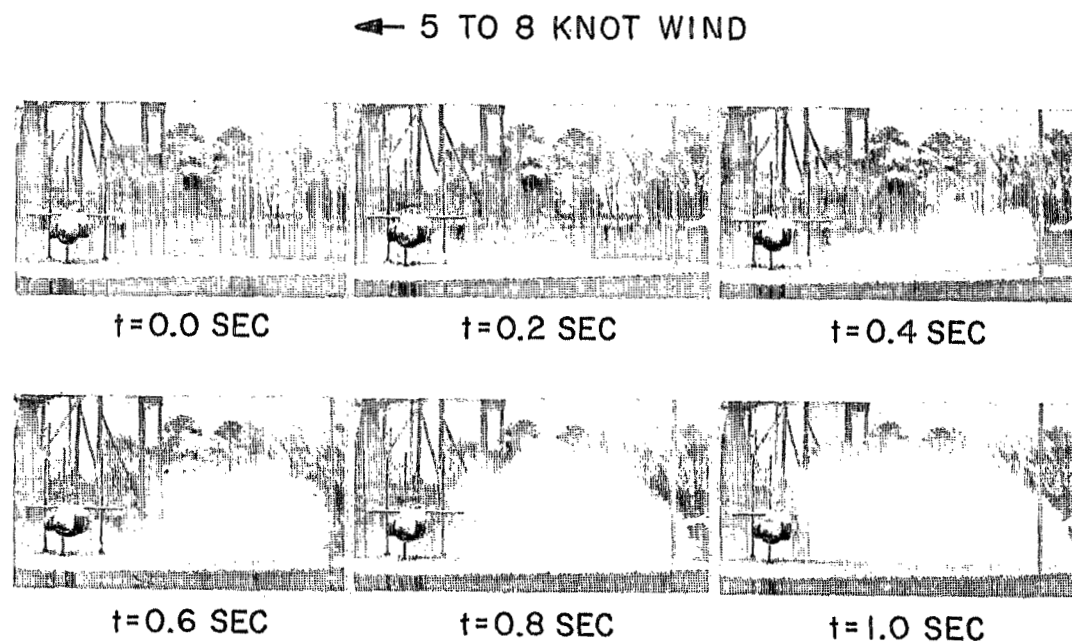


Figure 38.- Sequence of photographs showing the rapid envelopment of an airplane by the hot-gas cloud from the engine exhaust. Full power; top inlet; single nozzle.

L-2652-8

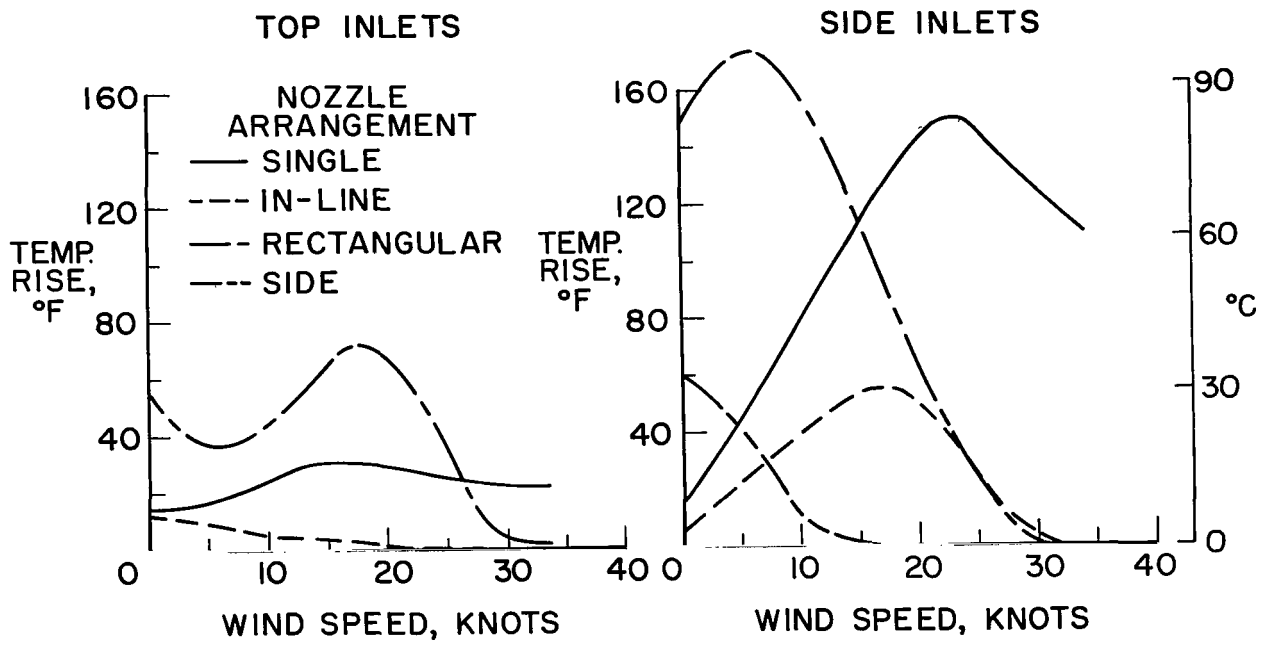


Figure 39.- Inlet air temperature rise caused by head wind blowing the vertical exhaust from several nozzle configurations near the ground.

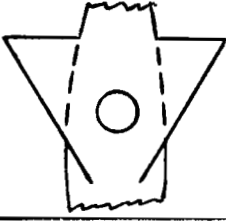
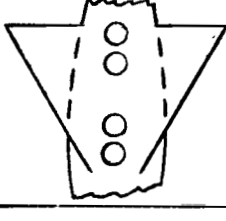
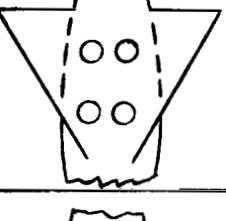
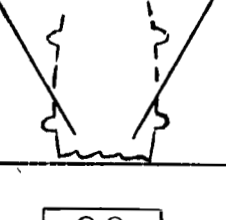
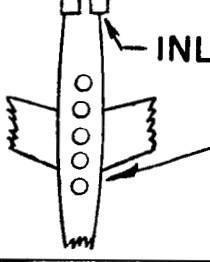
BASIC CONFIGURATION	INLET AIR TEMPERATURE RISE					
	NO WIND		HEAD WIND		SIDE WIND	
	°F	°C	°F	°C	°F	°C
	20	11	160	89	160	89
	10	6	60	33	60	33
	140	78	180	100	200	111
	90	50	110	61	120	67
	150	83	—	—	—	—
	100	55	—	—	—	—

Figure 40.- Summary of test results obtained for large-scale NASA hot-gas ingestion models.

——— T/W = 1.05
 - - - - T/W = 1.10

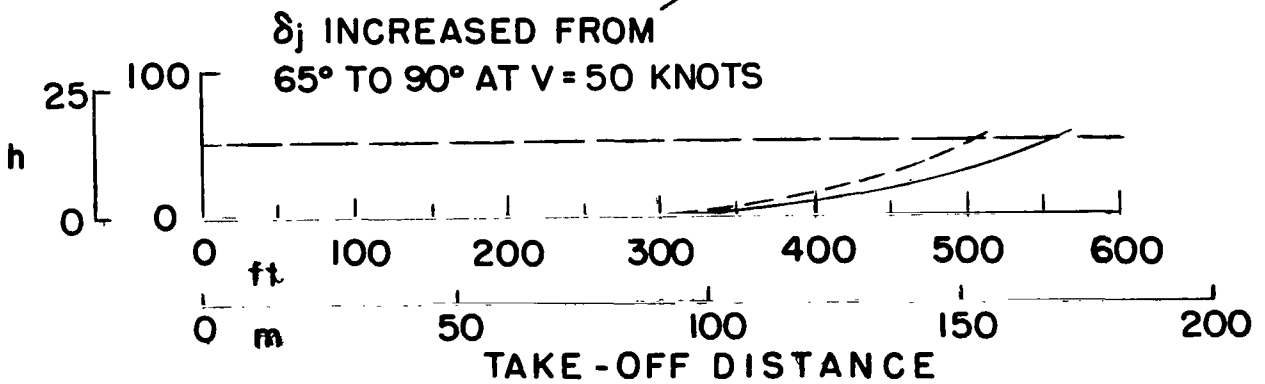
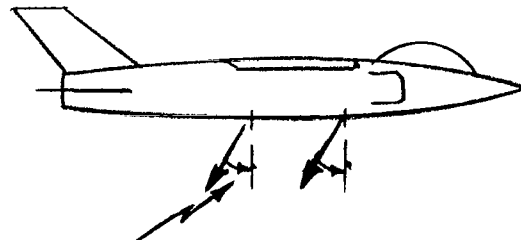
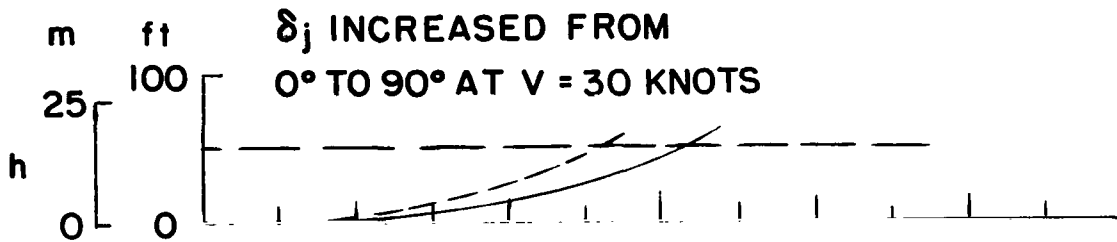
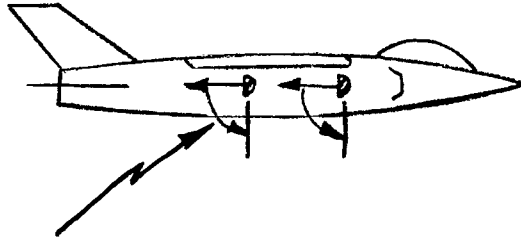


Figure 41.- Rolling vertical take-off performance of two airplane configurations; lift-off is delayed until the forward speed is sufficient to prevent hot-gas ingestion.

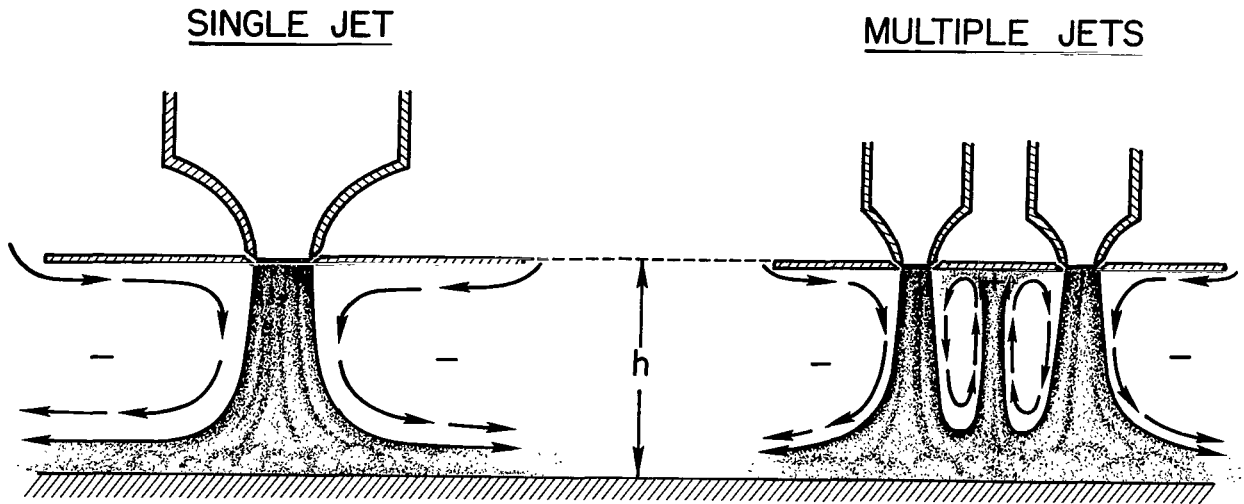


Figure 42.- Sketch of the jet-induced flow for single and multiple jets exiting vertically near the ground.

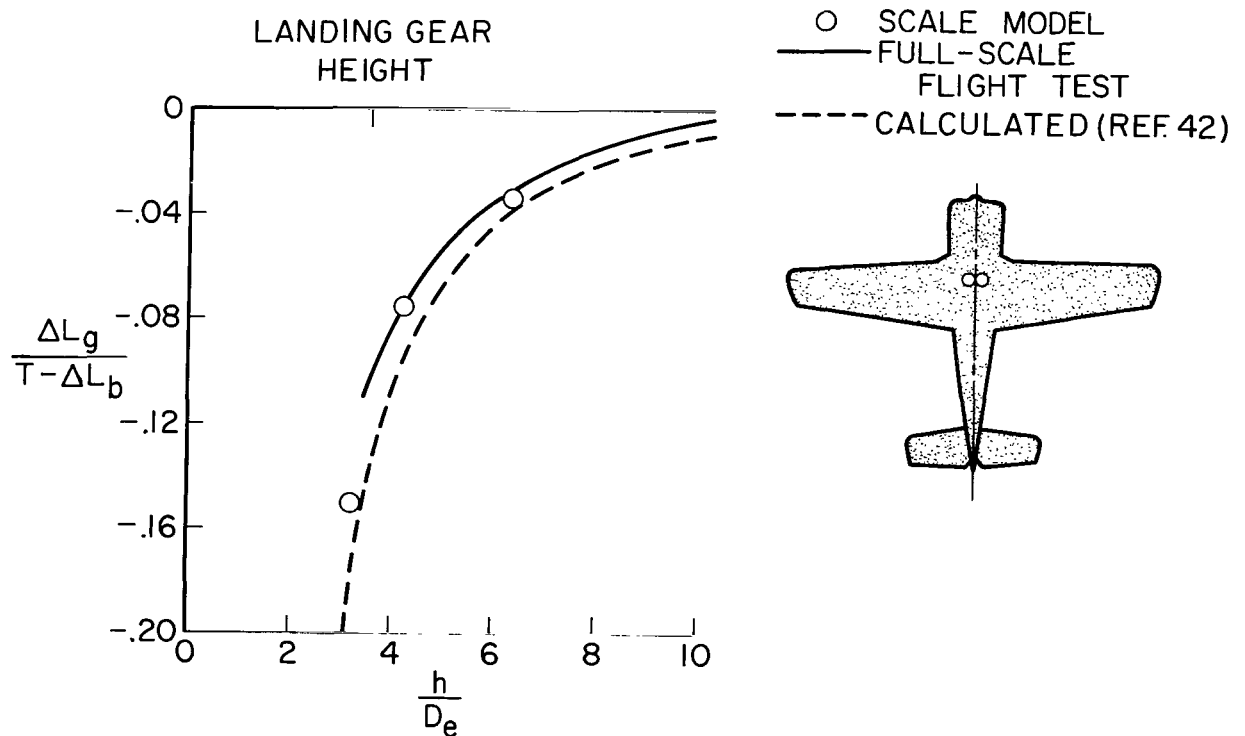


Figure 43.- Jet-induced lift loss near the ground for the X-14A airplane as given by small-scale model data, flight data, and calculated estimation. (From ref. 1.)

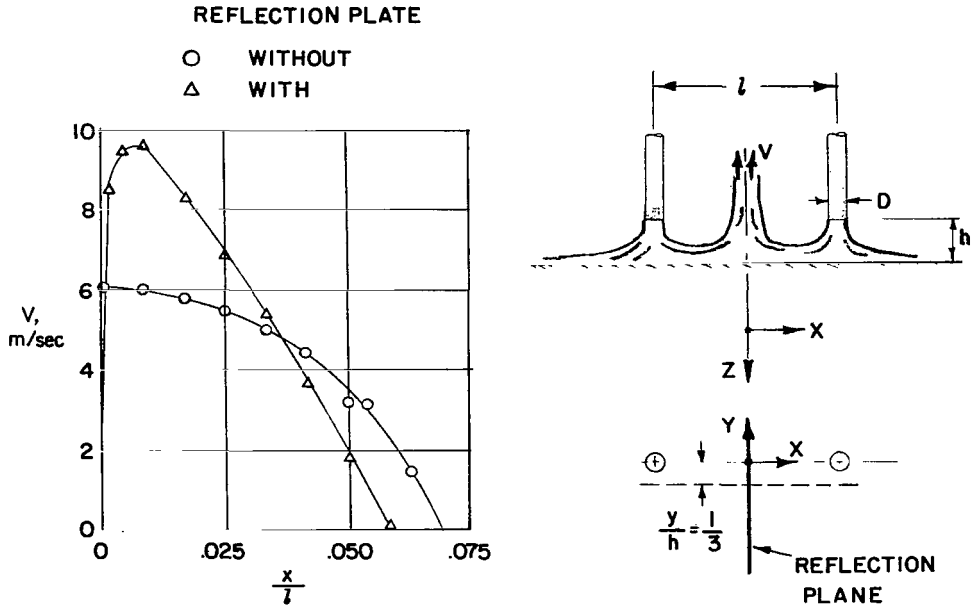


Figure 44.- Effect of a reflection plane on the measured upflow velocities in the fountain flow caused by two jets exiting vertically near the ground. The nozzles were at a height (h/D) of 3 and the upflow velocities were measured in the nozzle exit plane at a lateral distance (y/h) of $1/3$. (From ref. 43.)

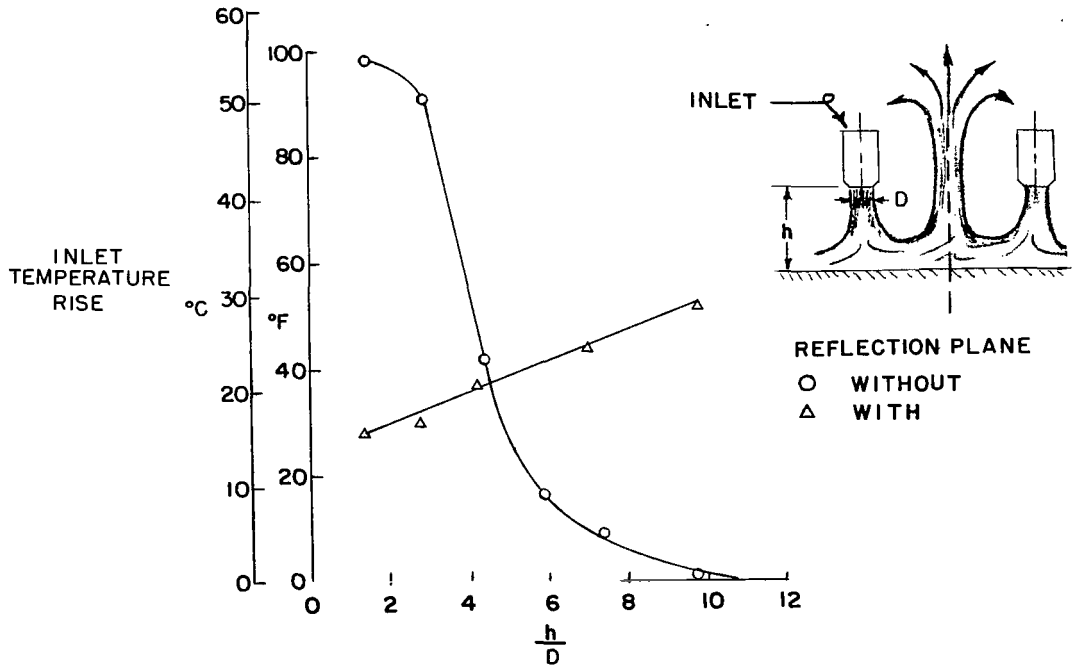
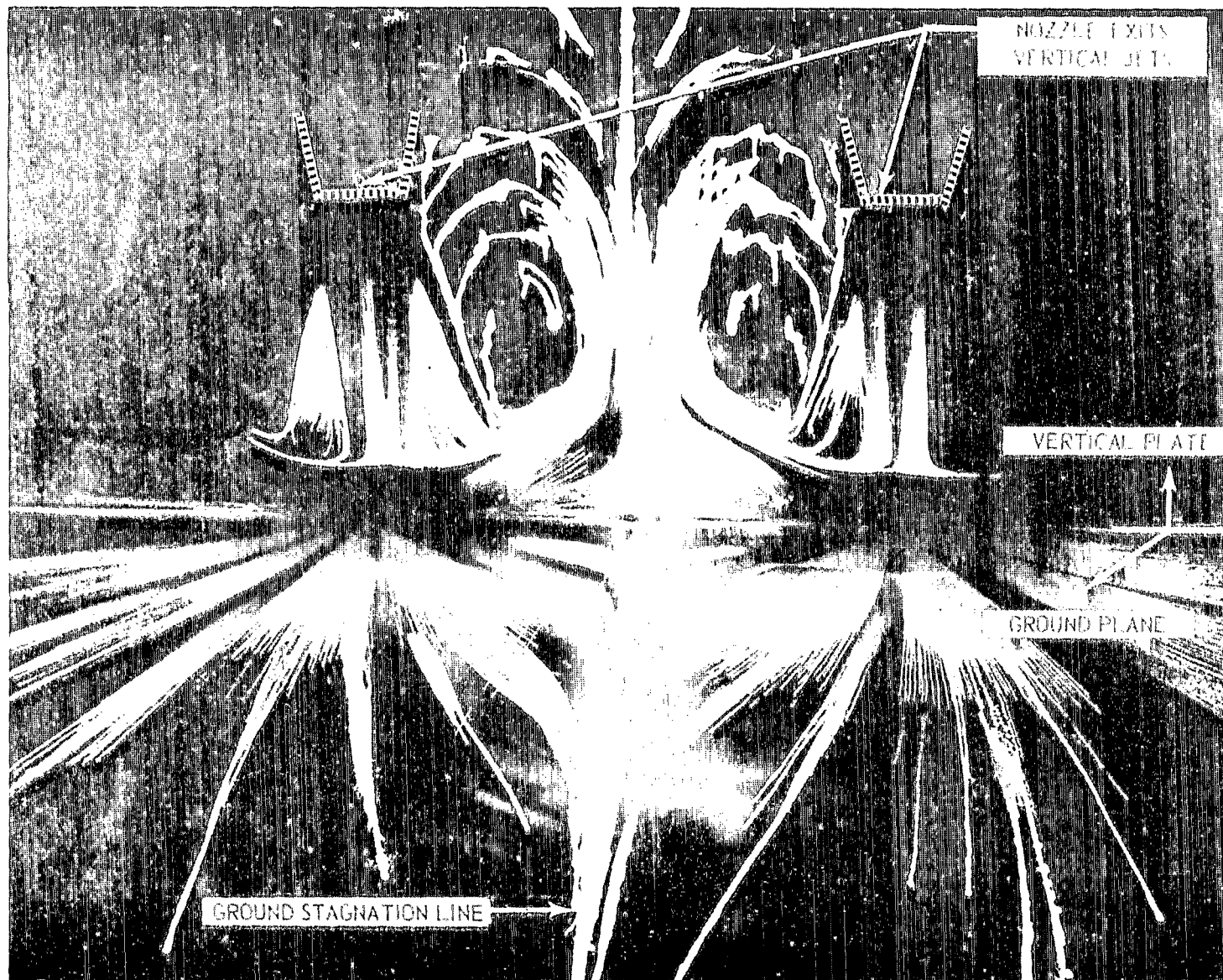


Figure 45.- Effect of a reflection plane on the measured inlet air temperature rise resulting from the fountain flow caused by two jets exiting vertically near the ground. (From ref. 38.)



L-69-5112
Figure 46.- Photograph of the flow field caused by two jets exiting vertically near the ground with equal nozzle pressures.
(From ref. 44.)

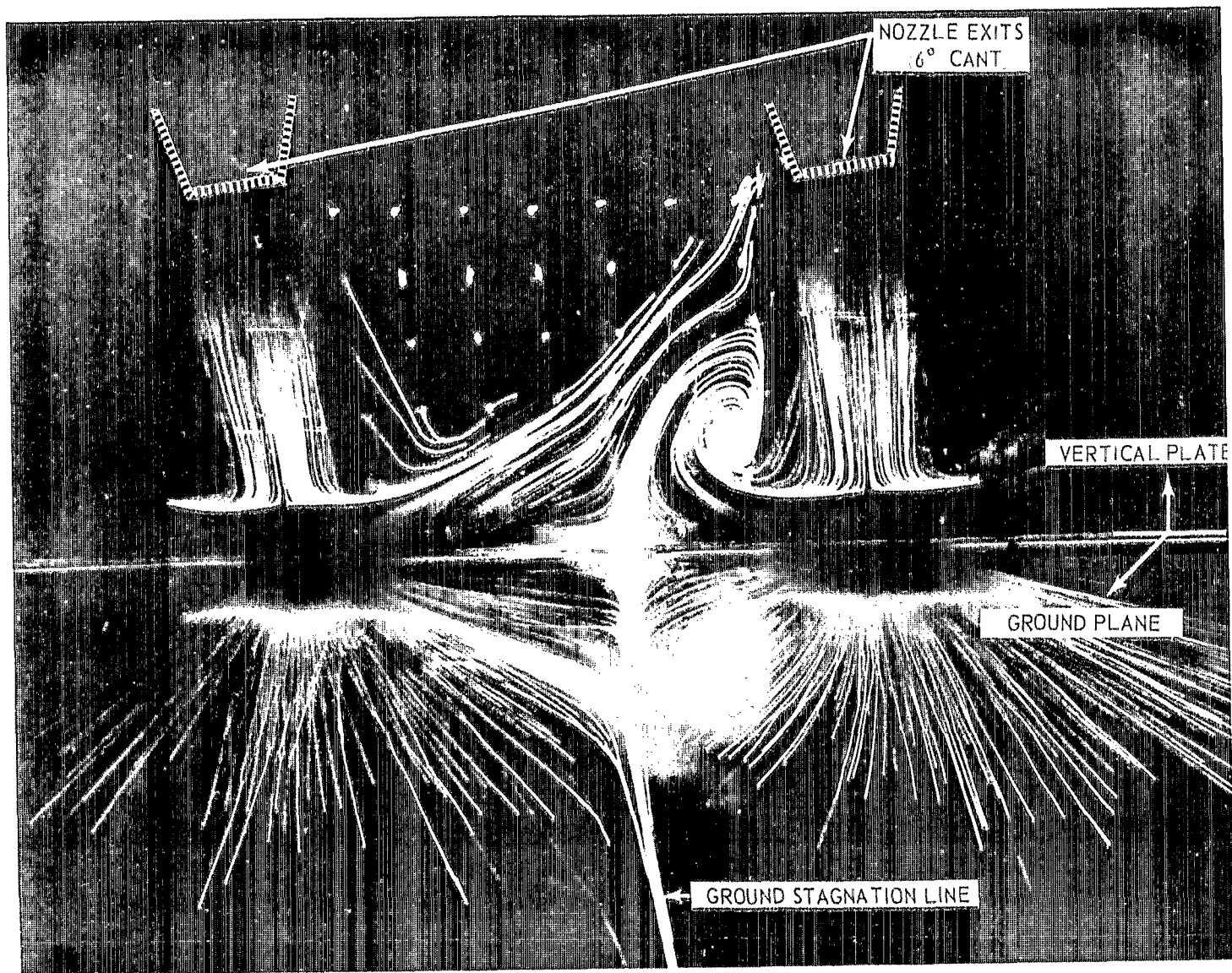


Figure 47.- Photograph of the flow field caused by two jets exiting near the ground with the nozzles canted 6° from vertical and with equal nozzle pressures.
(From ref. 44.)

L-69-5113

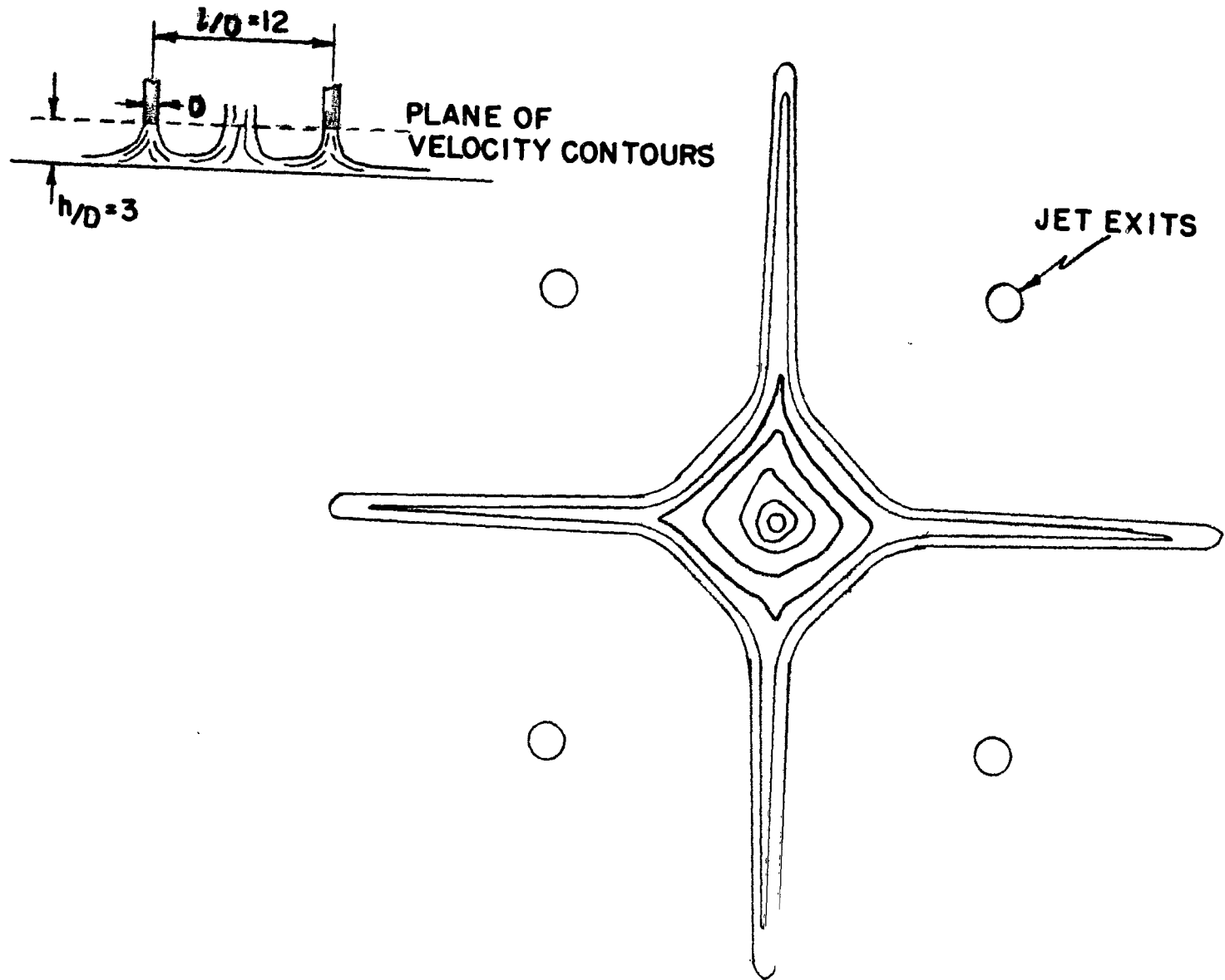


Figure 48.- Contours of constant upflow velocity in the plane of exit of a pair of nozzles three diameters above the ground. (From ref. 43.)

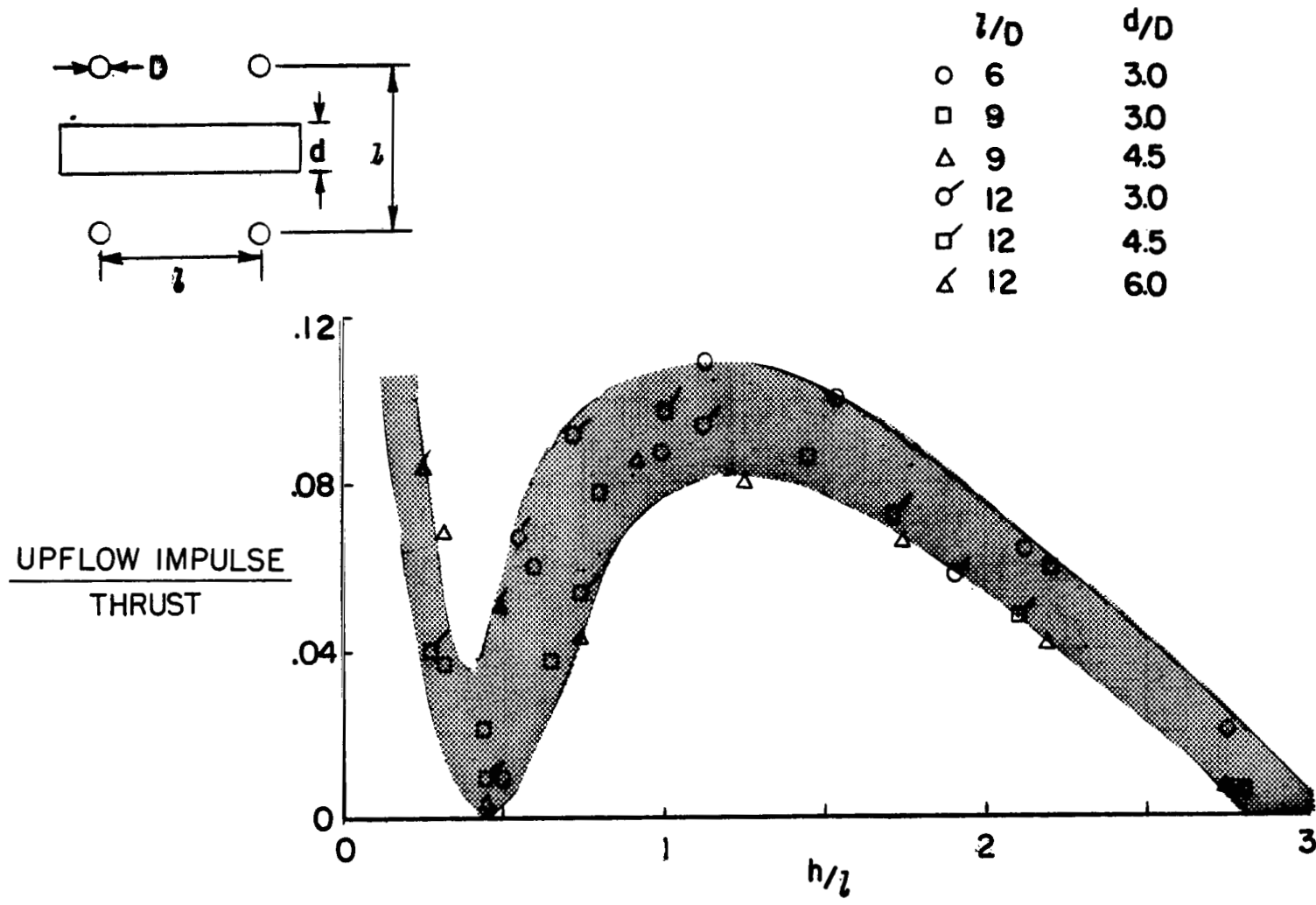


Figure 49.- Summary plot of nondimensionalized upflow impulse as a function of the ratio of nozzle height to nozzle spacing. (From ref. 43.)

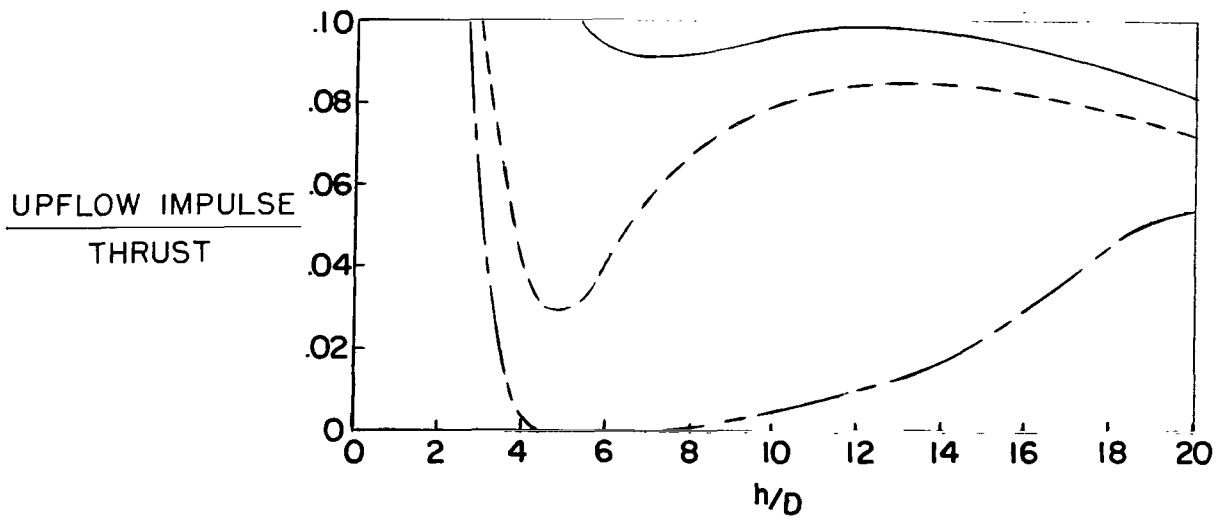
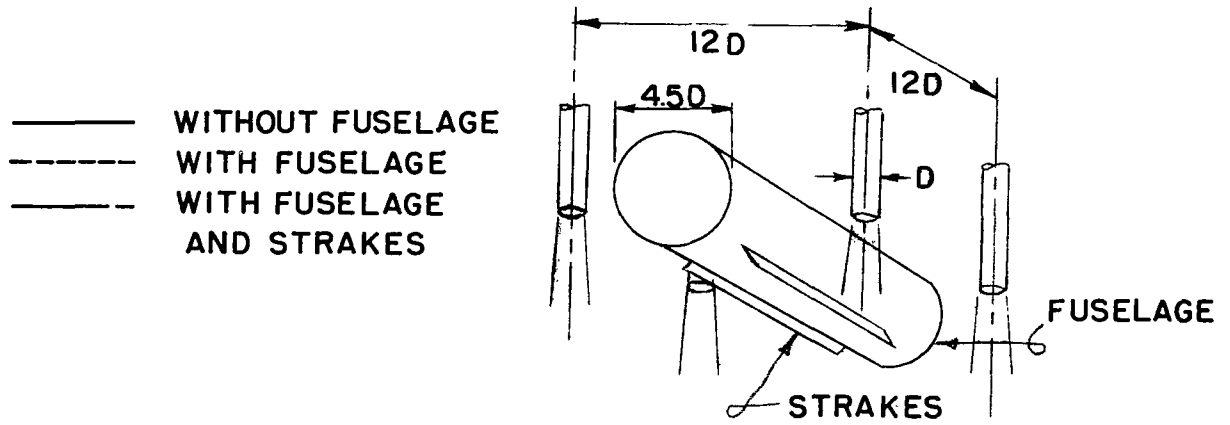


Figure 50.- Effect of fuselage on the nondimensional upflow impulse as a function of nozzle height. (From ref. 43.)

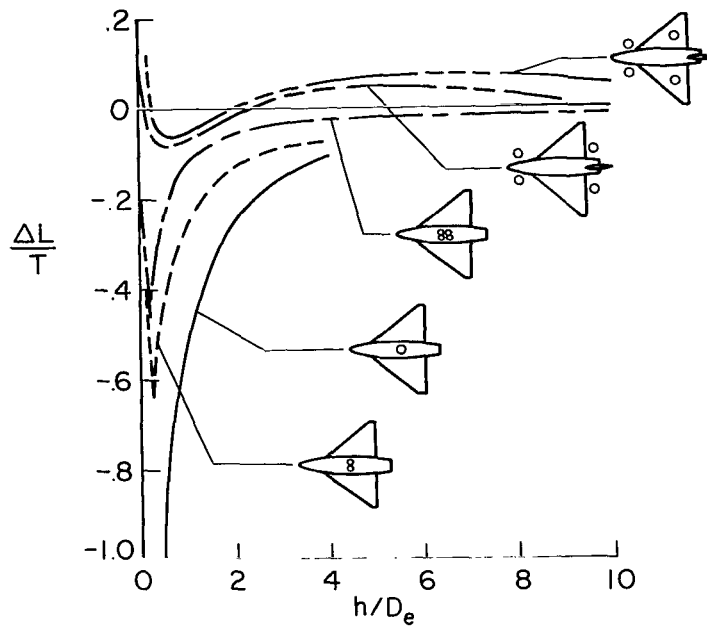


Figure 51.- Effect of multiple-jet pattern on the lift loss caused by ground effects. (From ref. 48.)

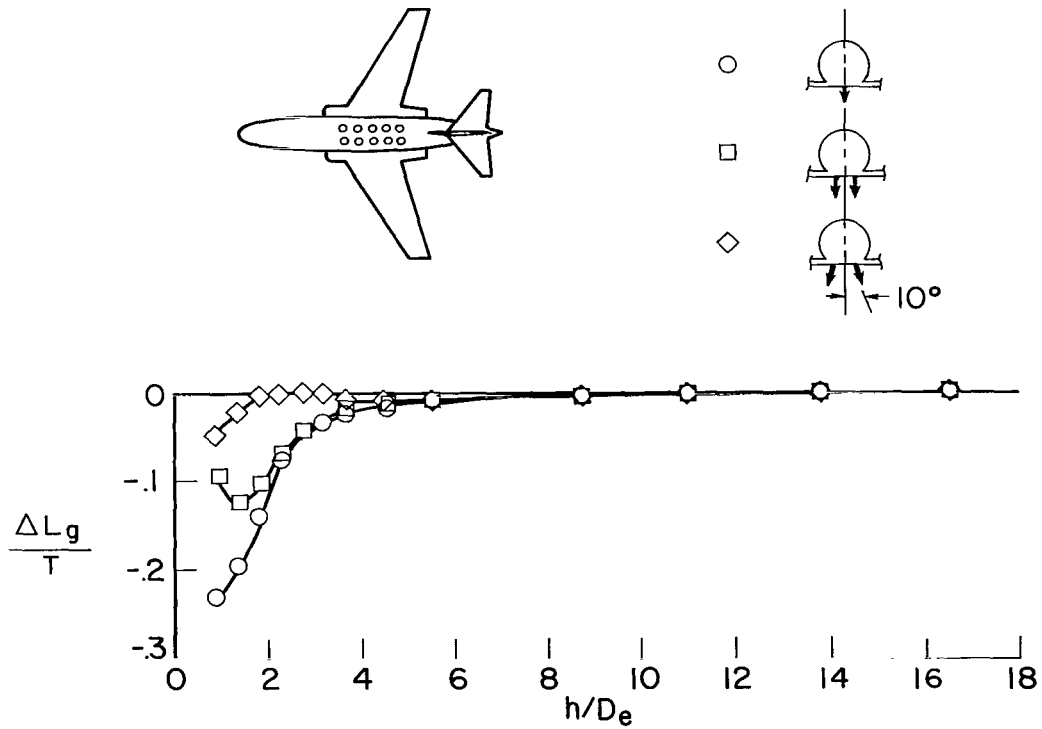


Figure 52.- Effect of outboard cant of multiple-jet nozzles on the lift loss caused by ground effects.

NATIONAL AERONAUTICS AND SPACE ADMINISTRATION

WASHINGTON, D. C. 20546

OFFICIAL BUSINESS

FIRST CLASS MAIL



POSTAGE AND FEES PAID
NATIONAL AERONAUTICS AND
SPACE ADMINISTRATION

POSTMASTER: If Undeliverable (Section 158
Postal Manual) Do Not Return

"The aeronautical and space activities of the United States shall be conducted so as to contribute . . . to the expansion of human knowledge of phenomena in the atmosphere and space. The Administration shall provide for the widest practicable and appropriate dissemination of information concerning its activities and the results thereof."

— NATIONAL AERONAUTICS AND SPACE ACT OF 1958

NASA SCIENTIFIC AND TECHNICAL PUBLICATIONS

TECHNICAL REPORTS: Scientific and technical information considered important, complete, and a lasting contribution to existing knowledge.

TECHNICAL NOTES: Information less broad in scope but nevertheless of importance as a contribution to existing knowledge.

TECHNICAL MEMORANDUMS: Information receiving limited distribution because of preliminary data, security classification, or other reasons.

CONTRACTOR REPORTS: Scientific and technical information generated under a NASA contract or grant and considered an important contribution to existing knowledge.

TECHNICAL TRANSLATIONS: Information published in a foreign language considered to merit NASA distribution in English.

SPECIAL PUBLICATIONS: Information derived from or of value to NASA activities. Publications include conference proceedings, monographs, data compilations, handbooks, sourcebooks, and special bibliographies.

TECHNOLOGY UTILIZATION PUBLICATIONS: Information on technology used by NASA that may be of particular interest in commercial and other non-aerospace applications. Publications include Tech Briefs, Technology Utilization Reports and Notes, and Technology Surveys.

Details on the availability of these publications may be obtained from:

**SCIENTIFIC AND TECHNICAL INFORMATION DIVISION
NATIONAL AERONAUTICS AND SPACE ADMINISTRATION
Washington, D.C. 20546**